UNIVERSIDADE DE BRASÍLIA

FACULDADE DE TECNOLOGIA

DEPARTAMENTO DE ENGENHARIA CIVIL E AMBIENTAL

ANÁLISE DO COMPORTAMENTO DE ESTRADAS NÃO PAVIMENTADAS REFORÇADAS COM GEOCÉLULAS FABRICADAS COM PNEUS USADOS

MARIA PAULA SUSUNAGA SALAZAR

ORIENTADOR: ENNIO MARQUES PALMEIRA

COORIENTADOR: IVONNE ALEJANDRA GUTIERREZ GONGORA

TESE DE DOUTORADO EM GEOTECNIA

PUBLICAÇÃO: G.TD-210/2025

BRASÍLIA / DF: OUTUBRO / 2025

UNIVERSIDADE DE BRASÍLIA
FACULDADE DE TECNOLOGIA
DEPARTAMENTO DE ENGENHARIA CIVIL E AMBIENTAL

ANÁLISE DO COMPORTAMENTO DE ESTRADAS NÃO PAVIMENTADAS REFORÇADAS COM GEOCÉLULAS FABRICADAS COM PNEUS USADOS

MARIA PAULA SUSUNAGA SALAZAR

TESE DE DOUTORADO SUBMETIDA AO DEPARTAMENTO DE ENGENHARIA CIVIL DA UNIVERSIDADE DE BRASÍLIA COMO PARTE DOS REQUISITOS NECESSÁRIOS PARA A OBTENÇÃO DO GRAU DE DOUTOR.

APROVADA POR:

_____
ENNIO MARQUES PALMEIRA, Ph.D. (UnB)
(ORIENTADOR)

_____
IVONNE ALEJANDRA GUTIERREZ GONGORA, D.Sc. (UnB)
(COORIENTADOR)

_____
RAFAEL CERQUEIRA SILVA, D.Sc. (UnB)
(EXAMINADOR INTERNO)

_____
JOSÉ ORLANDO AVESANI NETO, D.Sc. (USP)
(EXAMINADOR EXTERNO)

_____
KARLA PIMENTEL MAIA, D.Sc. (VALE)
(EXAMINADOR EXTERNO)

DATA: BRASÍLIA/DF, 31 de outubro 2025

FICHA CATALOGRÁFICA

SUSUNAGA SALAZAR, MARIA PAULA

Análise do comportamento de estradas não pavimentadas reforçadas com geocélulas fabricadas com pneus usados. [Distrito Federal] 2025

xxii, 134 p., 210 mm x 297 mm (ENC/FT/UnB, Doutora, Geotecnia, 2025)

Tese de Doutorado - Universidade de Brasília. Faculdade de Tecnologia. Departamento de Engenharia Civil

1. Geosynthetics
2. Geocells
3. Soil reinforcement
4. Unpaved roads

I. ENC/FT/UnB

II. Título (série)

REFERÊNCIA BIBLIOGRÁFICA

SUSUNAGA SALAZAR, M. P. (2025). Análise do comportamento de estradas não pavimentadas reforçadas com geocélulas fabricadas com pneus usados. Tese de Doutorado, Publicação **G.TD-210/2025**, Departamento de Engenharia Civil, Universidade de Brasília, Brasília, DF, 134 p.

CESSÃO DE DIREITOS

NOME DO AUTOR: Maria Paula Susunaga Salazar

TÍTULO DA TESE DE DOUTORADO: análise do comportamento de estradas não pavimentadas reforçadas com geocélulas fabricadas com pneus usados.

GRAU / ANO: Doutor /2025

Maria Paula Susunaga Salazar
Calle 70b N 8ª 04 Ibagué Tolima
Colombia
ingcivilsusunaga@gmail.co

UNIVERSITY OF BRASÍLIA
FACULTY OF TECHNOLOGY
DEPARTMENT OF CIVIL AND ENVIRONMENTAL ENGINEERING
POSTGRADUATE PROGRAM IN GEOTECHNICS

PERFORMANCE EVALUATION OF RECYCLED-TIRE GEOCELLS FOR THE REINFORCEMENT OF UNPAVED ROADS

MARIA PAULA SUSUNAGA SALAZAR

SUPERVISOR: ENNIO MARQUES PALMEIRA
CO- SUPERVISOR: IVONNE ALEJANDRA GUTIERREZ GONGORA

DOCTORAL THESIS IN GEOTECHNICS

PUBLICATION: G.TD-210/2025
BRASÍLIA / DF: OCTOBER/ 2025

UNIVERSITY OF BRASÍLIA
FACULTY OF TECHNOLOGY
DEPARTMENT OF CIVIL AND ENVIRONMENTAL ENGINEERING

PERFORMANCE EVALUATION OF RECYCLED-TIRE GEOCELLS FOR THE REINFORCEMENT OF UNPAVED ROADS

MARIA PAULA SUSUNAGA SALAZAR

DOCTORAL DISSERTATION SUBMITTED TO THE DEPARTMENT OF CIVIL ENGINEERING AT THE UNIVERSITY OF BRASÍLIA AS PART OF THE REQUIREMENTS FOR THE DEGREE OF DOCTOR.

APROVED BY:

_____
ENNIO MARQUES PALMEIRA, Ph.D. (UnB)
(SUPERVISOR)

_____
IVONNE ALEJANDRA GUTIERREZ GONGORA, D.Sc. (UnB)
(CO-SUPERVISOR)

_____
RAFAEL CERQUEIRA SILVA, D.Sc. (UnB)
((INTERNAL EXAMINER)

_____
JOSÉ ORLANDO AVESANI NETO, D.Sc. (USP)
(EXTERNAL EXAMINER)

_____
KARLA PIMENTEL MAIA, D.Sc. (VALE)
(EXTERNAL EXAMINER)

DATA: BRASÍLIA/DF, 31 de October 2025

CATALOGING IN PUBLICATION DATA

SUSUNAGA SALAZAR, MARIA PAULA

Performance evaluation of recycled-tire geocells for the reinforcement of unpaved roads. [Distrito Federal] 2025

xxii, 134 p., 210 mm x 297 mm (ENC/FT/UnB, Doutora, Geotecnia, 2025)

Doctoral these – University of Brasília. Faculty of Technology. Department of Civil and Environmental Engineering.

1. Geosynthetics
2. Geocells
3. Soil reinforcement
4. Unpaved roads

II. ENC/FT/UnB

II. Título (série)

BIBLIOGRAPHIC REFERENCE

SUSUNAGA SALAZAR, M. P. (2025). Performance Evaluation of Recycled-Tire Geocells for the Reinforcement of Unpaved Roads. Doctoral Thesis, Publication **G.TD-210/2025**, Department of Civil and Environmental Engineering, University of Brasília, Brasília, DF, 134 p.

ASSIGNMENT OF RIGHTS

Maria Paula Susunaga Salazar
Address: Calle 70b N 8ª 04 Ibagué Tolima
Country: Colombia
Email: ingcivilsusunaga@gmail.com

Dedicated to:
Jorge Iván y Pastora

ACKNOWLEDGMENTS

This work is the result of many years of effort, during which I have been accompanied by fundamental people who have significantly contributed to achieving this goal. In this space, I wish to express my deepest gratitude to all of them.

First and foremost, I would like to thank God for guiding me along the way and allowing me to reach this point in my life, successfully completing a crucial stage of my most meaningful research journey.

I am deeply grateful to the University of Ibagué and the University of Brasília for their financial support and flexibility, which made it possible to carry out the research stage of this work in Colombia, thereby strengthening the scope and quality of the study.

I extend my sincere thanks to my advisor, Professor Ennio Marques Palmeira, for his constant guidance and expertise; for always being available whenever I needed support, and for staying close despite the distance, just an email away. I also wish to thank Ivonne, who became more than a co-supervisor—she turned into a friend and a fundamental pillar during this process. Today, I remember her words; she always believed that I would be able to complete this stage. Thank you for your trust.

My heartfelt gratitude goes to my family, my greatest source of strength and companionship. To Juan David, my husband and my greatest love, who stood by me unconditionally throughout this entire journey. To my little Jorge, who arrived in the midst of this process and became a powerful motivation to keep moving forward and achieve this milestone. To my grandparents and my mother, who, even without fully understanding the technical details, were always attentive to my well-being and progress. To my aunt Gloria, who provided me with key tools to keep going when I felt I had none left.

Some friendships become family, and I wish to thank my dear friends Natalia, Consuelo, Ana María, Tania, Kathe, Jaime and Liliane, who have always been there to listen and support me.
Throughout this journey, I also had the support of systems, electronics, and mechanical engineers who made possible the development of the sensors and the data acquisition system.

My thanks go to María Camila Merchán, Bricheld, Jairo, and Andrés for their active participation in implementing the technical part of the project.

This research was conducted at the Soil and Pavement Laboratory of the University of Ibagué, and I am deeply grateful to the entire lab team, especially Engineer Camilo Zuzunaga, for his help, support, and companionship during the experimental tests.

Without hesitation, I want to express my gratitude to my students, who, at a time when I could not find a way forward, drove this project with their effort and dedication. Thank you to each of the "*aguacates*" who are part of the GEOPAV research group.

Finally, to my colleagues, with whom I shared laughter and also challenging moments; your advice and experience were invaluable in strengthening this research work.

ABSTRACT

Unpaved roads are a fundamental component of transportation infrastructure in developing countries, enabling territorial integration, access to goods and services, and the strengthening of rural economies. However, their structural performance is often constrained by the low bearing capacity of subgrade soils, variable moisture conditions, and insufficient maintenance. In this context, the use of geosynthetics, particularly geocells, has proven to be an effective technique for enhancing the mechanical behavior of granular layers by providing confinement and promoting a more uniform distribution of applied loads.

This thesis presents an experimental investigation on the behavior of a granular base material reinforced with geocells manufactured from recycled tires. The material was subjected to repeated vertical loading using a cyclic loading device specifically designed for this purpose. The system applied a constant load at a frequency of 1.2 Hz while recording vertical displacements, stresses transmitted to the subgrade, and the applied load. A total of twenty-six laboratory tests were performed, varying parameters such as geocell height and position within the layer, geocell type (recycled or commercial), and infill material (granular base or selected soil). Each configuration was evaluated under two loading conditions: an initial state and a post-maintenance state, the latter consisting of replenishing the surface infill material.

The results showed that the use of geocells substantially reduced the accumulated deformations compared to unreinforced sections, whereas the stresses transmitted to the subgrade did not exhibit significant variation. Configurations with greater geocell height and optimal placement within the layer thickness demonstrated enhanced structural performance under repeated loading. Moreover, geocells made from recycled tires exhibited mechanical behavior comparable to that of commercial geocells, confirming their technical and environmental feasibility as sustainable alternatives. These findings contribute to a deeper understanding of the effects of cellular confinement on granular layers subjected to cyclic loading and support the use of recycled materials for the reinforcement of unpaved roads.

RESUMO

As estradas não pavimentadas constituem um componente fundamental da infraestrutura de transporte em países em desenvolvimento, pois permitem a integração territorial, o acesso a bens e serviços e o fortalecimento das economias rurais. No entanto, seu desempenho estrutural é frequentemente limitado pela baixa capacidade de suporte dos solos de fundação, pelas condições variáveis de umidade e pela ausência de manutenção adequada. Nesse contexto, o uso de geossintéticos, em especial das geocélulas, tem se mostrado uma técnica eficaz para aprimorar o comportamento mecânico das camadas granulares, proporcionando confinamento e uma distribuição mais uniforme das cargas aplicadas.

Esta tese apresenta uma investigação experimental sobre o comportamento de um material granular tipo base reforçado com geocélulas fabricadas a partir de pneus reciclados. O material foi submetido a carregamentos verticais repetidos por meio de um equipamento de carga cíclica desenvolvido especificamente para esse propósito. O sistema aplicou uma carga constante com frequência de 1,2 Hz, registrando deslocamentos verticais, tensões transmitidas ao subleito e a carga aplicada. Foram realizados vinte e seis ensaios laboratoriais, variando parâmetros como a altura e a posição das geocélulas dentro da camada, o tipo de geocélula (reciclada ou comercial) e o tipo de material de preenchimento (base granular ou solo selecionado). Cada configuração foi avaliada sob duas condições de carregamento: um estado inicial e um estado pós-manutenção, consistindo na reposição do material de preenchimento superficial.

Os resultados mostraram que o uso de geocélulas reduziu substancialmente as deformações acumuladas em comparação às seções não reforçadas, enquanto as tensões transmitidas ao subleito não apresentaram variações significativas. As configurações com maior altura de geocélula e posicionamento adequado dentro da espessura da camada demonstraram melhor desempenho estrutural sob carregamentos repetidos. Além disso, as geocélulas produzidas com pneus reciclados apresentaram comportamento mecânico comparável ao das geocélulas comerciais, confirmando sua viabilidade técnica e ambiental como alternativa sustentável. Esses resultados ampliam a compreensão dos efeitos do confinamento celular em camadas granulares submetidas a carregamentos cíclicos e reforçam o uso de materiais reciclados no reforço de estradas não pavimentadas.

INDEX

LIST OF FIGURES

LIST OF TABLES

LIST OF SYMBOLS, NOMENCLATURE, AND ABREVIATIONS

B	Footing width
b, L	Length
Bg	Breakage index
c	Length and width of the pocket
C	Soil cohesion
CBR	California Bearing Ratio test
CE	Circular Economy
cm	Centimeters
DNP	National Planning Department
FI	Flexibility index
FLAC3D	Program for numerical modeling
g/cm³	Dry density
G-15	Smallest tire, 15 cm
G-20	Largest tire, 20 cm
h	Height
HDPE	High Density Polyethylene
HDPEGs	High-Density Polyethylene Geocells
Hz	Hertz
IF	Improvement Factor
INVIAS	National Institute of Roads (Colombia)
kN	Kilonewton
kPa	Kilopascal
LL	Liquid limit
m²	Square meter
MIF	Modulus Improvement Factor
mm	Millimeter
mm/cycle	Settlement per load cycle
MNT	After maintenance
MPa	Megapascal
Nc, Nq, Nγ	Bearing capacity factors
NPA	Polymer alloys
Nr	Number of load cycles sustained by the reinforced section
Nu	Number of load cycles sustained by the unreinforced section
p	Applied vertical stress
PBGs	Polymeric Blend Geocells
PET	Polyethylene terephthalate (bottles)
PETGs	Polyester Geocells with injected joints
Pl	Plastic limit
PP	Polypropylene
Pr	Bearing capacity of the reinforced soil

Pu	Classical bearing capacity of the unreinforced soil
q	Acting surcharge
q	Stress on the soil with geocells (reinforced)
q0	Stress on the unreinforced soil
qf	Bearing capacity of the unreinforced foundation
qult	Ultimate bearing capacity
RC	Reinforced concrete
RCA	Commercial geocell, placed on the subgrade
RCA-MNT	Commercial geocell, placed on the subgrade, maintenance
RCI, RCM	Commercial geocells
RCM	Commercial geocell, installed at mid-layer of the embankment
RCM-MNT	Commercial geocell, installed at mid-layer of the embankment, maintenance
RGI15	Tirecell, 15 cm height, placed on the subgrade
RGI15-MNT	Tirecell, 15 cm height, placed on the subgrade, maintenance
RGI20	Tirecell, 20 cm height, placed on the subgrade
RGI20-MNT	Tirecell, 20 cm height, placed on the subgrade, maintenance
RGM15	Tirecell, 15 cm height, installed at mid-layer of the embankment
RGM15-MNT	Tirecell, 15 cm height, installed at mid-layer of the embankment, maintenance
RGS15	Tirecell, 15 cm height, installed 5 cm below the surface
RGS15-MNT	Tirecell, 15 cm height, installed 5 cm below the surface, maintenance
RRCI	Commercial geocell, placed on the subgrade with recebo infill
RRCI-MNT	Commercial geocell, placed on the subgrade with recebo infill, maintenance
RRCM	Commercial geocell, installed at mid-layer of the embankment with recebo infill
RRCM-MNT	Commercial geocell, installed at mid-layer of the embankment with recebo infill, maintenance
RRG15	Tirecell, 15 cm height, placed on the subgrade with recebo infill
RRG15-MNT	Tirecell, 15 cm height, placed on the subgrade with recebo infill, maintenance
RRGI20	Tirecell, 20 cm height, placed on the subgrade with recebo infill

RRGI20-MNT	Tirecell, 20 cm height, placed on the subgrade with recebo infill, maintenance
Sc, Sq, Sγ	Shape factors of the footing
Spost	Accumulated settlement measured during the cycle after maintenance intervention
Spre	Accumulated settlement measured during the initial stage of the test
T	Tensile stress developed in the geocell
TBR	Traffic Benefit Ratio
u	Depth
URR	Section without reinforcement in recebo infill
URR-MNT	Section without reinforcement in recebo infill, maintenance
w %	Water content
γ	Unit weight of the soil
Δq	Improvement due to confinement effect
Δqmemb	Improvement due to the membrane effect
Δqslab	Improvement due to the slab effect
τ	Shear resistance

CHAPTER 1

1. INTRODUCTION

Unpaved roads are essential to global transportation infrastructure, particularly in rural areas and developing countries. They constitute a significant percentage of the total road network, exceeding 80% in Latin America and the Caribbean (Chauvet, 2018), and play a crucial role in community connectivity, economic development, and access to basic services (Styer et al., 2024). However, their maintenance and structural performance face numerous challenges due to their high vulnerability to climatic factors, dynamic loads, and erosion processes (Harral, 1988).

Unpaved roads in Colombia constitute a fundamental part of the country's transportation infrastructure, accounting for approximately 69% of the national road network, with a significant presence in rural areas. These roads are essential for connecting remote communities, facilitating access to markets, basic services, and economic opportunities. The National Government recognizes their importance and implements investment and maintenance strategies through the National Planning Department (DNP) and entities such as INVÍAS. However, ensuring their proper condition remains a significant challenge, as only 19% of tertiary roads are in optimal condition, while 41% are in fair condition, and 40% are in poor condition. The lack of paving, combined with factors such as adverse weather conditions, erosion, and limited maintenance resources, complicates the long-term sustainability of these roads.

Paved and unpaved roads that traverse sections with low bearing capacity face significant challenges in terms of stability and durability. Traditionally, increasing the thickness of structural layers is used to enhance load-bearing capacity; however, this approach results in higher material consumption, increased costs, and environmental issues related to aggregate extraction. In this context, the use of geosynthetic materials, such as geocells, geotextiles, and/or geogrids, has proven to be an efficient solution for stabilizing weak subgrades. These materials allow for a more uniform load distribution, reduce permanent deformations, and optimize structural design by decreasing the base layer thickness without compromising the road’s mechanical performance (Poorahong et al., 2024).

The circular economy (CE) is proposed as a fundamental strategy to mitigate the environmental impacts associated with the depletion of non-renewable resources and the exponential increase in waste. In 2010, global waste production reached approximately 1.3 billion tons, and projections indicate that this amount could rise to 2.2 billion tons by 2025, highlighting the urgent need to adopt sustainable material management and waste reduction models (Segui, 2018).

The principles of the circular economy align closely with the United Nations' Sustainable Development Goals (SDGs), especially SDGs 12 (Responsible Consumption and Production), 9 (Industry, Innovation, and Infrastructure), 11 (Sustainable Cities and Communities), and 13 (Climate Action). These goals emphasize transitioning toward resource-efficient systems, technological innovation, and environmentally responsible infrastructure development. This reinforces the importance of circular practices in the engineering and construction sectors.

The construction industry accounts for up to 60% of natural material extraction (Kamali et al., 2019), which highlights the urgency of adopting sustainable strategies that promote material reuse and foster a circular economy. Given the sector’s high resource consumption, optimizing the use of recycled materials, reducing waste, and minimizing environmental impact are essential measures to enhance the industry's sustainability.

Within the same context, the increase in vehicle manufacturing has led to a proportional rise in the number of discarded tires, with estimates projecting the generation of 2.67 billion units by 2027 (Kunecki, 2023). This massive accumulation poses a serious environmental threat, as tire particles contaminate freshwater ecosystems and coastal estuaries, negatively impacting biodiversity (World Economic Forum, 2024). Additionally, the improper disposal of these waste materials presents a high fire risk, especially when they accumulate in unregulated landfills or are managed inefficiently.
In response to this issue, there has been a growing interest in developing sustainable strategies for the reuse of used tires, driven by the need to reduce their environmental impact. Among the most notable alternatives is their use in pavement construction and their incorporation into various industrial applications (Phys.org, 2024), thereby promoting the transition toward a circular economy model and more efficient waste management.

This work evaluates the behavior of geocells manufactured with used tires, these elements are focused on the generation of a circular economy based on three important problems: the deficiency of tertiary roads, the need to reduce the consumption of materials in the construction of pavements and the reuse of a hazardous waste such as used tires.

Geocells are materials that help improve road performance. Within the road structure, they prevent deformation of the fill material, increasing its lifespan and reducing maintenance costs (Palmeira, 2018). However, most traditional geocells are made from synthetic polymers derived from petroleum, which has a significant environmental impact. In this context, the development of geocells made from recycled tires emerges as a sustainable alternative that not only preserves the required mechanical properties but also contributes to the management of a waste material with a high environmental impact.

Research such as that of Lei et al., (2024) has shown that the incorporation of geocells in soils contributes significantly to the reduction of deformations and to the increase of soil strength, thanks to their confinement capacity. In addition, these materials have gained wide acceptance due to their effectiveness in load distribution, soil reinforcement and reduction of deformations under cyclic loads (Banerjee et al., 2024). Geocells vary in aspects such as height, joint spacing and fabrication material, allowing their optimization according to the specific requirements of each project. These particularities make the use of geocells as reinforcement a more efficient and effective alternative compared to other geosynthetics, improving both structural performance and functionality in various infrastructure applications (Biabani et al., 2016).

This research focuses on the evaluation of the performance of geocells manufactured with recycled tires as a reinforcement element in unpaved roads. The behavior of deformations and pressures generated by traffic on soils stabilized with this type of geocells will be analyzed in order to determine their effectiveness in improving the stability and durability of the road structure under cyclic loading conditions in a scaled laboratory model. The results of this study will allow generating technical knowledge on the feasibility of this solution and its potential contribution to the sustainability of road infrastructure.

1.1. JUSTIFICATION

The improvement of rural roads is a determining factor for the socio-economic development of remote communities, as it not only optimizes mobility and access to markets, but also fosters integration with urban centers, reducing inequality gaps and promoting sustainable growth. Recent research, such as those of Anega (2023) and Armen (2025), has shown that the optimization of rural road infrastructure has a direct impact on the economic transformation of communities. This impact translates into a greater diversification of productive activities, the strengthening of local commerce and the generation of new employment opportunities. In addition, improved connectivity facilitates the transition of traditional economic sectors towards more competitive and sustainable models, thus promoting the well-being and quality of life of the inhabitants of these regions.

Given the importance of developing more efficient, resistant and durable rural roads, this research focuses on evaluating the performance of the reinforcement of these infrastructures by means of geocells made of recycled tires. The study aims to analyze the impact of tire geocells on the reduction of deformations and the extension of the life of rural roads. By taking advantage of a polluting waste such as discarded tires, this solution not only contributes to the stability and durability of road infrastructure, but also promotes environmental sustainability through the reuse of recycled materials. In this sense, the study seeks to provide a viable and ecological alternative for the reinforcement of rural roads, with both technical and environmental benefits.

1.2. PROBLEM STATEMENT

Tertiary roads play a crucial role in the connectivity of rural communities, facilitating access to markets, basic services, and economic opportunities (Correa, 2017). However, their structural and functional performance is compromised by the low bearing capacity of the soils (Ahmed et al., 2024), the action of dynamic loads, and the lack of proper maintenance. Limited investment in road infrastructure and dependence on conventional materials have led to a recurring issue of premature deterioration, increasing rehabilitation costs and affecting the long-term sustainability of these roads.

Tertiary roads face significant deterioration challenges, mainly due to the appearance of undesirable rutting and deformations, which compromise their functionality and sustainability. Studies have shown that the incorporation of geosynthetics in unpaved roads optimizes stress distribution, reduces deformations and prolongs their service life (Singh et al., 2022) However, despite the benefits proven in the laboratory, their performance in real conditions still requires further research, especially in different types of soils and traffic loads. In this context, the use of geocells made from recycled tires is presented as a sustainable alternative, capable of improving the stability of tertiary roads, reducing maintenance costs and taking advantage of recycled materials, promoting a more efficient and environmentally responsible road infrastructure.

Globally, the accumulation of discarded tires represents a serious environmental and economic problem, since their improper management generates negative impacts on soil, water bodies and air quality. It is estimated that 75% of discarded tires contain empty spaces, which makes their storage and transportation difficult, generating significant costs. In addition, due to their high durability and flammability, their prolonged accumulation increases the risk of catastrophic fires, releasing large amounts of smoke, hydrocarbons and toxic metals, which contributes to soil and groundwater contamination (Hashamfirooz et al., 2025). The reuse of this material in the construction of road infrastructure would not only help reduce environmental pollution, but would also reduce dependence on conventional materials, promoting circular economy and sustainability in the civil engineering sector.

Given this context, it is necessary to evaluate the impact of the use of geocells made from recycled tires on the structural and functional performance of tertiary roads. Specifically, it is necessary to analyze their effectiveness in terms of deformation reduction, pressure distribution and resistance to aggregate fracture, in order to determine their viability as a technically and environmentally sustainable solution for the improvement of these infrastructures. In this regard, the present research seeks to answer the following question: how does the use of geocells made from used tires influence the structural and functional performance of tertiary roads in terms of reducing deformations, pressure distribution, and resistance to aggregate fracture?

The study will provide key information for decision-making in the design and maintenance of tertiary roads, contributing to the development of innovative solutions that improve the stability of these infrastructures and reduce their environmental impact.

1.3. OBJECTIVES

1.3.1. General Objective

Evaluate the performance of geocells manufactured from recycled tires as reinforcement elements in unpaved roads on low-load-bearing soils, analyzing their impact on reducing deformations and pavement pressures.

1.3.2. Specific Objectives

- Characterize the physical and mechanical properties of geocells made from recycled tires (height, thickness, strength, flexibility, and durability) and their relationship to the structural behavior of unpaved roads.
- Quantify the influence of reinforcement with recycled tire geocells through comparative tests with and without their presence, evaluating their effect on load-bearing capacity, stress redistribution, and the reduction of permanent deformations in the pavement.
- Analyze the impact of geocell placement within the fill material, assessing their structural performance when installed at different depths within the granular layer (near the subgrade, in the middle of the layer, or close to the pavement surface).

CHAPTER 2

2. LITERATURE REVIEW

This chapter presents a review on geocells, covering their definition, manufacturing materials, confinement mechanism, and applications in soil stabilization and structural reinforcement in civil engineering. Their main characteristics, the materials used for their fabrication, and their impact on improving the geotechnical performance of soils and structures will be analyzed. Therefore, recent studies that have evaluated the behavior of geocells under different conditions will be explored, highlighting their effectiveness in soil stabilization, road base reinforcement, erosion control, and the construction of retaining walls. Finally, technological advances in the manufacturing of geocells using sustainable materials, such as recycled polymers and natural fibers, will be discussed, emphasizing their contribution to environmental engineering and resource optimization in modern infrastructure.

2.1.GEOSYNTHETICS AND GEOCELLS

The use of geosynthetics in soil and aggregate stabilization has been widely documented in transportation infrastructure, such as roads, railroads and airports. These materials provide structural improvements through different mechanisms:

- **Geogrids:** Enhance particle interlocking, improving soil shear strength and providing reinforcement and lateral confinement.
- **Geostrips:** polymeric strips that reinforce soil masses in substitution to metallic strips.
- **Geotextiles:** Act as permeable layers that separate and reinforce soil masses, contributing to stability through friction and tension, which reduces lateral deformation.
- **Geocells:** Three-dimensional structures that create lateral confinement of aggregates or soils, increasing system rigidity and significantly improving load distribution and soil bearing capacity.

Thanks to these mechanisms, the use of geosynthetics not only optimizes stability and load distribution, but also reduces settlement and deformation, improving the structural performance of pavements and foundations. (Tutumluer et al., 2025)

Geocells are a geosynthetic material with a three-dimensional honeycomb structure, composed of polymer strips interconnected by nodes (Lei et al., 2024). Figure 2.1 illustrates the installation and filling process of geocells: (A). Geocells function by confining the material within them, with their primary purpose being ground reinforcement and protection. When stacked, they can also be used to form retaining walls. One advantage of geocells is that they are supplied compressed and, upon arrival at the construction site, they can be expanded, which facilitates their transportation (Palmeira, 2018). Figure 2.2 shows the typical geometry of compressed and expanded geocells.

Figure 2.1- Example of geocell installation in the field: (A) Installation. (B) Filling of the geocells.(Feng et al., 2024).

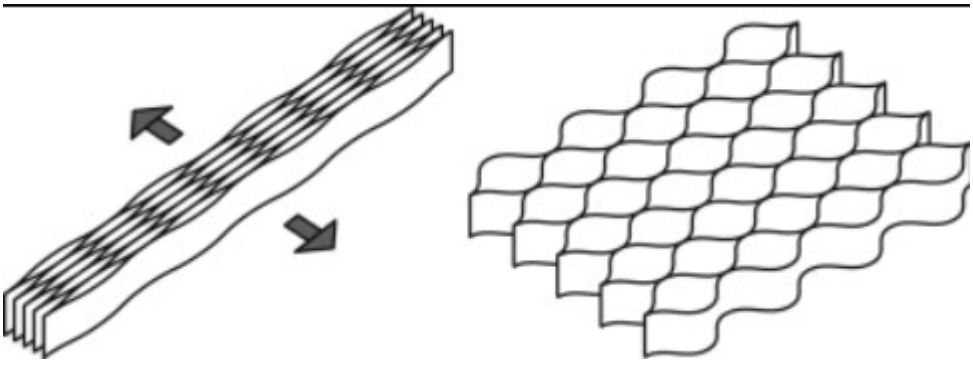

Figure 2.2-Typical geometry of geocell (Yang, 2010).

This type of geosynthetic represents a rather recent technique in geotechnical engineering, designed to enhance soil stability and strength through an efficient confinement mechanism. Its functionality is based on the complete containment of material within its cellular compartments, entirely preventing lateral dispersion. This restriction creates a reinforcing effect that increases soil rigidity and cohesion, forming a stronger composite material. As a result, the geocell layer acts as a structural cushion that evenly distributes foundation loads over a larger area. (Dash et al., 2003)

Geocells basically work on the principle of lateral confinement, which occurs through two main mechanisms, as shown in Figure 2.3. First, the friction between the filler material and the geocell wall limits the lateral displacement of the soil particles, improving their shear strength and stability. Secondly, the geocell-reinforced base acts as a cushion, restricting the upward movement of the soil outside the load area. This contributes to a better stress distribution and an increase in the bearing capacity of the reinforced soil (Pokharel et al., 2010).

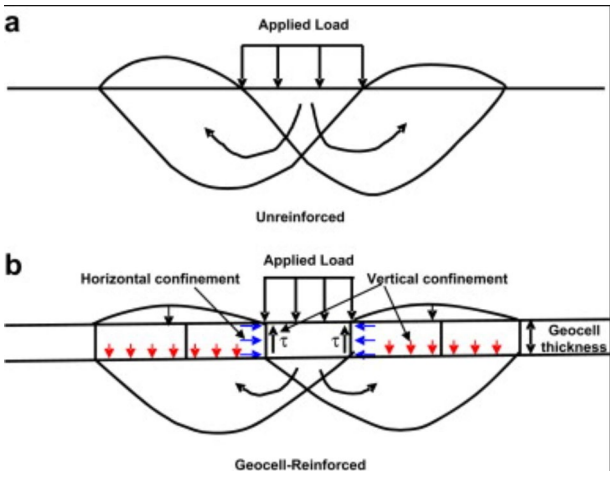

Figure 2.3 -Unreinforced and geocell-reinforced bases (Pokharel et al., 2010).

There are geocells made of different types of materials, the most popular of which are high density polyethylene (HDPE) and polypropylene. (PP)(Parsa et al., 2024), but there are also known studies with geocells made from non-woven geotextiles (Abiryan, 2017), polymer alloys (NPA) (Y. Zhao et al., 2025), natural fibers such as coconut (Sreevalsa et al., 2019), recycled tires(Badiger et al., 2024) or manufactured from other materials. Regardless of the material used, studies show that cellular confinement works as a reinforcement of the materials yielding positive results in material behavior.

Given its impact on improving the geotechnical performance of soils, various studies have evaluated the effectiveness of geocells under different conditions. Recent research has demonstrated their usefulness in soft soil stabilization, settlement reduction, and load-bearing capacity improvement.

2.2. FACTORS AFFECTING THE PERFORMANCE OF GEOCELLS

The use of geocells in geotechnical engineering has proven to be an effective technique for the reinforcement of soils and granular materials, improving bearing capacity, reducing deformation and increasing the stability of various structures (Emersleben & Meyer, 2008; Fazeli Dehkordi et al., 2023).However, the effectiveness of geocell reinforcement depends on multiple factors that influence its performance. This section presents a review of the key factors affecting the efficiency of geocell reinforcement, based on previous studies and relevant scientific literature. Figure 2.4 graphically illustrates the geometric parameters of geocells, where h represents the height, u the depth of installation, and b the length.

In addition to the above, the bearing capacity improvement factor (I_f) is defined as the increase in strength of the reinforced soil compared to unreinforced soil. It is calculated as the ratio between the applied stress on the soil with geocells (q) and the applied stress on the unreinforced soil (q_0) at the same displacement level. Figure 2.5 graphically illustrates the calculation of the bearing capacity improvement factor. According to experimental studies, this index can be determined at any point on the load-deformation curve. However, when it is evaluated at the displacement level corresponding to the failure of the unreinforced soil, the ultimate bearing capacity ($qult$) is used. This allows for the quantification of the improvement in load-bearing capacity due to the use of geocells. The improvement factor, in turn, depends on variables such as material stiffness, installation depth, and the characteristics of the supporting soil, among others.

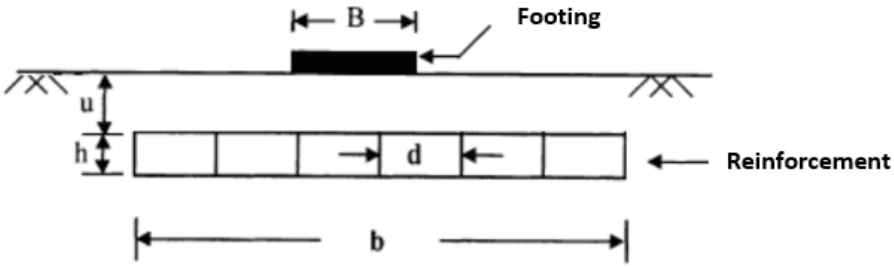

Figure 2.4 - Geometric parameters of a geocell reinforcement system (Avesani, 2013).

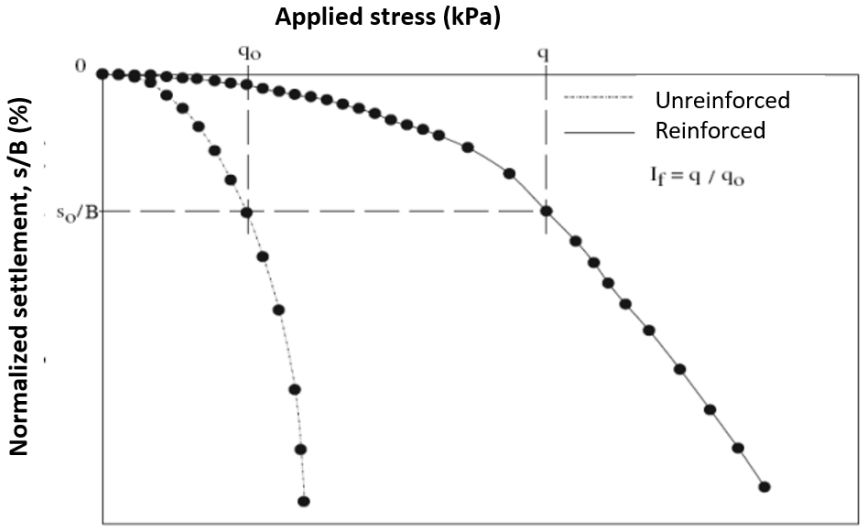

Figure 2.5 - Parameters used in the calculation of the bearing capacity improvement factor (Avesani, 2013).

2.2.1. Height of the geocells

The height of geocells is a critical parameter in soil reinforcement, as it directly influences bearing capacity and stress distribution within the reinforced system. Experimental studies have shown that an increase in height enhances lateral confinement of the infill material, increasing shear strength and improving soil stability. (Pokharel et al., 2010). However, various studies have identified an optimal height, beyond which the improvement in bearing capacity stabilizes or even decreases due to reduced load transfer efficiency and potential local deformations in the geocell walls. (Krishna, 2023).

Some studies show that as the height of the geocell increases, the bearing capacity of the reinforced soil also increases. (Shin et al., 2017) conducted a study with three different heights (120 mm, 180 mm and 240 mm) and showed that the allowable bearing capacity

and ultimate bearing capacity increase progressively as the geocell height increases. As shown in Figure 2.6, the maximum bearing capacity is reached with the 300×240 mm configuration, where the ultimate bearing capacity reached 601.63 kPa and the allowable bearing capacity 200.88 kPa, confirming that greater lateral confinement of the backfill material improves the mechanical behavior of the reinforced system.

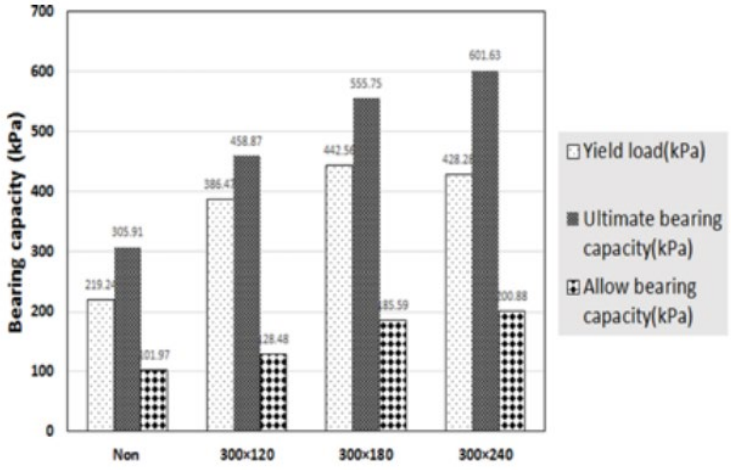

Figure 2.6 - Bearing capacity for each geocell height used(Shin et al., 2017).

Shimizu (1990) found that an increase in the height and area of the geocell significantly improves the bearing capacity of the reinforced foundation. This enhancement is attributed to the geocell's ability to provide greater lateral confinement and stress distribution, which reduces settlements and improves system stability. Additionally, they determined that the magnitude of the increase in bearing capacity is correlated with the horizontal stiffness of the cell material, as higher stiffness allows for better deformation control and more efficient distribution of applied loads on the reinforced soil.

Regarding the optimal height of geocells, various studies have been conducted which, through research involving different materials and geometric configurations, have established optimal height ranges depending on the application and load conditions. In particular, the studies by Demirdogen et al., (2024), Zhao et al., (2025) and Banerjee et al., (2024) have evaluated the performance of geocells in shallow foundations, subgrades, and flexible pavements, respectively, identifying how height influences bearing capacity, settlement reduction and stress distribution. Table 2.1 Table 2.2 and Table 2.3 summarize the main findings of these studies, enabling a direct comparison of their results and

recommendations. The analysis shows that the optimal height in all three studies ranges between 100 mm and 150 mm.

Table 2.1 - Optimal height range based on the type of geocell for subgrade reinforcement.(Zhao et al., 2024, 2025).

Geocell Types	Optimal Height (mm)	Key Observations
HDPEGs (High-Density Polyethylene Geocells)	100 - 150 mm	Improves lateral confinement, but heights above 150 mm may reduce reinforcement efficiency.
PETGs (Polyester Geocells with Injected Joints)	50 - 100 mm	Less sensitive to height variations; performance does not significantly improve with greater heights.
PBGs (Polymeric Blend Geocells)	100 - 150 mm	Similar to HDPEGs but with better creep resistance; greater height allows for better load distribution.

Table 2.2.2 - Optimal height of geocells in flexible pavements (Banerjee et al., 2024).

Condition	Optimal Geocell Height
Pavement with high loads and repeated traffic	150 mm
Cost-effective solution with good performance	100 mm with SW330
Soils with low bearing capacity	150 mm
Applications with low loads	100 mm

Table 2.3 - Influence of geocell height on shallow foundations (Demirdogen et al., 2024).

Geocell Height (mm)	Observed Effect
120 mm	Increase in bearing capacity compared to unreinforced soils. Considered a reference point.
150 mm	Improves bearing capacity by 6% under concentric load. No significant improvement under eccentric load.
Greater than 150 mm	No additional benefits observed; wall buckling may occur.

2.2.2. Cell Shapes

Geocells have evolved in their geometric design to optimize soil reinforcement performance and improve bearing capacity. The shape of the cells is a key factor influencing structural rigidity, stress distribution, and the efficiency of material confinement. Various geometric configurations exist, including circular, rectangular, rhomboidal, hexagonal, square, and honeycomb (see Figure 2.7), each exhibiting distinct characteristics that influence the performance of the reinforced system (Krishna, 2023). The following section presents studies that analyze the reinforcement behavior according to cell shape.

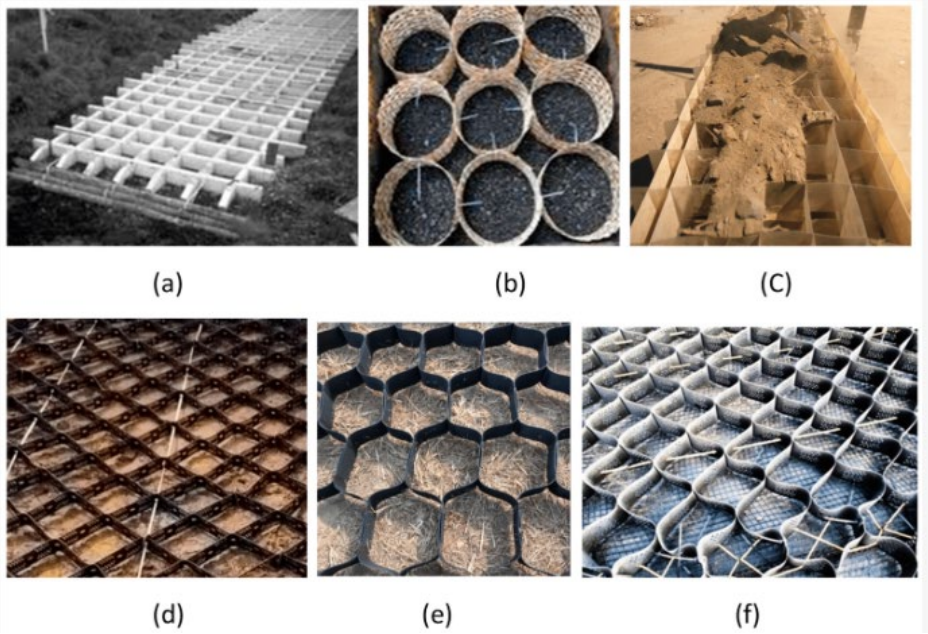

Figure 2.7 - Geometric Configurations of Commercial Geocells. (a) square, (b) circular, (c) deformed rectangular, (d) rhomboidal, (e) hexagonal, (f) diamond-shaped. (Krishna, 2023).

(Sherin (2017) evaluated the performance of three types of geocells with different geometric shapes: circular, square, and rhomboidal. The study results indicated that the circular and square shapes exhibited similar behavior in terms of improving the soil's bearing capacity. However, the rhomboidal shape, specifically the annular configuration, demonstrated a 28.5% improvement in bearing capacity compared to the other shapes due to its greater structural rigidity. In all analyzed cases, the use of geocells significantly enhanced the soil's bearing capacity, optimizing its load-bearing behavior and reducing settlements.

Pokharel et al. (2010) conducted a comparative study on circular and elliptical geocells to evaluate their performance in terms of structural rigidity and bearing capacity. The results demonstrated that circular geocells exhibited greater structural rigidity and improved bearing capacity compared to elliptical geocells. These findings suggest that cell geometry plays a fundamental role in the efficiency of lateral confinement and stress distribution within the reinforced system, which should be carefully considered in the design and application of geocells in geotechnical projects.

2.2.3. Soil Fill

The infill material in geocells plays a crucial role in enhancing the mechanical properties of the reinforced soil, as it directly influences bearing capacity, structural rigidity, and shear resistance of the system (Krishna, 2023). Studies have shown that coarse, well-graded granular soils generate greater friction at the soil-geocell interface, enhancing confinement efficiency and load distribution within the structure. Additionally, proper compaction of the infill material increases the soil's relative density, leading to higher deformation resistance and improved load-bearing capacity. However, the use of marginal soils as infill material has also proven effective in various applications, provided that certain criteria are met, such as low plasticity and good drainage. These properties enable the mobilization of the necessary rigidity and stability to enhance the performance of geocell reinforcement (Sireesh et al., 2009).

The study by Sireesh et al. (2009)analyzed the impact of infill material density on the performance of geocells for soil reinforcement. It was found that denser soils provide a greater improvement in bearing capacity compared to lower-density soils. It was observed that in dense soils, the three-dimensional structure of the geocell restricts volumetric dilation caused by foundation penetration, enhancing its efficiency in load distribution. Additionally, the confinement provided by geocells in dense soils allows for better stress distribution and increased rigidity of the reinforced system. As a result, the study concluded that the use of dense infill materials is optimal for improving the stability and performance of geocells, recommending proper compaction to maximize their benefits.

The study conducted by (Pokharel et al. (2010) demonstrates that the infill material plays a crucial role, as its performance and quality directly influence bearing capacity and the efficiency of geocell reinforcement. The study focused on granular materials without fines, which exhibited lower cohesion and greater sensitivity to moisture, reducing effectiveness compared to materials with a certain fine content and higher cohesion. In particular, the material with fines exhibited better resistance under unsaturated conditions, providing greater stability to the reinforced system. However, it was found that the cohesion in the base material can minimize the benefit of lateral confinement generated by the geocell under static loads. In addition, the density and compaction of the backfill material significantly affected the stress transmission and the bearing capacity of the system. It is concluded that the proper selection of the backfill material should consider its cohesion, drainage capacity and response to moisture variations to optimize the performance of the geocell reinforcement.

Another study conducted by Zhao (2023) focused on the influence of different infill materials on the behavior of geocell reinforcement in cohesive soils, demonstrated that the selection of infill material plays a crucial role in bearing capacity and settlement reduction in geocell-reinforced cohesive soils. It was found that geocell performance should not be analyzed in isolation, but should be considered in conjunction with the mechanical properties of the backfill material. Soils with low cohesion and reduced modulus showed less improvement in bearing capacity, while materials with higher modulus and lower cohesion showed a positive impact on reinforcement efficiency. Numerical studies indicated that a cohesionless soil with a modulus of 20 MPa and a friction angle of 40° is the most suitable option for improving geocell performance. In addition, it was observed that increasing the cohesion of the foundation soil contributes to improve the bearing capacity, but may reduce the effectiveness of the lateral confinement of the geocell, suggesting that the backfill material should be carefully selected to optimize the structural performance of the system.

The efficiency of geocells with different infill materials depends not only on the type of material but also on factors such as granulometry, compaction, and moisture content. The following section details how each of these variables influences geocell efficiency.

Granulometry: The particle size distribution of the infill material plays a fundamental role in the efficiency of geocell reinforcement, as it influences compaction, internal friction, and load distribution within the reinforced system. Dash et al. (2003) demonstrated that well-graded soils significantly enhance bearing capacity by promoting greater particle interaction and improving confinement within the geocell structure. In their experimental study, the use of poorly graded sand (SP) showed that, although geocells enhance soil stability, confinement efficiency could have been greater with a more uniformly graded material. Additionally, they emphasized that the presence of fine particles could reduce reinforcement strength due to lower compactability and increased susceptibility to deformation. On the other hand, the three-dimensional numerical study conducted by Hegde & Sitharam, (2015) supported these findings by modeling the behavior of geocell-reinforced soils under different granulometric conditions. Their results indicated that well-graded materials generate greater internal friction, optimizing interaction with the geocell walls and improving stress distribution within the system. Additionally, they found that materials with a high fine particle content tend to reduce confinement efficiency, leading to more pronounced settlements and lower rigidity in the reinforced soil structure. Therefore, both studies conclude that the selection of infill material should prioritize well-graded granulometry with high shear strength while avoiding soils with excessive fines to maximize stability and bearing capacity in geocell reinforcement.

Compaction: Hegde & Sitharam (2015) reported that proper compaction of the infill material is essential to maximize efficiency, especially in granular materials, where compaction at 95% or more of the maximum Proctor density significantly increases shear strength and reduces maintenance costs. In cohesive soils, inadequate compaction can drastically reduce efficiency by increasing plastic deformation and the risk of failure.

Moisture Content: The moisture content significantly influences the efficiency of geocell reinforcement. Tafreshi & Dawson (2010) analyzed how moisture content affects the bearing capacity and stability of geocells, concluding that an optimal moisture level is essential to maximize their structural performance. Under high moisture conditions, the shear strength of the fill material decreases, reducing the effectiveness of the confinement provided by the cells and resulting in greater deformations in the reinforced structure. On the other hand, when the moisture content is too low, the fill material may not achieve its

maximum density during compaction, limiting its load-bearing capacity and reducing the reinforcement efficiency. The results indicated that the optimal performance of geocells is achieved when the soil moisture is close to the optimal compaction moisture content, which maximizes the internal friction of the material and its interaction with the geocell wall (Tafreshi & Dawson, 2010).

2.3. USES OF GEOCELLS

Geocells have proven to be an innovative and versatile solution in civil engineering, providing significant improvements in soil stability. The following sections provide a comprehensive overview of their most common applications.

2.3.1. Soil Stabilization and Reinforcement

Soil stabilization using geocells is a widely applied technique in geotechnical engineering to enhance the bearing capacity and shear strength of soils with low structural quality. Thanks to their honeycomb-like three-dimensional structure, geocells confine granular materials within their compartments, preventing lateral dispersion and increasing the stiffness of the soil-reinforcement system This confinement generates a slab effect, enabling the uniform distribution of loads and reducing differential settlements (Lei et al., 2024).

Various studies have demonstrated that the implementation of geocells on low-capacity soils significantly enhances their strength and load-bearing capacity, optimizing structural performance in roads, loading platforms and foundations (Biabani et al., 2016; Pokharela et al., 2018; Xlender et al., 2016). Additionally, their use in expansive and soft soils has proven to be an effective strategy for increasing long-term stability, minimizing maintenance, and reducing infrastructure-related costs.

Duddu et al. (2024) conducted a study focused on the stabilization of sandy soil using geocells and geogrids. Figure 2.8 illustrates the materials and locations used in the study. The results showed that both types of geosynthetics significantly improved the soil's deformation modulus. This study evaluated the performance of stabilized soils by

comparing various reinforcement configurations using geocells and biaxial and triaxial geogrids. The results indicated that the application of these materials increased the Modulus Improvement Factor (MIF) within a range of 1.0 to 2.5, depending on the type, geometry, and location of the reinforcement. These findings confirm the effectiveness of cellular confinement and soil-geosynthetic interaction in improving the mechanical behavior of the subgrade, highlighting the role of geocells as an efficient solution for soil stabilization in road infrastructure.

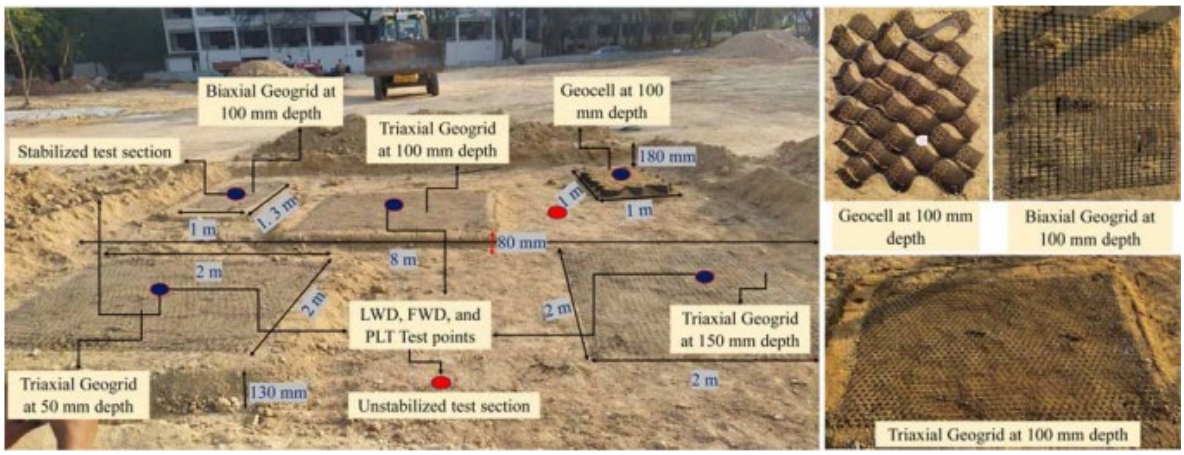

Figure 2.8 - Location of reinforcement points and geosynthetic materials in stabilized and non-stabilized soils in the study of Duddu et al. (2024).

A study was conducted using geocells made from PET bottles (Figure 2.9) to evaluate their performance in soil reinforcement and stabilization, specifically in fills with fly ash (FA) (Dandin et al., 2024). This approach investigated whether the use of complete PET bottles, as a substitute for high-density polyethylene (HDPE) geocells, could provide confinement and structural improvement in low-bearing-capacity soils. Full-scale tests demonstrated that the inclusion of PET bottles reduced the rate of settlement accumulation, promoting more resilient and elastic behavior compared to unreinforced soils (Dandin et al., 2024).

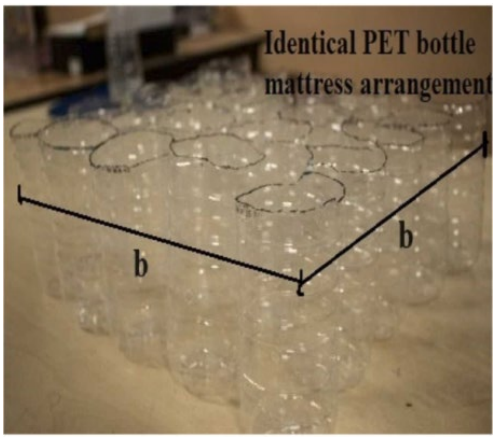

Figure 2.9 - Geocells Made from PET Bottles (Dandin et al., 2024).

In the study conducted by Parsa et al. (2024), the reinforcement mechanism and the stress-strain behavior of geocells made from non-woven geotextiles were evaluated. Three series of plate load tests were conducted on reinforced sand beds, featuring configurations that included single cells and cell groups arranged in predetermined patterns. The experiments analyzed the soil's bearing capacity, the vertical displacement of the surface, and the axial deformation of the cell walls, considering different cell sizes and quantities. The results indicated that cells with compartment sizes matching the diameter of the loading plate exhibited superior structural performance, optimizing load distribution and reducing settlements.

Other studies have shown that geocells also help mitigate instability caused by freeze-thaw cycles in pavements in cold regions. In this context, Huang et al. (2021) conducted eleven tests on geocell-reinforced and unreinforced sands, observing that after multiple freeze-thaw cycles, the geocells reduced frost heave and thaw settlement of the sand by 18% and 34%, respectively. Additionally, an increase in soil stiffness and bearing capacity by 40% and 253%, respectively, was observed, highlighting the effectiveness of geocells in enhancing the stability of pavement bases under extreme climatic conditions.

Yoon et al. (2008) studied geocells made from used tires (Figure 2.10) as reinforcement for sandy soil and observed a significant reduction in soil settlement, demonstrating superior performance compared to traditional geocells. This improvement was attributed to the greater stiffness of recycled tires as a reinforcement material. Plate load tests were conducted to evaluate key parameters, including the number of connection bolts, the

relative density of the sand, the embedment depth, and the number of reinforcement layers. The results show that tire-based geocells provide substantial improvements in the mechanical behavior of the soil, particularly at low densities, positioning them as a sustainable and effective alternative to commercial geocells.

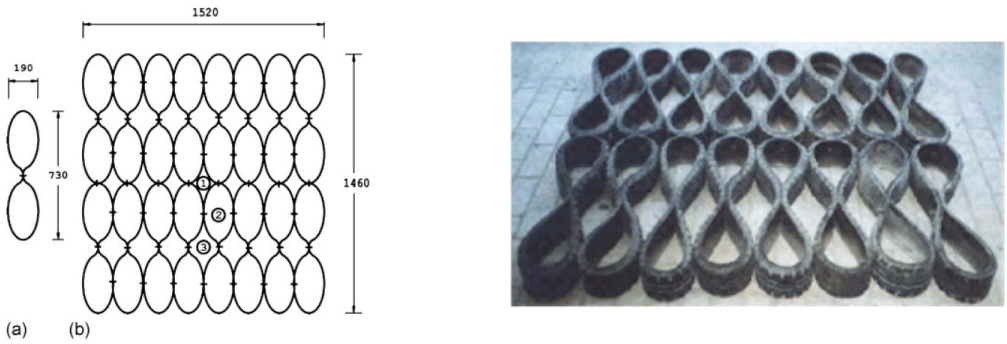

Figure 2.10 - Three-dimensional mesh used by Yoon et al., (2008).

Badiger et al., (2024) investigated the use of geocells made from recycled tire strips as reinforcement for pavement base materials. The results showed that pavement sections reinforced with geocells, both commercial and those made from recycled tires, experienced a significant reduction in permanent deformation compared to unreinforced sections. This decrease in deformation is attributed to the confinement and membrane effects provided by the cellular reinforcement, which enhance load distribution and increase pavement resistance to repetitive loads, thereby contributing to greater infrastructure durability.

In addition to the aforementioned studies, Sreevalsa et al. (2019) conducted research on geocells made from coconut fibers (Figure 2.11), comparing them with high-density polyethylene (HDPE) geocells. The results showed that the greater flexibility and energy absorption capacity of the natural fiber allowed for a more efficient load distribution, improving the stability of the reinforced soil. Furthermore, it was observed that the brittleness of HDPE leads to a sudden increase in settlements when certain load thresholds are exceeded, whereas coconut fiber geocells exhibit a more gradual and stable behavior. These findings highlight the potential of natural fiber geocells as a sustainable and high-performance alternative for soil stabilization in road infrastructure and geotechnical engineering projects.

Figure 2.11 - Coir geocells (Sreevalsa, 2019).

These findings demonstrate that geocells can be manufactured using alternative materials, offering an effective solution for soil confinement. In addition to being a viable alternative to traditional geocells, this innovation represents a sustainable method for soil stabilization, with applications in road infrastructure, foundations, and structural fills. Their implementation not only enhances the mechanical performance of the soil but also contributes to reducing plastic waste, promoting more eco-friendly and efficient solutions in geotechnical engineering.

2.3.2. Slope Stability and Erosion Control

Geocells have proven to be an effective solution for slope stability by providing a dual function of structural reinforcement and erosion control. Their use in the soil's surface layer reduces material loss and enhances soil cohesion while creating a favorable environment for vegetation establishment. This combination of mechanical reinforcement and biological stabilization strengthens the slope against the actions of water and wind, preventing particle detachment and minimizing erosive effects. However, during the initial construction stages, when the root system has not yet developed sufficient strength, the slope remains vulnerable to damage from rain or runoff. In this context, geocells act as a cellular confinement system that protects the soil until the vegetation matures. Furthermore, their interaction with the root system forms a continuous lateral linkage that reinforces the slope's integrity over the long term, consolidating stability and reducing the

need for frequent maintenance (Markiewicz, 2024). Figure 2.12 presents a general schematic view of erosion control using geocells.

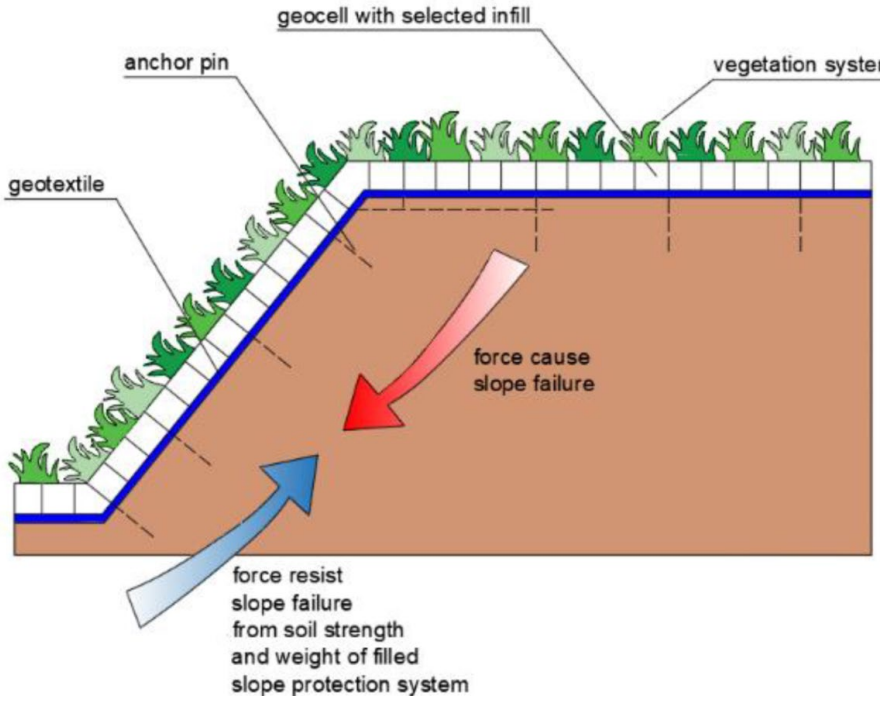

Figure 2.12 - General scheme of erosion control with geocells (Markiewicz, 2024).

Geocells have proven to be an effective solution for enhancing the stability of slopes and road embankments, with a notable positive impact on shear strength under various failure conditions. Recent research has delved into their influence, considering factors such as geocell arrangement, the angle between the reinforced layer and the shear plane, and the aspect ratio of the cellular structure. Through numerical simulations using FLAC3D (Figure 2.13) and large-scale direct shear tests, it has been demonstrated that geocell-reinforced layers exhibit significant anisotropy, indicating that their mechanical behavior varies depending on the orientation of the failure plane(Y. Zhao et al., 2024). Furthermore, it has been verified that increasing the aspect ratio or height of the geocell enhances its confinement capacity, resulting in a 156% increase in apparent cohesion and a 13% increase in the friction angle. These findings reinforce the effectiveness of geocells in slope stabilization, highlighting their role in reducing erosion and preventing landslides, making them a sustainable and efficient alternative in geotechnical engineering (Zhao et al., 2024).

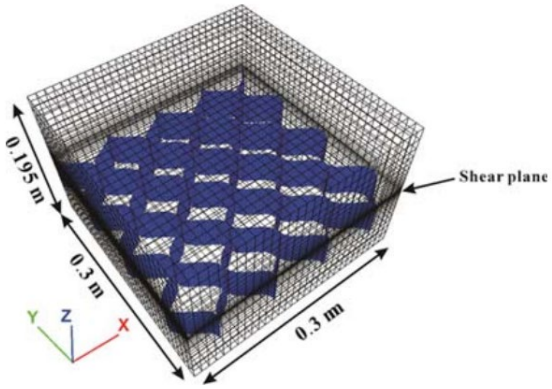

Figure 2.13 - Isometric View of the Model Simulating DST-B (Direct Shear Test) (Y. Zhao et al., 2024).

Hidalgo et al. (2020) investigated the use of geocells made from recycled tires through pullout tests and numerical modeling, concluding that this technology represents a sustainable alternative for the large-scale reuse of discarded tires. The results indicated that the system's performance depends significantly on the level of compaction and the quality of the infill material, as optimal compaction and suitable material enhance structural strength, tire-soil interaction and overall stability. These findings underscore the potential of recycled tires as a viable geotechnical resource, promoting environmental sustainability by reducing waste and providing efficient and reliable solutions for the construction of resilient infrastructure. Figure 2.14 illustrates a retaining wall constructed using geocells made from recycled tires.

Figure 2.14 - Retaining wall prototype (Hidalgo, 2020).

2.3.3. Foundation Reinforcement

Geocells have emerged as an innovative and efficient solution for reinforcing shallow foundations, offering significant improvements in load-bearing capacity and settlement reduction in low-strength soils. Three key factors influence their performance: the properties of the geocell material, the cellular geometry, and the relative density of the underlying soil. Research has shown that higher compaction levels in the infill material and the subgrade soil enhance the structural strength of the system, promoting better load distribution.(Hegde & Sitharam, 2015).

Geocells have proven to be an effective solution for slope foundation stabilization, optimizing the bearing capacity and structural behavior of footings in reinforced soils. Recent studies have evaluated the performance of reinforced concrete (RC) footings on slopes stabilized with geocells compared to unreinforced soils. The results of large-scale tests indicate that the inclusion of geocells not only improves the load distribution, but also increases the bearing capacity by more than 300%, mitigating differential settlement and increasing the efficiency of the foundation system. Likewise, it has been identified that the distance between footings and their proximity to the edge of the slope influence their structural performance, highlighting the importance of optimal spacing in the design of slope foundations. These findings reinforce the role of geocells in geotechnical engineering as an effective technique for slope stability and improvement of structural support in sloping soils (Fazeli Dehkordi et al., 2023).

2.4. UNPAVED ROADS

Rural roads are essential for the communities that rely on them daily, as they facilitate the transportation of goods and access to basic services such as healthcare and education. Consequently, they play a crucial role in the economic development of rural regions (Kebede, 2024) by fostering market opportunities for these populations (Gebresilasse, 2023). However, the understanding of their structural behavior and socioeconomic implications remains limited. Given that a significant proportion of the global population resides in rural areas, rural road improvement projects have a profound impact on these

communities; yet, the precise magnitude of this impact is not well understood (Chen et al., 2023).

The deterioration of rural roads increases mobilization and vehicle operation costs, complicating the transportation of people and goods. This situation limits access to economic opportunities and essential services, disproportionately affecting communities farthest from urban centers and contributing to heightened poverty in these regions (Mbabazi, 2019).

For this reason, it is essential to develop alternatives that incorporate pavement engineering design to extend their service life and reduce maintenance intervals. These roads often exhibit fragility due to their nature, as they are typically constructed with earth or locally sourced materials, often without surface coating or structural design of the roadway body (CODASP, 1988).

According to Guitierrez, (2015), for unpaved roads to be considered suitable for service, they must meet the following criteria:

- Good load-bearing capacity;
- Adequate rolling and adhesion conditions;
- Safety and comfort;
- Effective drainage.

Unpaved roads can exhibit a range of defects that negatively affect their performance (CODASP, 1988):

- **Excessive Dust:** This phenomenon occurs when a vehicle travels on the road and raises a significant amount of soil particles, typically during periods of severe drought (See Figure 2.15).

Figure 2.15 - Excessive dust on unpaved roads (Retrieved from https://jethrojeff.com/)**.**

Undulations: These are irregularities on the road surface in the form of material accumulations perpendicular to the traffic direction, spaced no more than 50 cm apart (Figure 2.16).

Figure 2.16 - Ondulations on unpaved roads (Ibagón et al., 2025).

- **Rutting:** These are marks on the road surface in the direction of vehicular traffic. They are generated due to the low bearing capacity of the soil and the repeated application of vehicle loads, leading to soil compaction and permanent deformations (See Figure 2.17).

Figure 2.17 - Rutting on unpaved roads (Retrieved from https://www.roadex.org/e-learning/lessons/permanent-deformation/permanent-deformation-rutting-classification/).

- **Potholes:** These are tray-shaped depressions on the road, caused by traffic and poor drainage. This defect is highly degenerative, with its deterioration accelerating due to rain and increased moisture on the road (See Figure 2.18).

Figure 2.18 - Potholes on unpaved roads.

Pokharel et al. (2011) demonstrated that using geocells in tertiary roads significantly enhances the load-bearing capacity and structural stability of the road surface, reducing differential settlements and improving load distribution. The study evaluated the performance of unpaved road sections reinforced with geocells under repetitive loading

conditions, observing a reduction in permanent deformation and increased resistance to surface erosion. Additionally, the results indicated that incorporating geocells optimizes the lateral confinement of granular materials, contributing to greater stiffness in the soil-reinforcement system and extending the road's service life. Complementary studies have validated these findings, highlighting that geocell reinforcement is an effective and sustainable strategy for improving rural road navigability, particularly in regions with low-load-bearing soils or adverse climatic conditions.

Another study conducted with geocells made from polymer alloy (NPA) for unpaved roads was carried out by Pokharel et al. (2011). This research analyzed four experimental sections, as shown in Figure 2.19, two of which were unreinforced, allowing a comparison of lateral deformation. The results demonstrated that the use of NPA geocells significantly improved the stability of unpaved roads, reducing permanent deformation and increasing the soil's load-bearing capacity. The study observed that the sections reinforced with geocells exhibited less rut formation and better stress distribution under repeated loading compared to unreinforced sections. Additionally, monitoring through strain gauges revealed that the geocells beneath the wheel path experienced tensile stresses, while areas outside this path were subjected to compressive stresses. These findings highlight the effectiveness of NPA geocells in enhancing the structural strength of unpaved roads, extending their service life, and reducing maintenance costs, particularly in regions with unfavorable soil conditions and repetitive traffic loads.

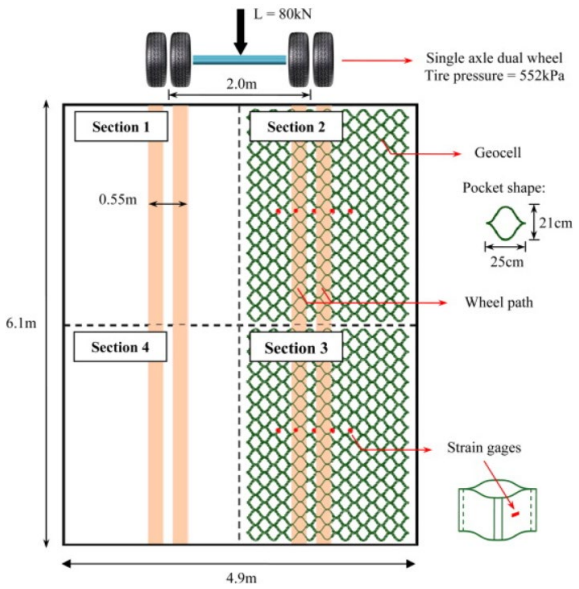

Figure 2.19 - Test setup Configuration Pokharel et al., (2011).

2.5. Theoretical Models of Bearing Capacity in Geocell-Reinforced Soils

In the analysis of soils and pavements reinforced with geocells, several theoretical calculation methods have been proposed to explain and quantify the structural improvement mechanisms associated with cellular confinement. These approaches have evolved from early adaptations of classical bearing capacity models to more recent formulations that incorporate stiffness factors and cyclic loading behavior.

2.5.1. Method proposed by Koerner

In 1994, Koerner introduced an approach for analyzing soils reinforced with geocells. This approach is based on adapting the plastic limit equilibrium mechanism, which is traditionally used to calculate the bearing capacity of shallow foundations under static loads. This approach builds on the classical models of Terzaghi (1943), Terzaghi and Peck (1967), and Vesic (1972), which describe how failure surfaces develop in unreinforced soils.

However, when a geocell layer is introduced, the situation changes. According to Koerner, the walls of the cells act as barriers that interrupt the conventional failure surface. This generates additional lateral confinement, producing frictional stresses between the infill material and the geocell walls. These stresses make the granular mixture stiffer and reduce its tendency to move. This decreases the stresses transmitted to the underlying layers. Figure 2.20 illustrates the reinforcement system.

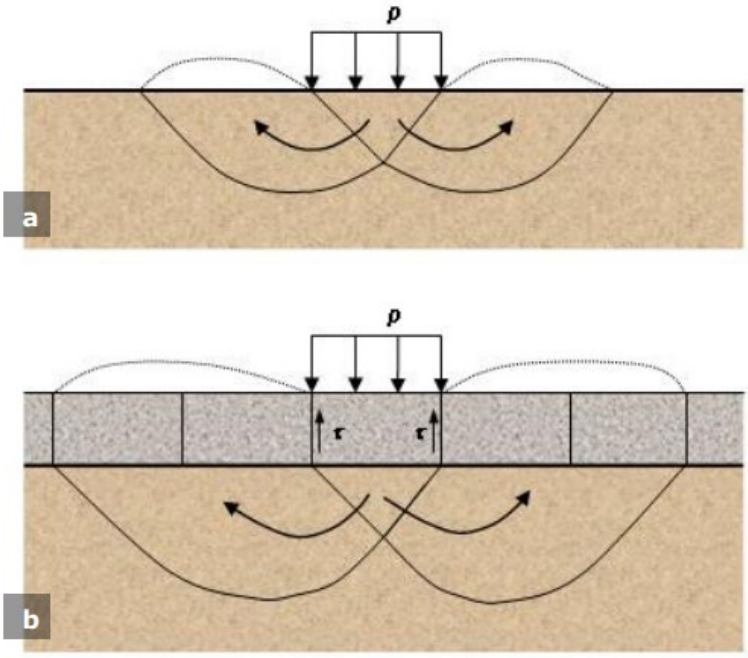

Figure 2.20. Failure mechanisms by bearing capacity of a soil: a) without the geocell confinement system; b) with the geocell confinement system(Koerner, 1994).

The model states that failure within an individual cell occurs only when the applied vertical stress exceeds a certain threshold. (p) exceeds the shear resistance at the interface between the soil and the cell wall (τ). Once this condition is reached, the infill material moves downward, transferring the load to deeper strata. However, this transfer does not occur directly since the reinforcement dissipates some of the stress. This results in a significant improvement in the system's bearing capacity (Koerner, 1994).

The equation that defines the ultimate bearing capacity of soil reinforced with geocells is expressed as the sum of two components: the additional contribution generated by the shear resistance at the soil–cell wall interface (2τ), and the conventional bearing capacity of the unreinforced soil (pu). The latter term, pu, corresponds to the classical bearing capacity expression derived from the works of Terzaghi and Vesic, in which soil cohesion (c), the acting surcharge (q), the unit weight of the soil (γ), and the footing width (B) are involved, adjusted by the bearing capacity factors (Nc, Nq, Nγ) and the shape factors of the footing (Sc, Sq, Sγ). Consequently, the equation reflects how the presence of geocells not only confines the granular material but also introduces an additional shear resistance mechanism that increases the overall bearing capacity of the system compared to an unreinforced soil.

$$p_r = \underbrace{2\tau + cN_cS_c + qN_qS_q + \tfrac{1}{2}\gamma BN_\gamma S_\gamma}_{p_u} \quad (2.1)$$

where:

p_r = bearing capacity of the reinforced soil;

p_u = bearing capacity of the unreinforced soil;

c = cohesion of the foundation soil;

q = surcharge acting on the foundation – considered as the geocell itself plus any possible surface loads;

γ = unit weight of the foundation soil;

B = width of the footing;

Nc,Nq,Nγ = bearing capacity factors;

Sc,Sq,Sγ = shape factors of the footing;

τ = interface shear resistance between the geocell walls and the infill material.

2.5.2. Method proposed by Avesani Neto (2013)

Avesani Neto, Bueno, and Futai (2013) developed a theoretical method that proposes an analytical approach to estimating the bearing capacity of soils reinforced with geocells. This approach integrates the effects of confinement and stress redistribution, which are characteristic of this type of three-dimensional reinforcement. Unlike other approaches based on empirical factors or analogies with two-dimensional geotextiles, Avesani's model is based on a physical representation of cellular behavior. It takes into account interactions between the infill material, geocell walls, and subgrade.

The model assumes that the reinforced bearing capacity (*pr*) is the sum of the unreinforced bearing capacity (*pu*) and the improvement induced by the reinforcement (*I*), expressed as follows:

$$\boldsymbol{pr = pu + I} \quad (2.2)$$

Where *pu* is calculated using the classical Terzaghi (1943) equations, incorporating the bearing capacity factors Nc, Nγ, and Nq according to the system geometry and soil type. The term I represents the increment produced by the geocell and depends on its geometry (height h, cell size d), the properties of the infill material (unit weight and friction angle φ), and the applied loading conditions.

According to Avesani *et al.*, the structural improvement of the reinforced system is governed by two main mechanisms.

The lateral confinement effect.
Geocells induce an increase in horizontal stresses within the infill, which restricts lateral expansion and generates additional passive pressure against the cell walls. This interaction enhances the shear resistance of the soil according to the following relationship:

$$\tau = k0\ p tan\delta \tag{2.3}$$

Where k_0 is the coefficient of lateral earth pressure at rest, p is the applied pressure, and φ is the interface friction angle between the soil and the geocell wall (usually approximated as 2/3 φ).

Stress redistribution effect:
The three-dimensional confinement provided by the geocell redistributes the applied stresses over a larger area, reducing localized deformations and improving the load-spreading capacity of the reinforced layer.

This improvement is derived from the lateral confinement and stress redistribution mechanisms generated within the cellular structure, which enhance the shear resistance and load-spreading capacity of the reinforced layer. The resulting relationship is expressed as:

$$p_r = p_u + 4\frac{h}{d}k_0 p \tan\delta(1-e) \tag{2.4}$$

where the second term represents the increase in bearing capacity attributed to the three-dimensional confinement provided by the geocell.

The model was validated through static load tests and comparisons with experimental data from various sources, which showed a strong correlation between the predicted and measured values.

CHAPTER 3

3. METHODOLOGY

This research was based on an experimental approach developed in the laboratory of the University of Ibagué, located in the city of Ibagué, Tolima Department, Colombia, aimed at evaluating the mechanical performance of geocells manufactured from recycled tires for the reinforcement of unpaved roads. Controlled tests were conducted on full-scale physical models, employing various configurations of geocell height and placement within the soil layer. The results were also compared with those obtained using commercial geocells to identify differences in surface deformation and pressure distribution on the subgrade.

A controlled loading system was employed to simulate real traffic conditions in a reproducible manner. Pressure sensors and deformation measuring devices were used to monitor the response of the materials under repeated loads. The collected data were processed and analyzed to assess the effectiveness of recycled geocells in comparison with commercial alternatives.

The experimental design of this research seeks to provide evidence on the feasibility of using recycled materials in road infrastructure, promoting sustainable solutions in civil engineering. The results obtained provide a foundation for analyzing the behavior of tire-derived geocells and their potential application in enhancing the structural performance of unpaved roads.

3.1. DESIGN OF GEOCELLS MANUFACTURED WITH USED TIRES

The design of the geocells was based on optimizing the use of recycled tires, minimizing transformation processes to reduce the carbon footprint and facilitate large-scale production. Tires ranging from rim size 13 to rim size 20 were selected to ensure dimensional homogeneity in the height and width of the figure-eight-shaped structures, maintaining a tolerance of ±3 mm. This standardization improved the geometric uniformity and optimized the confinement capacity of the granular material.

The design consisted of removing the lateral sidewalls of the tire, leaving only the tread to serve as the functional element. Subsequently, the two ends of each tread segment were joined using pneumatic metal staples, forming a figure-eight configuration, as shown in Figure 3.1.

Figure 3.1- Design of the Process for Manufacturing Geocells with Used Tires.

Geocells function through lateral confinement and internal friction, two essential mechanisms for enhancing the stability of granular materials. Lateral confinement restricts the horizontal movement of the infill material, thereby increasing its load-bearing capacity, while the friction between the geocell walls and the confined material improves resistance to shear stress. Recycled tires are well-suited for this system due to their high mechanical strength, flexibility, and surface texture, which promote interaction with aggregates and maximize material confinement within the structural mesh. Figure 3.2. shows a magnified view of the inner surface of the tire, whose rough texture contributes to increasing friction and mechanical interaction between the geocell and the surrounding soil, resulting in enhanced lateral confinement and, consequently, improved structural performance of the reinforced system.

Figure 3.2 - Expanded form of the tread patterns on tires.

For the design of the manufacturing process, a comparative analysis of different types of tires and fastening methods was conducted to ensure the structural homogeneity of the

reinforcement mesh. Plastic ties were initially evaluated, followed by metallic wire ties, and finally, the use of pneumatic staples, which allowed the tire to be perforated and the modules to be joined in two steps more efficiently.

Plastic ties were discarded due to their low mechanical strength and high susceptibility to fractures during the transport and handling of the meshes. Similarly, the use of metallic wire was ruled out, as it required perforating the rubber to thread and secure the wire—a labor-intensive and less efficient process compared to metallic staples.

The cell height is a fundamental parameter in the design of geocells, as it directly influences the confinement capacity of the granular material and the structural performance of the system, as detailed in the literature review. For this design, two ranges of recycled tires were selected: the first includes tires from rim size 13 to rim size 16, and the second, tires from rim size 17 to rim size 20. As a result of the previous analysis, two differentiated cell heights were established: between 11 cm and 16 cm for the first group, and between 17 cm and 23 cm for the second. These variations in height (h), length (L), and length and width of the pocket (c) (See Figure 3.3) generate modules with differentiated dimensions within the confinement mesh, enabling the analysis of their structural performance as a function of their geometric properties.

Table 3.1 presents the specific dimensions of the "8" configuration modules for both tire groups, which will be designated as G-15 and G-20, corresponding to the smallest and largest tires, respectively With the physical properties of the "8" modules clearly defined, the assembly process for 1 m² of geocells was initiated. During this process, the number of required modules was verified, determining that approximately 16 tires per m² are needed for G-15 geocells, while 8 are required for G-20 geocells.

The consumption of recycled tires was determined based on the number of modules needed to create each type of geocell and the total area covered. According to Table 3.1, the G-15 geocell uses 16 recycled tires per square meter of manufactured surface, with an average height of 15 cm. The G-20 geocell, with a height of 20 cm, requires eight tires per square meter because its modules are larger and cover a greater area. These values establish the quantity of recycled material used to construct the geocells and serve as a basis for quantifying the total volume of tires repurposed during fabrication.

Figure 3.3 - Physical properties of the modules of 8.

Table 3.1 - Physical properties of the geocells G-15 and G-20.

Property	G-15 (cm)	G-20 (cm)
Height (h)	11-16	16-23
Length (L)	62	73
Pocket Length (B)	36	43
Pocket Width (C)	22	25
Number of Modules per 1 m²	16	8

This design of the geocells optimized the use of recycled tires, ensuring an efficient confinement system with minimal material transformation. The "8" configuration and the standardization of heights facilitated structurally stable assembly. With these parameters defined, the manufacturing process was initiated, ensuring the correct formation of the reinforcement mesh.

3.2. MANUFACTURING OF GEOCELLS WITH USED TIRES

The manufacturing process was structured into four fundamental stages: material transport and storage, component cutting, modular unit assembly, and the formation of the three-dimensional mesh.

Material Storage:

The material was stored under controlled conditions in a covered area to prevent water accumulation inside the tires and reduce the risk of disease vector proliferation. Periodic inspection protocols were established to ensure the proper disposal of the recycled

material and minimize any premature deterioration due to exposure to environmental agents.

Component Cutting:

During the preparation and cutting phase, the lateral sides of the tires were removed using a high-precision industrial scalpel. This method was chosen due to its ability to create clean and uniform cuts, ensuring that the tread retained its original structure without significant material loss.

Modular Unit Assembly:

The modules were joined by fixing the two ends of each tread segment to form a figure-eight structure. To ensure a strong and durable connection, a fastening system using metal staples applied with high-pressure pneumatic machines was employed. This method optimized the structural strength of each module without compromising its flexibility.

Formation of the Three-Dimensional Mesh:

Finally, the figure-eight structures were interconnected following a regular pattern to ensure the stability of the cellular matrix. The arrangement of the connection points was designed to optimize the lateral confinement of the granular material and improve load distribution within the structure. Quality control measures were implemented to verify the geometry of the mesh, the strength of the connections, and the uniformity of the final structure before its field implementation.

Figure 3.4 illustrates the manufacturing process of the geocells made from recycled tires, as previously detailed in this section. It shows the key stages of the procedure, from material preparation to final assembly, ensuring the correct formation of the structural mesh.

(a)

(b)

(c)

(d)

(e)

(f)

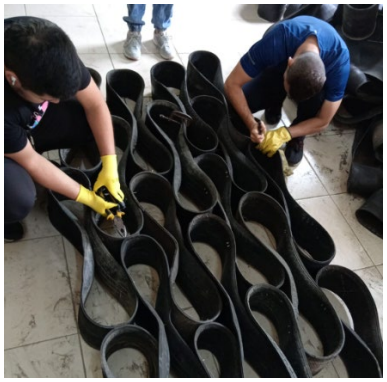

(g)

(h)

Figure 3.4 - Manufacturing process of the three-dimensional mesh with used tires: (a) Transportation (b) Storage (c) Cutting of sidewalls (d) Flipping (f) Assembly of modules (g) Staple fixing (h) Finished cell.

The fabrication of geocells from recycled tires has been explored by various researchers interested in sustainable alternatives for soil reinforcement like Badiger et al., (2024), Hidalgo, (2018) and Yoon et al., (2008)). Notably, the research conducted by Hidalgo (2018) led to the development of patent NC2019/0018673. This patent provides a detailed description of the manufacturing process, including the cutting, layout, and assembly of tire segments to form modular geocell-type reinforcement units.

3.3. PHYSICAL PROPERTIES OF COMMERCIAL GEOCELLS

The geocells used in this study are made of virgin high-density polyethylene (HDPE), a thermoplastic material that offers high tensile strength, durability, and stability under cyclic loading and environmental exposure. They were selected as a reference for comparing performance with geocells fabricated from recycled tires in the experimental program.

Table 3.2 presents the physical properties of the commercial geocells, according to the manufacturer's specifications and the corresponding ASTM standards.

Table 3.2 - Properties of the commercial geocells.

PROPERTIES	COMMERCIAL GEOCELL
Material	Virgin HDPE
Density	0.945 – 0.960
Thickness (textured)	1.50 (±10%)
Rib spacing	445
Open cell dimensions (±3%)	315 × 304
Cell height (±3%)	150
Expanded section dimensions (±3%)	5.04 × 9.12
Expanded section area (±3%)	45.96

These properties ensure adequate confinement of the granular material and uniform stress distribution within the pavement structure. This configuration is considered representative of road reinforcement and provides a basis for comparison with geocells made from alternative materials.

3.3. SOIL MATERIALS USED

This section describes the materials used in the formation of the unpaved road structure within the full-scale testing chamber. It details the characteristics of the subgrade soil, which serves as the main support layer, and the structural materials used in the base layer. For the structural layer, two types of materials were employed:

1. **Gravel**: A granular material typical of the region, widely used in unpaved roads due to its availability and acceptable mechanical behavior under moderate traffic conditions.
2. **Selected Material**: A processed granular base with enhanced mechanical properties, chosen for its higher load-bearing capacity and better structural performance under repetitive loading conditions.

Both materials were characterized to assess their suitability within the road structure and their interaction with the geocell system made from recycled tires. Below, further information is provided on each of the materials used.

3.3.1. Subgrade material

The subgrade material used was extracted from the University of Ibagué and classified according to the SUCS system as a silty sand (SM). The characterization tests conducted are presented in Table 3.3.

Table 3.3 - Properties of the material used as subgrade.

Property	Result
Classification according to SUCS(INVIAS, 2013a)	SM
Liquid Limit (LL) (%)(INV E 125-13, 2013)	36.9
Plastic Limit (PL) (%)(INV E 126-13, 2013)	26.2
Plasticity Index (PI) (%)(INV E 126-13, 2013)	10.7
Specific Gravity (INV E 128-13, 2013)	2.66
CBR (%)(INV E 148-13, 2013)	2
Dry Density (g/cm³)(INV E 142-13, 2013)	1.5

Figure 3.5 shows the result of the modified Proctor test, where an optimal moisture content of 25% and a maximum dry density of 1.50 g/cm³ were obtained. Figure 3.6 presents the particle size distribution curve of the subgrade material.

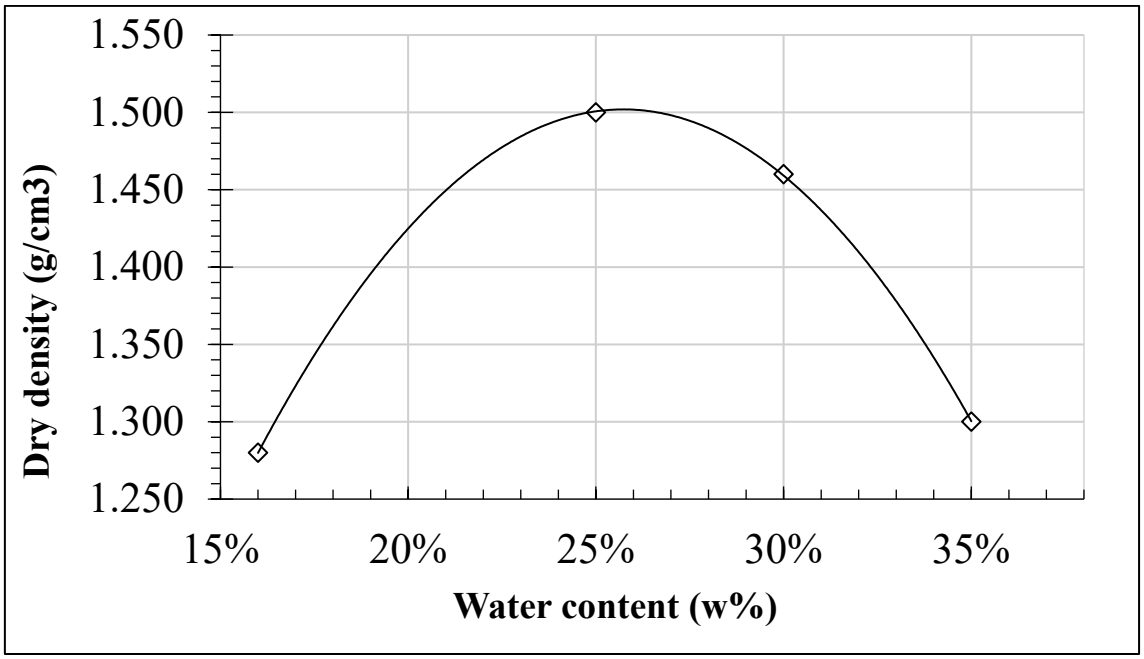

Figure 3.5 - Subgrade material compaction curve.

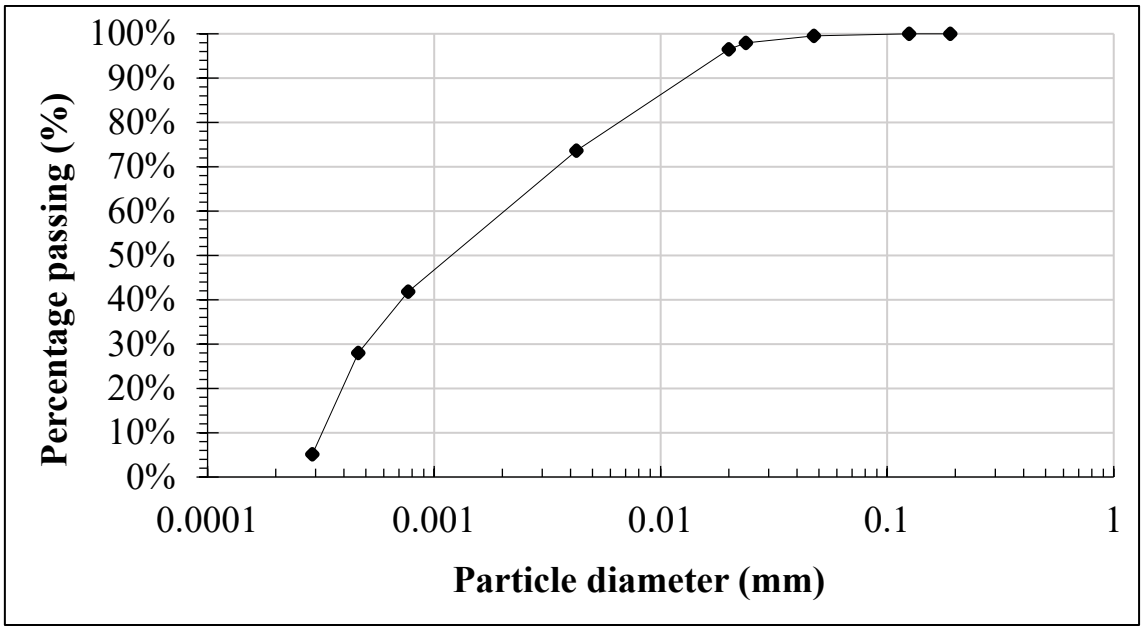

Figure 3.6 -Grain size distribution curve of the subgrade material.

Once the geocells were fabricated, it was necessary to select the appropriate materials for their application in the structural layer of the unpaved road. The characterization of these

materials allows for the evaluation of their interaction with the reinforcement system and their ability to improve the pavement's performance.

3.3.2. Structural materials

The structural layer of the unpaved road plays a fundamental role in load distribution and system stability. Two types of materials were used for its formation: gravel, a typical granular material of the region, and base material, selected for its better mechanical properties and higher load-bearing capacity.

This section presents the characteristics and properties of each of these materials, including their particle size distribution, density, moisture content, mechanical strength, and behavior under load, with the aim of evaluating their performance within the road structure and their interaction with the recycled tire geocell system.

Selected Base Material

The base material used in the structural layer of the unpaved road was classified according to the USCS (Unified Soil Classification System) as GM-GW, indicating a well-graded gravel and sand mixture with fine silty particles. This type of material is suitable for use in support layers due to its stability and high drainage capacity.

The physical and mechanical properties of the base material were determined through laboratory testing. Table 3.4 and Figure 3.7 show the results of the tests conducted.

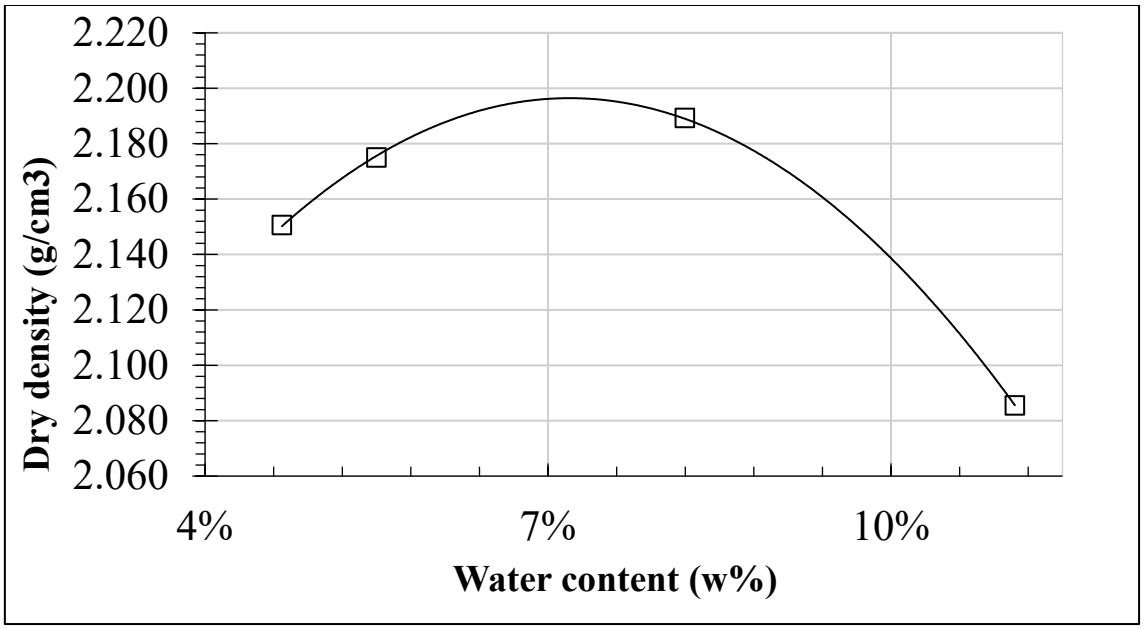

Figure 3.7 - Compaction curve of the base material.

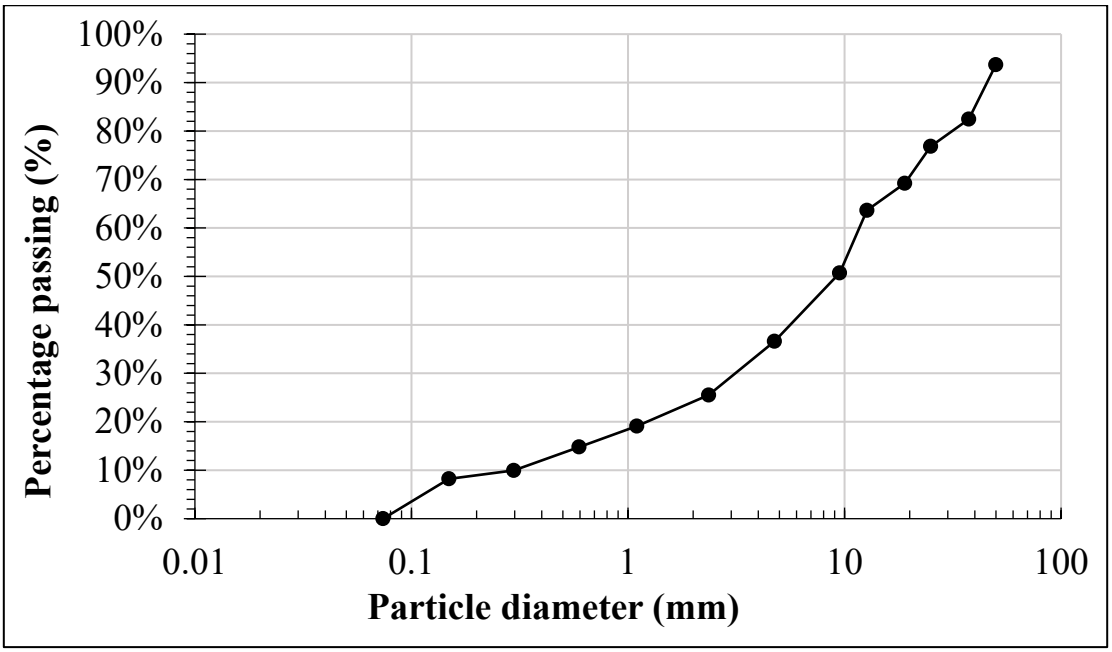

Figure 3.8 - Grain size distribution curve of the base material.

Table 3.4 - Properties of the selected base type material.

Property	Result
Classification according to SUCS(INVIAS, 2013)	GM-GW
Dry Density (g/cm³)	2.19
CBR (%)	111.54
Percentage of Clay Lumps (%)	0.21
Los Angeles Abrasion (%)	35

Typical Regional Material: Gravel

Gravel is a granular material widely used in unpaved roads due to its availability and suitable mechanical characteristics for support layers in regions with moderate traffic. In this research, a material classified according to the USCS (Unified Soil Classification System) as SW (Well-Graded Sand) was used, indicating that it has a uniform particle distribution with no significant amount of cohesive fines.

The physical and mechanical properties of the gravel (regionally known as “Recebo”) were determined through laboratory testing. The results obtained are shown in Figure 3.9, Figure 3.10 and Table 3.5. According to the SUCS classification, the material is a well-graded sand (SW) with a moderate amount of clay lumps present. With a CBR value of 30% and a Los Angeles abrasion index of 85%, it is clear that the material has limited bearing capacity and durability, which is lower than what is required for a conventional granular base.

Therefore, Recebo is not suitable for direct use as a base layer. However, it can be used as a subbase material or reinforced when combined with confinement systems, such as geocells. These systems enhance the material's mechanical performance and reduce degradation by abrasion. In the context of unpaved roads, this material is a valuable, low-cost, locally available alternative, particularly in sustainable projects that aim to optimize the use of regional resources and reduce the extraction of quarry aggregates.

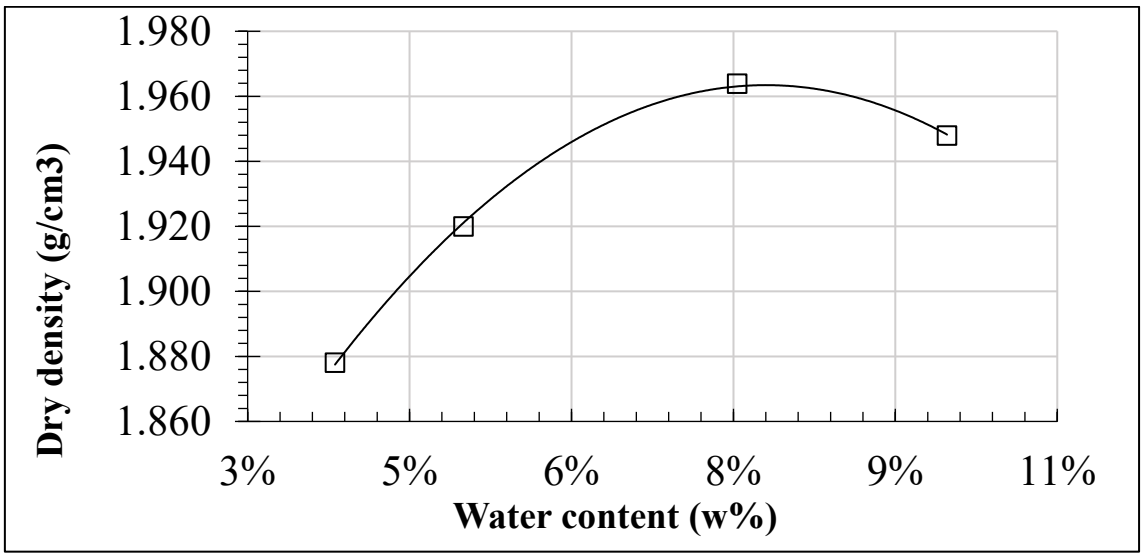

Figure 3.9 - Compaction curve for *Recebo* type material.

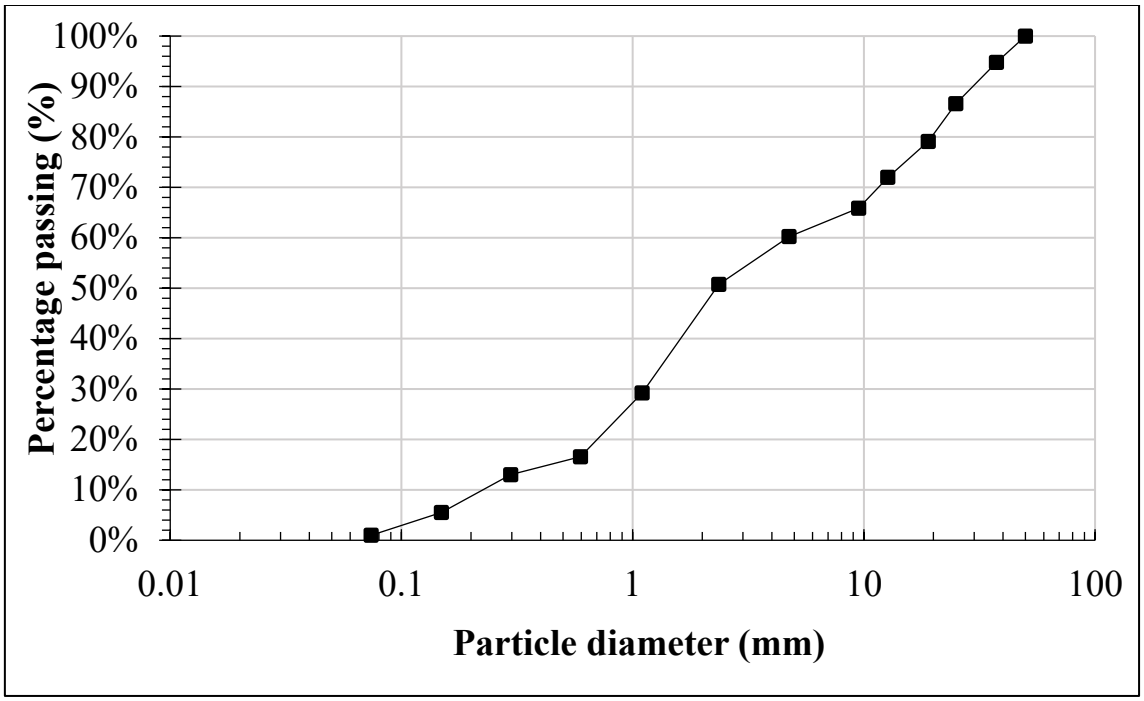

Figure 3.10 - Granulometric curve of the *Recebo* type material.

Table 3.5 - *Recebo* type material properties.

Property	Result
Classification according to SUCS	SW
Dry Density (g/cm³)	2.19
CBR (%)	30
Percentage of Clay Lumps (%)	29
Los Angeles Abrasion (%)	85

3.4. CYCLIC LOADING EQUIPMENT AND INSTRUMENTATION

This section provides a detailed description of the equipment used in the cyclic load tests to evaluate the performance of geocells made from recycled tires in unpaved roads. It includes specifications about the testing chamber, the loading system, the instrumentation used, and the data acquisition system, all fundamental elements to ensure the accuracy and reproducibility of the results. Figure 3.11 shows the main components and the equipment used.

Figure 3.11 - Cyclic loading equipment used.

3.4.1. Test chamber

The main equipment used in the research is a cyclic load chamber designed to simulate traffic conditions on unpaved road structures. This chamber has a cylindrical shape with an internal diameter of 1.2 meters and a height of 1 meter, dimensions sufficient to allow for the evaluation of the mechanical behavior of the structural layers of an unpaved road with and without recycled tire geocells.

The testing chamber is constructed from structural steel, with reinforcements at the base and lateral walls to prevent deformation during load application. Additionally, it is equipped with three access doors, which allow for the insertion and removal of materials in controlled layers, facilitating the assembly and disassembly of the testing system.
The selection of a 1.2 m diameter for the testing chamber is justified based on the size of the loading plate (18 cm in diameter) and the need to minimize edge effects in the stress distribution within the tested materials.

In load tests on soils and granular materials, it is essential that the dimensions of the chamber are sufficiently large to ensure that the effects of lateral confinement do not significantly affect the results. Technical literature (Biabani et al., 2016; Guitierrez, 2015) recommends that the chamber diameter be at least 5 to 10 times the diameter of the loading plate to avoid interference from the walls in the distribution of stresses and to ensure that the material's behavior under load is representative of field conditions. In the

present research, the diameter of the chamber (1.2 m) is approximately 6.67 times the diameter of the load plate (18 cm), which meets this criterion and allows the applied load to be distributed within the material without artificial lateral restrictions. Additionally, this size is adequate to accommodate different geocell reinforcement configurations without altering the confinement conditions and affecting the results.

The selection of this type of equipment responds to the need for controlled testing under repeated loading conditions that allows for the evaluation of the influence of recycled tire reinforcement on the stability and load-bearing capacity of unpaved roads.

3.4.2. Load Application System

The cyclic load system used in the research was designed to simulate real traffic conditions on an unpaved road. The pressure transmitted to the ground by a typical vehicle tire is approximately 600 kPa, so this value was taken as the reference for the tests.

The load applied in the test was 1.56 tons, transmitted through a circular plate with a diameter of 18 cm. Based on these parameters, the actual pressure exerted on the surface was calculated, resulting in a value of 600 kPa, ensuring that the test conditions are representative of the real behavior of an unpaved road subjected to vehicle traffic.

Additionally, the load was applied with a frequency of 1 Hz, which corresponds to the frequency used in resilient modulus tests, allowing for the evaluation of the material's mechanical behavior under repeated loading conditions. This procedure ensures that the results obtained are comparable to previous studies and can be applied in the characterization of the structural performance of the road reinforced with recycled tire geocells.

To define the test stopping criterion, two conditions were established: (1) to reach an accumulated vertical deformation equal to or greater than 3 inches (76.2 mm), or (2) to complete a total of 100,000 repeated loading cycles, whichever occurred first. The selection of these limits is based on both technical and practical criteria. First, a deformation equal to or greater than 3 inches is considered indicative of functional failure

of the structure, as it compromises the trafficability and integrity of the unpaved road system. Second, the threshold of 100,000 cycles is adopted as a reasonable representation of the accumulated traffic expected on rural roads with low traffic volume, as is typical in many areas of the country. This number of cycles simulates the loading conditions that such a road might experience over an approximate period of one year of operation, considering the repeated passage of light and occasionally heavy vehicles. Thus, these criteria ensure that the tests capture both the initial behavior and the long-term evolution of the different structural configurations, without unnecessarily prolonging the test once critical performance conditions are reached.

The load application was carried out using a hydraulic system shown in Figure 3.12, which operates through the movement of a piston driven by oil pressure. This system consists of a hydraulic oil reservoir, a pressure pump, a solenoid control valve, a hydraulic cylinder, and a set of high-pressure hoses that allow fluid flow. The hydraulic pump draws oil from the reservoir, generating the pressure required to move the piston. Through an inlet hose, the oil is directed to the hydraulic cylinder, where it pushes the piston down, applying the load to the test plate. During this process, the solenoid valve regulates the flow's entry and exit.

Once the load application is complete, the solenoid valve changes its configuration, allowing the oil to return to the reservoir through an outlet hose, which causes the piston to rise again, preparing it for the next loading cycle. This mechanism allows for the repetition of the test in a continuous cycle, precisely replicating the dynamic loading conditions to which unpaved roads are subjected under vehicular traffic.

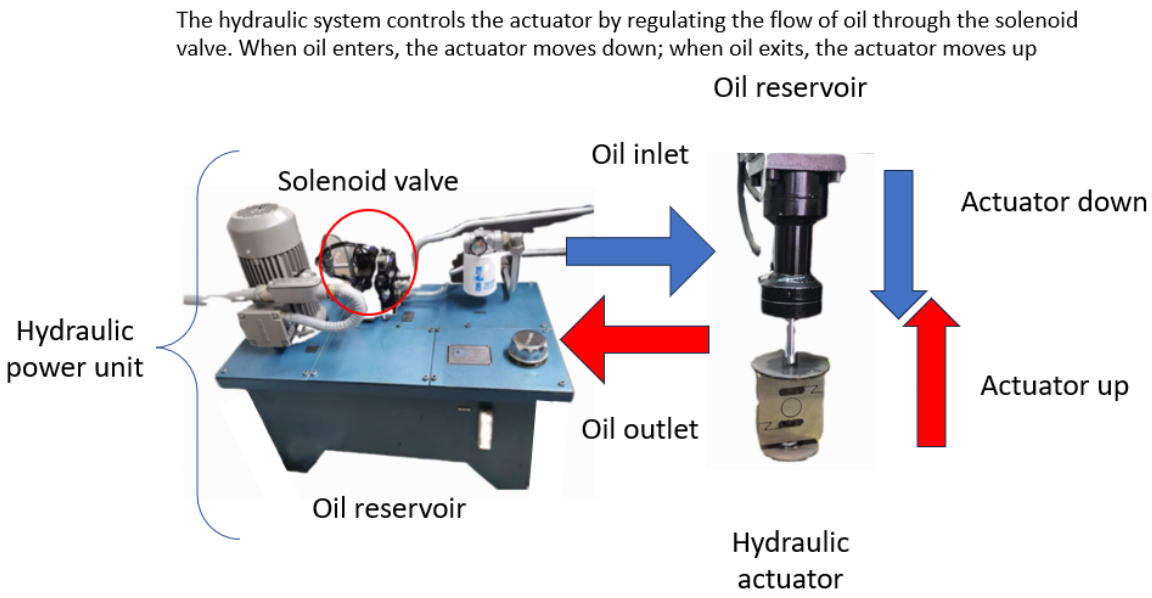

Figure 3.12 - Hydraulic system for load application.

The loading system is controlled using a software developed in LabVIEW, which sends commands to the solenoid valve to regulate the entry and exit of hydraulic oil based on the test parameters.

3.4.3. Instrumentation

To ensure the accuracy and reliability of the tests conducted in the testing chamber, an instrumentation system was implemented, consisting of various sensors and measurement devices. These elements allowed real-time recording of the mechanical responses of the system under cyclic loading, providing key information on material deformation, induced stresses, and the applied load.

The instrumentation system included displacement sensors, pressure sensors, a load cell, and data acquisition software. The integration of these devices into the experimental setup enabled the capture of high-resolution data and the subsequent evaluation of the mechanical behavior of the road reinforced with recycled tire geocells.

Displacement Sensors

For measuring displacements on the surface of the road, displacement sensors were used, which function as linear potentiometers that convert the movement of the cable into an electrical signal proportional to the displacement. These sensors have a maximum range of 15 cm and were strategically installed at key points on the surface of the road structure to record settlement and displacement caused by the applied load. Figure 3.13 shows the displacement sensors used.

The operating principle of the displacemente sensors is based on an internal spring mechanism that keeps the cable taut while measuring the position variation. As the surface of the road undergoes deformation, the sensor converts these changes into an output voltage, which is then recorded and processed by the data acquisition system. Their main advantage is the high precision and stability in displacement measurements, allowing continuous and uninterrupted recording of the changes in the evaluated structure.

The sensors were calibrated before installation through a procedure where known displacements and their corresponding voltage output values were recorded, generating a calibration curve that allowed correct interpretation of measurements during the tests. This process was crucial to ensure the reliability of the obtained data.

Figure 3.13 - Displacement sensor.

Load Sensor

The load cell used in this research is an "S" type sensor with a maximum capacity of 50 kN, employed to measure the load applied by the hydraulic actuator during the tests

(Figure 3.14). This device allows precise recording of the magnitude of the force transmitted to the test system, ensuring proper control of the cyclic loading application. The sensor works by converting mechanical force into a voltage signal, which is recorded by the data acquisition system. The calibration of the load cell was carried out by applying known loads in a controlled environment, generating a calibration curve that allows correlating the voltage signal with the actual applied load. During the tests, this information is crucial to verify that the load remains within the desired range and that the load-rest cycles comply with the conditions established in the methodology.

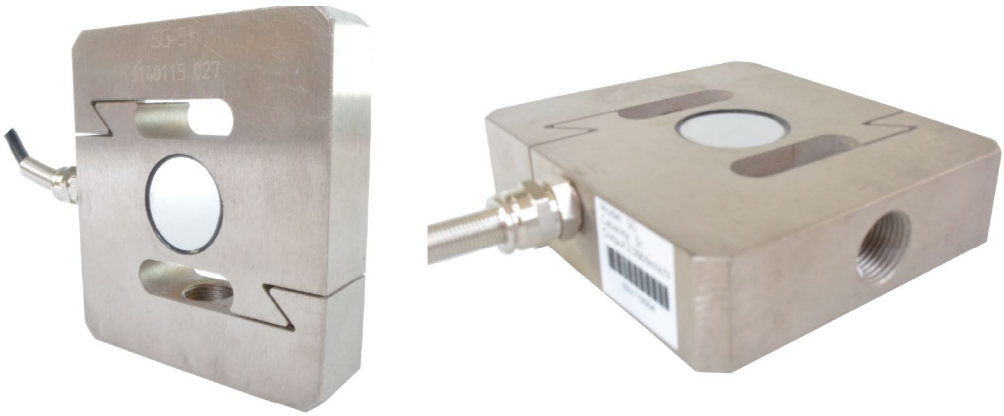

Figure 3.14 – "S" type load cell.

Pressure Sensor

To assess the distribution of stresses in the subgrade under cyclic loading, three electric total pressure cells were installed, which recorded the stresses generated by the application of load on the granular structure of the unpaved road. These sensors are essential for quantifying the magnitude of the stresses transmitted to the foundation soil and analyzing the effect of lateral confinement generated by the geocells on stress distribution.

The pressure cells used in this study are designed to measure total stresses within the soil. These cells consist of a stainless-steel body with a diameter of 6.5 cm, inside which four strain gauges are strategically placed to form a bridge (Figure 3.15), converting pressure variations into electrical signals proportional to the stress applied to the subgrade.
When cyclic loading is applied to the surface of the road, the granular material transmits the stresses to the subgrade, where the pressure cells detect the magnitude of the generated

stresses. These electrical signals are amplified and processed in the data acquisition system for further analysis.

Figure 3.15 - Total stress cells.

3.4.4. Data acquisition system

The data acquisition system developed in this research consists of several components that ensure the accurate and reliable capture of measurements during the tests. Each of these components serves a specific function in collecting, processing, and storing information, allowing for a detailed evaluation of the behavior of the soil reinforced with recycled tire geocells. Figure 16 shows the general structure of the system, where the sensors, data acquisition card, and real-time monitoring software are integrated, and the following explains each one.

1. Power Supply

The system is equipped with a regulated power supply, designed to provide the necessary energy to the sensors and the data acquisition card. The stability of the power supply is crucial to avoid fluctuations that could affect the accuracy of the measurements.

2. Signal Filtering and Amplification

The signals from the sensors may present interference or voltage levels that need adjustment before processing. Therefore, a filtering and amplification module is used to reduce electrical noise and optimize the signal for conversion in the data acquisition card.

3. Load Signal Conditioning

The load cell requires signal conditioning to ensure compatibility with the acquisition system. This module adjusts the signal's amplitude, ensuring accurate readings and preventing distortion in the measurement of the applied load.

4. Data Acquisition Card

For signal conversion and recording, a National Instruments data acquisition card is used, which allows for the simultaneous connection of multiple sensors. This device converts analog signals into digital data, facilitating processing and storage in the monitoring system.

Each of these stages contributes to the integrity of the data acquisition system, ensuring reliable and repeatable measurements that allow for the analysis of the performance of the soil reinforced with geocells under controlled conditions.

Figure 3.16 illustrates the configuration of the data acquisition system, emphasizing the primary components and their respective functions.

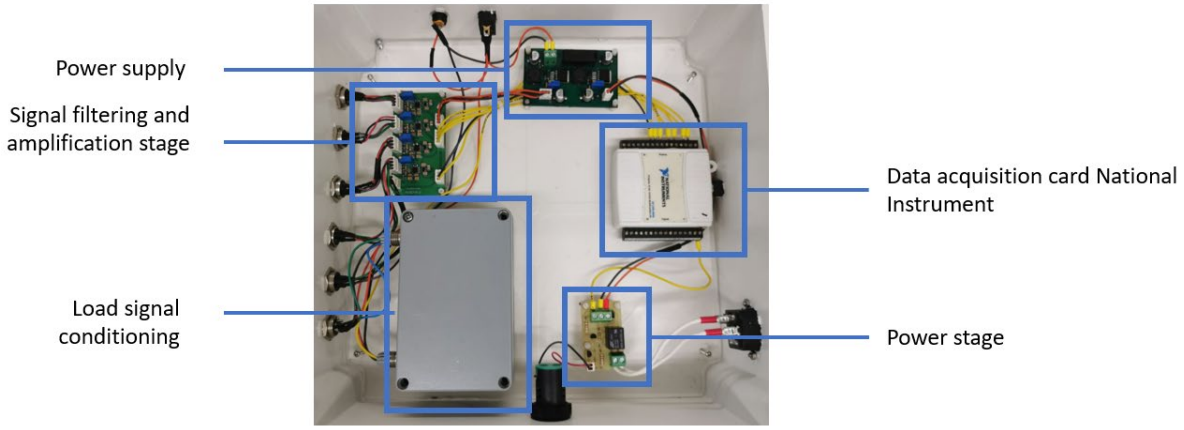

Figure 3.16 - Data acquisition system.

3.4.5. Data acquisition software

The monitoring and control of the tests were carried out using a software developed in LabVIEW, designed for real-time visualization of the measured parameters and the adjustment of experimental conditions. This software enabled the efficient integration of the sensors with the data acquisition system, ensuring continuous and accurate collection of relevant information for analyzing the structural performance of the soil reinforced with geocells made from recycled tires.

The control of the hydraulic actuator is managed directly from the software interface, allowing for the generation of signals that activate the solenoid valve responsible for regulating the oil flow in the hydraulic system. This enables precise adjustment of the cyclic load frequency, ensuring that the applied values remain within the time ranges established for the material evaluation.

Regarding data storage and export, the software allows for the automatic saving of records in formats compatible with numerical analysis tools. This facilitates the organization and structuring of data for subsequent processing, enabling the generation of reports and comparative graphs that contribute to the interpretation of the obtained results.

Before each test, a validation process of the data acquisition system was conducted to ensure the accuracy and reliability of the recorded measurements. This validation involved the application of known pressures, loads, and deformations, allowing for verification that the sensors, acquisition system, and software were functioning correctly. The software interface is simple and intuitive, as shown in Figure 3.17.

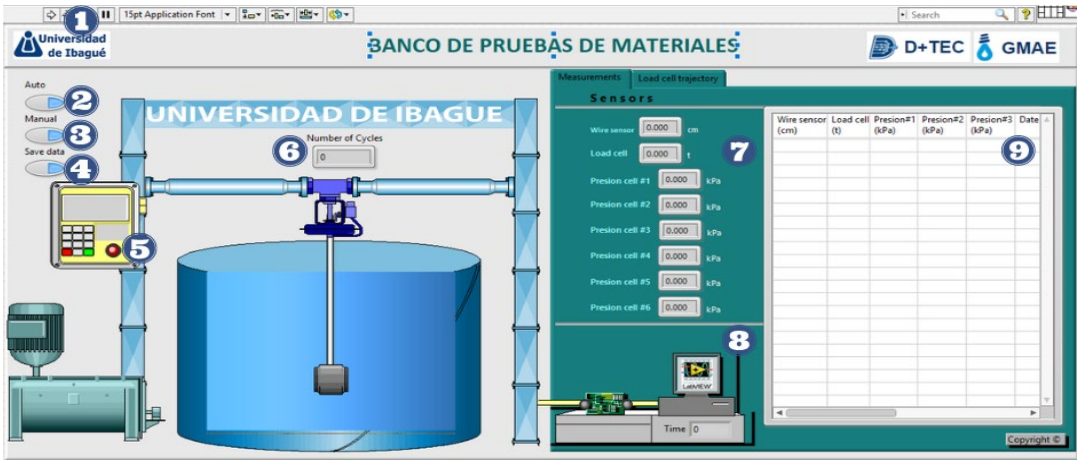

Figure 3.17 - Software interface.

3.4.6. Calibration procedure and sensor location

Calibration of the sensors used in the test is an essential procedure to ensure the accuracy of the measurements during the experiments. This process was conducted prior to each test to verify the precision of the measurements of applied load, displacements, and total stresses.

Calibration of the Pressure Cells

The pressure cells used in the research were subjected to a calibration process before their installation in the subgrade. Known stresses were applied to the surface of the cells, and their response in terms of output voltage was recorded. Based on these data, a calibration curve was established, allowing for a direct correlation between the obtained signal and the actual pressure applied.

The calibration protocol was carried out under controlled conditions and followed a specific sequence to minimize errors and ensure the repeatability of the results. Figure 3.18 shows the process carried out.

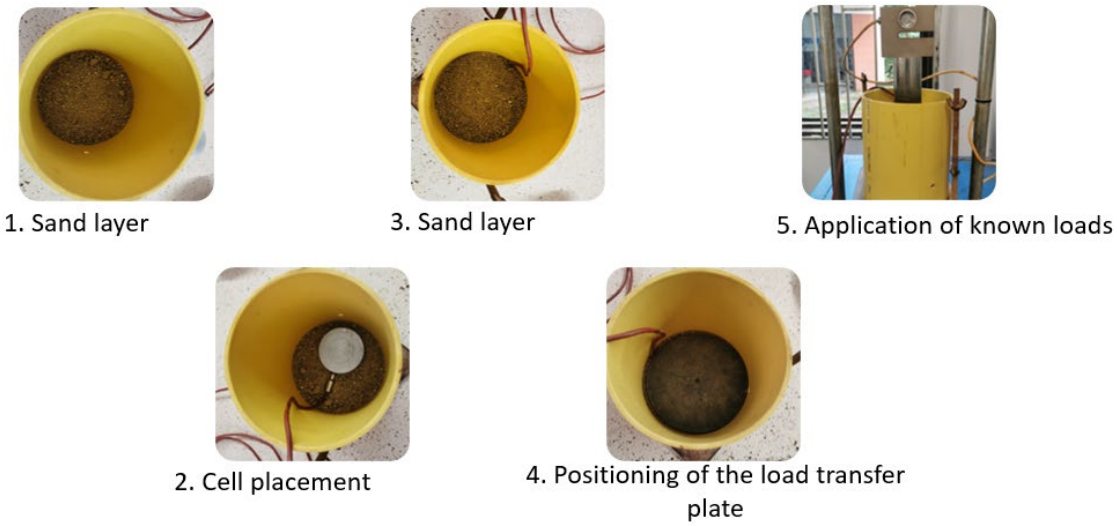

Figure 3.18 - Stress cell calibration protocol.

The calibration process involved the following steps:

1. **Preparation of the Calibration Base:**
   The process began with the preparation of a sand base, which served to provide uniform support for the pressure cell. A 5 cm thick layer of compacted sand was spread and leveled over the calibration surface. This layer ensured homogeneous contact between the cell and the loading system, avoiding irregularities that could affect the measurements.
2. **Positioning of the Pressure Cell:**
   Once the base was prepared, the pressure cell was carefully placed on the sand layer. Its alignment and leveling were verified to ensure that the applied stress would be uniformly distributed across its surface.
3. **Application of a Protective Layer:**
   To prevent displacement and improve sensor stability, an additional 3 cm layer of sand was placed over the cell. This layer provided uniform coverage and avoided external interference during load application. It is important to note that the sand used during calibration is the same as that used later during the test.
4. **Installation of the Load Transfer Plate:**
   A load transfer plate was placed on top of the sand layer to distribute the applied loads evenly during calibration. The plate was properly aligned to prevent stress concentrations that could distort the calibration results.

5. **Application of Known Forces and Data Recording:**
   Incremental forces were applied to the plate using a controlled loading system. For each load increment, the voltage output values generated by the pressure cell were recorded using the data acquisition system. This procedure allowed the establishment of a relationship between the applied pressure and the sensor output signal.
6. **Determination of the Calibration Curve:**
   The collected data were analyzed and graphically represented to determine the calibration curve of the pressure cell. From this curve, a fitting equation was derived to correlate the voltage values with the applied pressure. Finally, the calibration parameters were entered into the data acquisition software.

Load Cell Calibration

The load cell, responsible for measuring the force transmitted to the ground, was also calibrated through the application of controlled loads. A loading machine was used to apply different levels of force to the cell, recording the corresponding voltage output. The methodology was as follows:

1. Mounting in the hydraulic system: The load cell was secured to a rigid support structure.
2. Application of known forces: Loads ranging from minimum values to the maximum expected during the tests were applied.
3. Recording output voltages: These were compared with the expected theoretical values, adjusting the calibration curve according to the results obtained.
4. System validation: The tests were repeated to verify the reproducibility of the data.

Calibration of Displacement Sensors

The displacement sensors used to measure deformations on the surface of the structure were calibrated using controlled displacements. Adjustable supports were employed to move the sensors in known increments, recording the voltage output in response. The procedure included:

- Fixing the sensor to a rigid structure.
- Controlled displacement in 0.5 cm intervals.
- Recording output voltages and comparing them with actual displacements.

- Generating a calibration curve to adjust the measurements during the tests.

This calibration protocol was conducted prior to each test to ensure the reliability of the collected data and minimize measurement errors.

3.4.7. Sensor Location

Table 3.6 and Figure 3.19(a) present the distribution of the sensors used in the research, indicating their quantity, location, and the variable measured. The displacement sensors were installed on the surface of the test section, enabling the recording of settlements and deformations induced by the applied cyclic load. Their strategic location facilitated the capture of the surface displacements generated in the granular structure.

Table 3.6 - Location and number of sensors used in the test.

Sensor Type	Quantity	Location	Measured Variable
Displacement wire sensors	2	Surface of the roadway	Displacement
Total pressure cells	3	Within the subgrade	Total stresses
Load cell	1	In the line of action of the hydraulic actuator	Magnitude of the applied load

The total pressure cells were placed within the subgrade to measure the stresses transmitted to the foundation soil. These cells were positioned with a horizontal spacing of 47 cm and a vertical distance of 15 cm between each other, ensuring adequate coverage of the area affected by the applied load. Figure 3.19(b) illustrates the exact arrangement of these sensors within the testing system. Finally, the load cell was installed in the line of action of the hydraulic actuator to measure the magnitude of the force applied to the surface of the unpaved road.

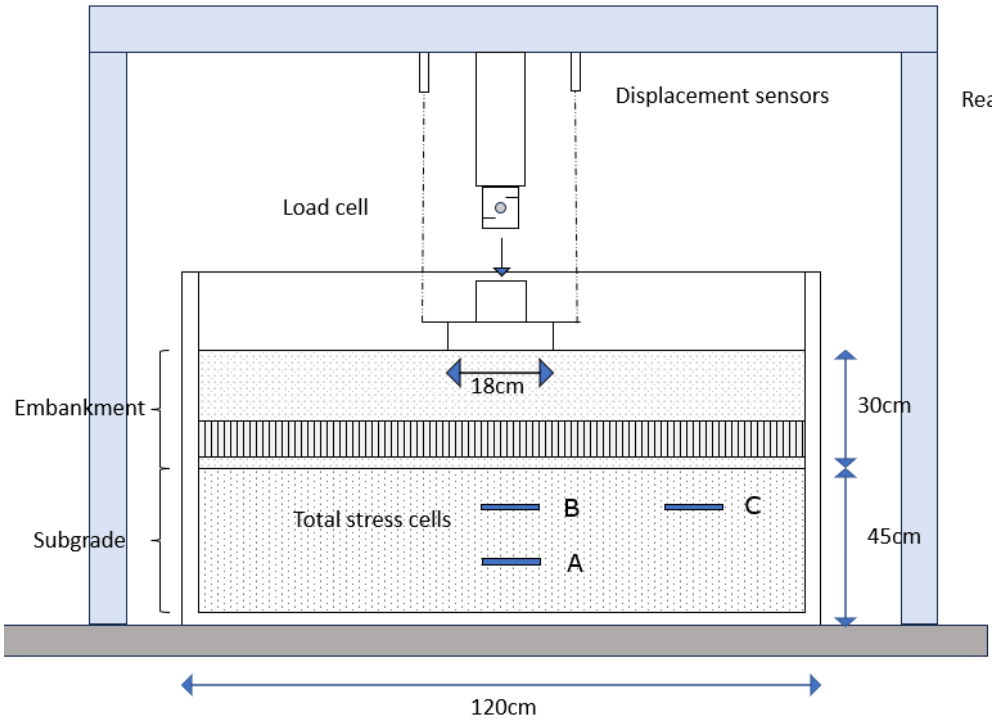

(a) Localization of sensor in the test.

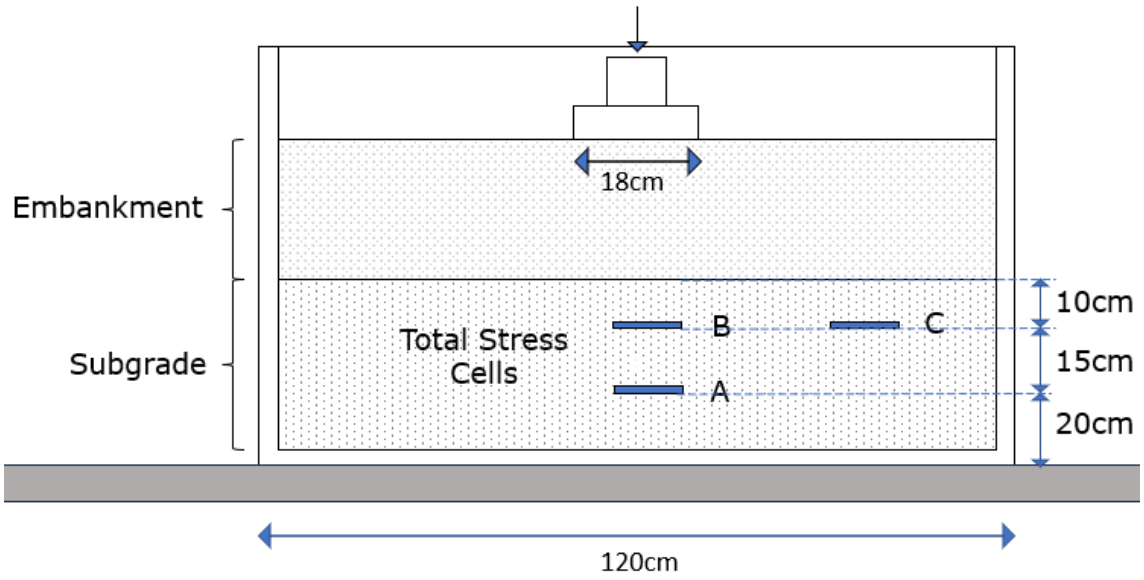

(b) Localization of cell in the test.

Figure 3.19 - Location of sensors in the tests.

3.4.8. Test set-up procedure

The setup of the test was carried out following a sequence of steps designed to ensure the proper installation of materials and sensors in the cyclic load chamber.

Step 1: Placement of the Subgrade

1. **Material Distribution**: The subgrade was placed in controlled layers inside the testing chamber.
2. **Compaction**: Each layer was uniformly compacted to reach the target density and moisture determined in previous laboratory tests. Manual tools and compaction equipment were used to ensure homogeneous preparation.
3. **Pressure Sensor Placement**: The installation of the total pressure cells followed a specific sequence to ensure accurate measurements. First, an excavation was made at the designated location within the subgrade. Then, a layer of sand was placed at the bottom of the hole to serve as a base and ensure uniform support. Next, the total pressure cell was carefully positioned and leveled on this sand layer. Once in position, another layer of sand was added to stabilize and protect the sensor before continuing with the placement of the remaining subgrade material.

   Figure 3.20 shows the location of the sensor within the test setup. The sand used is the same material previously employed during the calibration process, ensuring uniform contact conditions and consistent sensor response.

Figure 3.20 - Sequence of voltage cell installation.

Step 2: Installation of Geocell System

The installation of geocells made from recycled tires was carried out according to the specific location required for each test, either directly on the subgrade or within the structural layer of the embankment.

To ensure proper placement, the supporting surface was prepared as follows:

- For the subgrade configuration, the foundation soil was compacted to create a stable and level base.
- For the structural layer configuration, a layer of granular embankment material was placed and compacted up to the designated elevation where the geocell was to be installed.

Once the surface was prepared, the geocells were carefully deployed and positioned in the planned location. The cells were then filled and confined with the selected granular material (granular base or local *recebo*), ensuring full integration with the surrounding structure and avoiding discontinuities that could compromise the system's performance under cyclic loading.

Step 3: Placement of the Base Material

The base material layer was installed over the compacted surface following a controlled procedure to ensure structural stability and proper integration with the reinforcement system.

First, the distribution of the structural granular material was carried out using selected or base material, according to the experimental configuration established for each test. The material was spread evenly within the test chamber, avoiding segregation and ensuring homogeneous distribution.

Subsequently, the compaction was performed in successive layers, applying a standardized procedure to ensure compliance with the density and moisture parameters previously determined in the material characterization tests. Compaction was carried out using appropriate mechanical equipment to ensure uniform stress conditions and minimize the influence of irregularities on the mechanical response of the system. Quality

control was performed on each layer by measuring in-situ density to verify compliance with the established specifications.

Step 4: Installation of the Load Application System

The load plate assembly was carried out by positioning a circular plate with a diameter of 18 cm over the compacted base material surface. It was ensured that the contact surface between the plate and the granular material provided uniform support to avoid stress concentrations and guarantee the proper distribution of the applied load.

The load applied by the hydraulic actuator was verified to be 15.6 kN, ensuring that the pressure transmitted to the surface of the 18 cm diameter load plate was 600 kPa. Finally, the displacement sensors, specifically displacement transducers, were installed on top of the load plate.

The installation process of the reinforced sections is illustrated in Figure 3.21, which summarizes the main stages of construction: (a) laying and compacting the subgrade material, (b) placing the granular base layer, (c) positioning the geopneus in the designated location, (d) compacting the fill material within the geopneus to ensure proper confinement, and (e) placing the load transmission plate used for the cyclic loading tests.

(a)

(b)

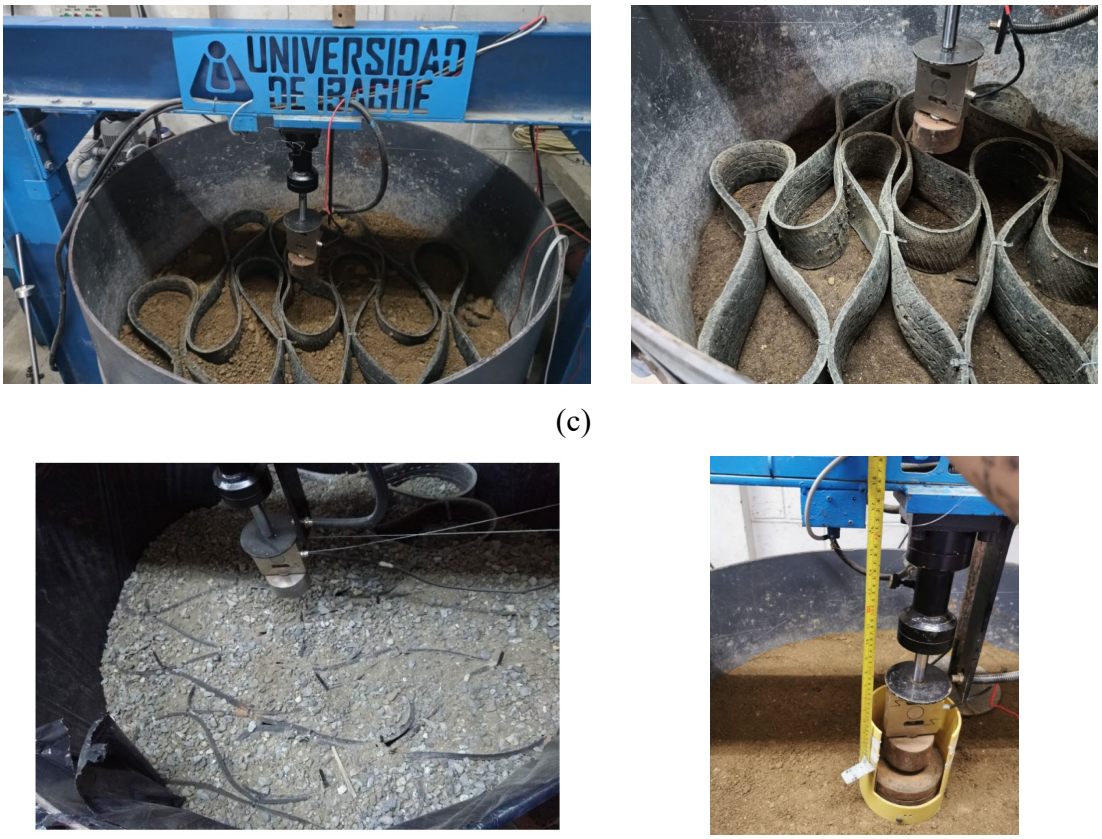

(c)

(d) (e)

Figure 3.21. Test assembly process. (a) subgrade preparation, (b) base layer placement, (c) geocell of tire positioning, (d) compaction inside geocell and (e) load transmission plate installation.

Step 5: Post-Maintenance Testing

Since the experimental methodology involved conducting tests on the same structure, a procedure for reconditioning the granular material was implemented to restore initial conditions after each test. After each test, the surface of the base material was inspected to identify accumulated deformations caused by the applied cyclic load. Based on the condition of the granular layer, material redistribution and leveling were carried out to ensure that the compaction remained within the pre-established values. The reconditioning process involved recompacting the granular material until its initial height was restored, allowing for the study of what occurs after road maintenance, as shown in Figure 3.22.

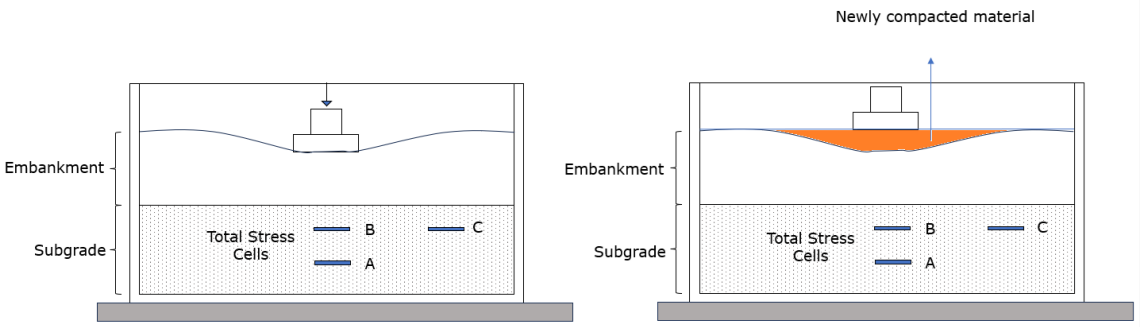

Figure 3.22. Road surface maintenance process. (a) Deformation observed in the tests after the initial construction stage (b) Start of the test after maintenance (with newly compacted material).

3.5. TESTS PERFORMED

To evaluate the structural performance of geocells made from recycled and commercial tires, a total of 26 tests were conducted under different structural configurations and initial conditions. These tests were designed to analyze the influence of the type of reinforcement, the location of the geocell within the structure, and the effect of surface maintenance on the road performance. The tests were classified according to the following criteria:

a) Type of Reinforcement

Three types of reinforcement were evaluated:

- **No reinforcement (test codes UR, URR):** These control tests represent a conventional road structure without any reinforcement.
- **Geocells made from recycled tires:** These tests aimed to study variations in height and locations within the structural material of the road.
- **Commercial geocells (test codes RCI, RCM):** Traditional confinement systems used as a reference.

b) Location of Reinforcement

The geocells were installed in **three distinct vertical positions** within the structural layer, as illustrated in Figure 3.23:

- **On top of the subgrade:** Geocell placed directly over subgrade (Figure 3.23a)
- **Mid-layer of the structural fill:** Geocell embedded at the mid-depth of the embankment (Figure 3.23b)
- **Near the road surface:** Geocell installed 5 cm below the surface (Figure 3.23c)

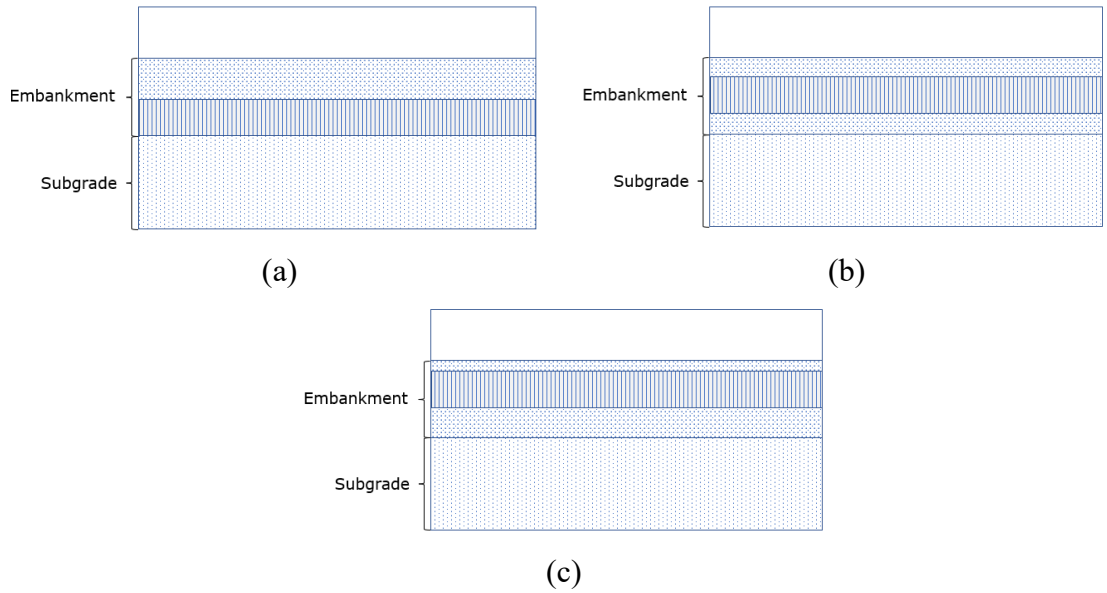

Figure 3.23. Reinforcement locations within the embankment: (a) on subgrade, (b) mid-layer, and (c) 5 cm below the road surface.

c) Test Scenario

Each test was carried out under two scenarios:

1. **Initial construction**: This condition represents the state immediately after initial construction.
2. **After of Maintenance:** This condition represents the state after filling the rut caused by the initial construction test. These tests are labeled with "-MNT" at the end of their codes.

d) Two types of granular materials were used to build the test sections:

1. **Base Material:** A high-quality granular base commonly used in road construction, selected for its superior mechanical properties and stability under traffic loads.
2. **Typical Local Material (*Recebo*):** A typical local soil material frequently used in rural road construction. This material was included to assess the geocells' reinforcement efficiency under conditions representative of low-cost, locally available resources.

For this study, an experimental plan was designed to realistically evaluate how different variables influence the performance of unpaved roads reinforced with geocells. Table 3.7

presents the complete test matrix, which includes all 26 experimental combinations. These tests involved two types of fill material (granular base and local recebo), different reinforcement configurations (unreinforced sections, 15 cm and 20 cm tire geocells, and commercial geocells), and multiple reinforcement positions within the structural layer (on top of the subgrade, in the middle of the layer, or 5 cm below the surface, as applicable in each case). Each combination was evaluated both in its initial construction state and after a maintenance stage. This experimental design enabled a practical and comprehensive analysis of the most relevant effects of each variable while reflecting real-world construction constraints that prevented the execution of every possible combination.

The experimental design was conceived to be as comprehensive and representative as possible. It aimed to capture the most relevant effects of each variable influencing the mechanical behavior of the reinforced layers. The selected combinations represented real field conditions while taking into account practical construction constraints that prevented executing all possible configurations. This approach ensured that the main influencing factors, such as geocell height, placement depth, and infill material type, were properly evaluated within the experimental framework.

Table 3.7. Experimental Matrix of Tests: Fill Material, Reinforcement Type, Location, and Condition.

	Fill Material	**Base Material**						**Typical Local Material (*Recebo*)**			
	Reinforcement location	Inferior		Middle		Upper		Inferior		Middle	
Type of Reinforcement	**Tire Geocell 15cm**	RGI15	RGI15-MNT	RGM15	RGM15-MNT	RGU15	RGU15-MNT	RRGI15	RRGI15-MNT	RRGM15	RRGM15-MNT
	Tire Geocell 20cm	RGI20	RGI20-MNT					RRGI20	RRGI20-MNT		
	Commercial Geocell	RCI	RCI-MNT	RCM	RCM-MNT			RRCI	RRCI-MNT	RRCM	RRCM-MNT
	Unreinforced	UR						URR			
		SUR-MNT						URR-MNT			

	Initial Condition
	After Maintenance

Table 3.8 and Table 3.9 show the name, description and configuration of each of the tests.

Table 3.8 - Tests carried out with base material.

Base material				
Test No.	Code	**Reinforcement**	**Configuration Scheme**	**Test Scenario**
1	UR	None	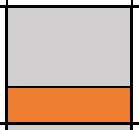	Initial construction stage
2	UR-MNT	None	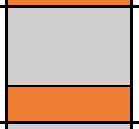	Maintenance stage
3	RGI15	Tire geocell, 15 cm high, placed on subgrade		Initial construction stage
4	RGI15-MNT	Tire geocell, 15 cm high, placed on subgrade	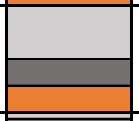	Maintenance stage
5	RGS15	Tire geocell, 15 cm high, installed 5 cm below the surface		Initial construction stage
6	RGS15-MNT	Tire geocell, 15 cm high, installed 5 cm below the surface		Maintenance stage
7	RGM15	Tire geocell, 15 cm high, installed mid-layer of embankment		Initial construction stage
8	RGM15-MNT	Tire geocell, 15 cm high, installed mid-layer of embankment		Maintenance stage
9	RGI20	Tire geocell, 20 cm high, placed on subgrade	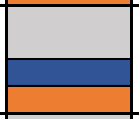	Initial construction stage
10	RGI20-MNT	Tire geocell, 20 cm high, placed on subgrade	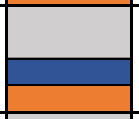	Maintenance stage
11	RCA	Commercial geocell, placed on subgrade		Initial construction stage
12	RCA-MNT	Commercial geocell, placed on subgrade		Maintenance stage
13	RCM	Commercial geocell, installed mid-layer of embankment	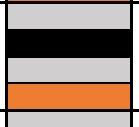	Initial construction stage
14	RCM-MNT	Commercial geocell, installed mid-layer of embankment		Maintenance stage

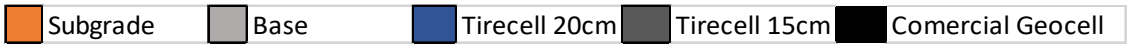

Table 3.9. Tests carried out with *recebo* material.

Typical Local Material (Recebo)				
Test No.	**Code**	**Reinforcement**	**Configuration Scheme**	**Test Scenario**
15	URR	None	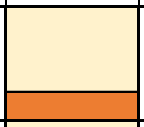	Initial construction stage
16	URR-MNT	None	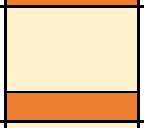	Maintenance stage
17	RRGI15	Tire geocell, 15 cm high, placed on subgrade		Initial construction stage
18	RRGI15-MNT	Tire geocell, 15 cm high, placed on subgrade	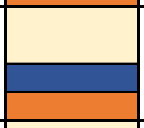	Maintenance stage
19	RRGM15	Tire geocell, 15 cm high, installed mid-layer of embankment		Initial construction stage
20	RRGM15-MNT	Tire geocell, 15 cm high, installed mid-layer of embankment		Maintenance stage
21	RRGI20	Tire geocell, 20 cm high, placed on subgrade		Initial construction stage
22	RRGI20-MNT	Tire geocell, 20 cm high, placed on subgrade		Maintenance stage
23	RRCI	Commercial geocell, placed on subgrade	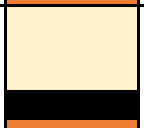	Initial construction stage
24	RRCI-MNT	Commercial geocell, placed on subgrade		Maintenance stage
25	RRCM	Commercial geocell, installed mid-layer of embankment		Initial construction stage
26	RRCM-MNT	Commercial geocell, installed mid-layer of embankment		Maintenance stage

3.6. FLEXIBILITY INDEX (FI)

This thesis introduces a Flexibility Index (FI) as a comparative tool to evaluate the efficiency of reinforcement systems used in the experimental sections during the early stages of loading. The purpose of this index is to quantify the ability of the unpaved road system to adapt to repeated loads through progressive deformations without compromising its structural integrity.

The calculation of FI is based on the accumulated deformation rate (v, expressed in mm/cycle) recorded during the initial loading cycles, specifically at cycle 3, identified as representative of the onset of the system's structural behavior. This choice is supported by previous studies (Pokharel et al., 2009; Thakur, 2016; Moghaddas Tafreshi & Dawson, 2012), which highlight the sensitivity of the firsts cycles in evaluating the initial mechanical response of the material and the reinforcement.

The Flexibility Index is formulated as follows:

$$FI = 1 - \frac{v_{\text{reinforced}}}{v_{\text{unreinforced}}} \tag{3.1}$$

where:

$vreinforced$: accumulated deformation rate measured at cycle 3 for the reinforced configuration (mm/cycle).
$vunreinforced$: accumulated deformation rate measured at cycle 3 for the unreinforced section (mm/cycle).

An FI value of 0 indicates that the reinforcement had no effect (the deformation rate is equal to that of the unreinforced system), whereas values approaching 1 represent a greater reduction in the initial deformation, reflecting a more effective reinforcement system.

This procedure was consistently applied to all test configurations for both fill materials (granular base and typical local *recebo*), providing a comparative parameter to classify and analyze the mechanical performance of reinforced solutions during the early stages of loading.

This methodology is presented as an original contribution of this thesis for evaluating the structural flexibility of reinforced unpaved roads.

3.7. POST-MAINTENANCE RELATIVE DEFORMATION INDEX (PM-RDI)

To assess how effective the maintenance intervention was in controlling residual settlements, this thesis proposes the use of the Post-Maintenance Relative Deformation Index (PM-RDI). This index provides a straightforward comparison between the accumulated settlement measured after maintenance and that recorded prior to the intervention, offering a clear measure of the efficiency of reinforced and unreinforced systems.

The PM-RDI is calculated using the following expression:

$$PM\text{-}RDI(\%) = \frac{S_{post}}{S_{pre}} \times 100 \tag{3.2}$$

***Spost*:** accumulated settlement measured during the cycle after the maintenance intervention (mm).
***Spre*:** accumulated settlement recorded during the initial stage of the test, before maintenance was performed (mm).

In practical terms, lower PM-RDI values indicate that maintenance successfully reduced post-intervention deformations, leading to greater structural stabilization. Conversely, higher PM-RDI values reveal a limited capacity to control residual settlements.

This procedure was consistently applied to all test configurations using both granular base and local recebo materials. The results were subsequently represented in comparative charts, allowing for a quick visualization of which reinforced solutions demonstrated better structural performance after maintenance.

3.8. BREAKAGE INDEX Bg(%)

To assess the degradation of the granular material used in the experimental sections, the Breakage Index (Bg) was determined following the methodology proposed by Marsa (1967) . This index quantifies the percentage of particle weight that underwent crushing during the tests. The calculation involves comparing the percentage of material retained on each sieve before and after testing, summing only the positive differences.

For this analysis, samples were carefully collected directly beneath the load transfer plate, within the structural layer, after completing the tests corresponding to the first loading cycle under initial conditions, prior to the maintenance stage. This approach allowed for evaluating the mechanical stability of the aggregates and understanding how geocell confinement influences the reduction of particle breakage.

3.9. TRAFFIC BENEFIT RATIO (TBR)

To evaluate the structural efficiency of geocell reinforcement in the experimental sections, this research employs the Traffic Benefit Ratio (TBR). This index allows for a direct comparison between the load-bearing capacity of a reinforced section and that of an unreinforced section under the same deformation limit criterion.

The TBR is calculated using the following expression:

$$TBR = \frac{N_r}{N_u} \tag{3.3}$$

where:

Nr: number of load cycles sustained by the reinforced section before reaching an accumulated deformation of 40 mm.
Nu: number of load cycles sustained by the unreinforced section to reach the same deformation limit.

The 40 mm deformation threshold was adopted to ensure comparability among configurations, consistent with practices reported in the technical literature. Several studies have used this parameter to quantify the structural benefits provided by geocell reinforcement in granular layers and subgrades, including Ramu (2022) Önal (2023) Pokharel et al. (2018) Badiger et al. (2024)and Saride (2015).

4. RESULTS AND DISCUSSION

This chapter presents a detailed analysis of the physical and mechanical behavior of an unpaved road structure reinforced with geocells manufactured from recycled tires. The evaluation was conducted through full-scale tests in a cyclic loading chamber. The results were organized according to the variables measured during the tests, including vertical displacements, total stresses in the subgrade, displacement velocity, particle breakage percentage, and the system's response following maintenance activities.

The primary objective of this analysis is to determine the effectiveness of geocell reinforcement by comparing performance across different configurations: without reinforcement, with reinforcement placed on the subgrade, and with reinforcement positioned on the structural layer. Additionally, the evolution of structural behavior before and after maintenance interventions is considered.

Graphs showing the evolution with respect to the number of load cycles, comparative tables, percentages of stress and deformation reduction, as well as flexibility indices and other variables are presented to assess whether the reinforcement provides technical benefits for unpaved roads. The results are discussed based on their technical significance and are compared with findings reported in the literature, providing evidence to support the validation of geocells made from used tires as sustainable road reinforcement elements.

4.1. DEFORMATION ANALYSIS IN UNPAVED ROADS REINFORCED WITH GEOCELLS

The mechanical behavior of unpaved road structures under repeated loading is primarily reflected in the accumulated deformations that develop within the pavement system. These deformations serve as indicators of the system’s strength, stiffness, and structural efficiency. In this study, various configurations were evaluated, both with and without reinforcement, including geocells made from recycled tires and commercial geocells, with variations in the location and height of the reinforcement.

This section presents a comprehensive analysis of the structural behavior based on experimental deformation records. Four complementary approaches are addressed:

- **Analysis of accumulated settlements**, to observe the total deformation under cyclic loading.
- **Analysis of settlement rate**, expressed in mm/cycle, which identifies critical transition phases.
- **System flexibility**, comparing reinforced systems with those without reinforcement.

These sections are aimed at fulfilling the specific research objectives related to the quantification of deformations and the influence of the geometry and location of the reinforcement.

4.1.1. Accumulated settlements for fill (typical local material)

The analysis of accumulated settlements reveals the vertical deformation of the system and allows for a direct comparison between the behavior of unreinforced and geocell-reinforced structures. Figure 4.1 illustrates that the unreinforced test (URR) experienced early failure, with deformation exceeding 290 mm. This behavior demonstrates the structural inadequacy of the unconfined system to withstand cyclic loads, showing progressive collapse from the initial loading cycles.

In addition, the tests included two different configurations based on the reinforcement location: one with geocells placed at the bottom of the granular layer, and another with reinforcement positioned at the center of the layer. The tests with reinforcement at the base (RRGI15, RRGI20, and RRCI) exhibited significantly lower deformations compared to the unreinforced case. Notably, the accumulated deformation observed in the test with the commercial geocell (RRCI) was similar to that recorded with the 20 cm recycled-tire geocell (RRGI20), suggesting a comparable structural performance between the two alternatives. However, the RRGI15 configuration showed unfavorable behavior, reaching the termination criterion at a permanent surface deformation of approximately 75 mm before completing 40,000 cycles.

The tests with geocells placed at the mid-depth of the granular layer were conducted using both the commercial geocell and the recycled-tire geocell with a height of 15 cm (configurations RRCM and RRGM15, respectively). Both systems exhibited similar levels of deformation, with accumulated settlements in the range of 50 mm to 80 mm, representing a reduction of approximately 75% compared to the unreinforced system. These two configurations highlight

the structural benefit of placing the reinforcement at mid-depth, as it enables better stress distribution, extends the service life of the system, and significantly reduces the magnitude of permanent settlements.

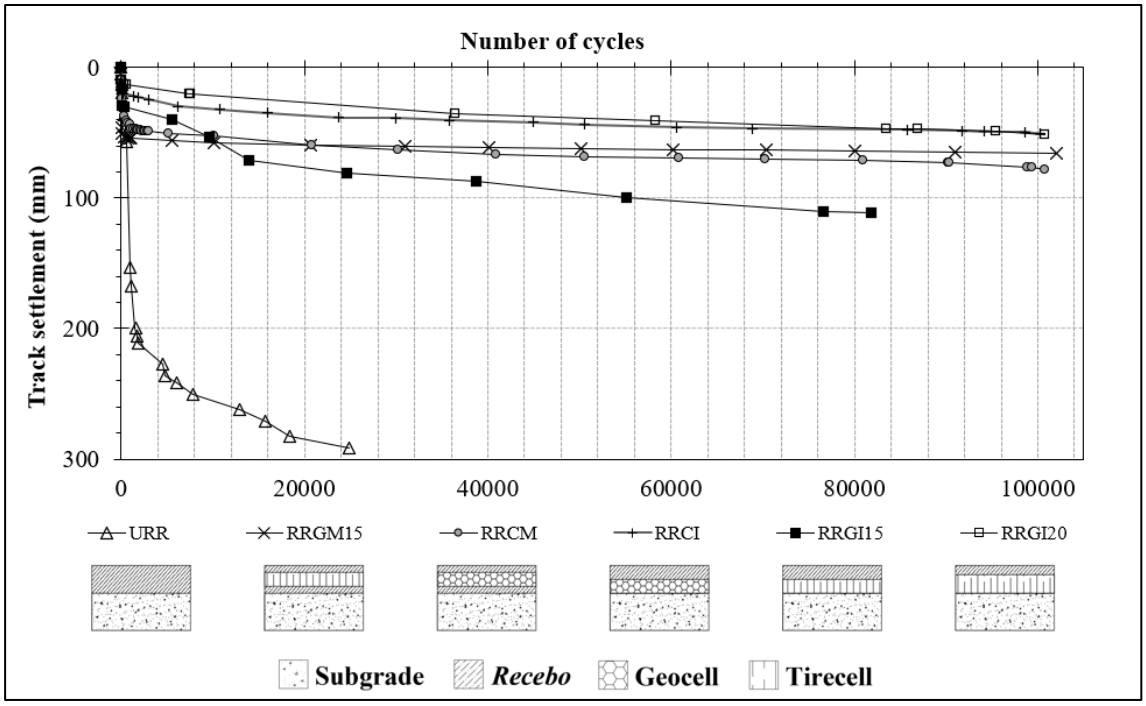

Figure 4.1. Accumulated Settlements for the Initial Condition with Recebo Material.

The configuration using the recycled-tire geocell with a height of 20 cm (RRGI20) exhibited particularly outstanding performance in terms of accumulated deformation. Throughout the test, this alternative maintained settlement values lower than those observed in configurations with shorter geocells, and even comparable to the commercial geocell. This result suggests that increasing the cell height may enhance the lateral confinement efficiency of the granular material, promoting a more effective redistribution of vertical stresses and thereby reducing permanent deformation. In this context, the use of 20 cm high geocells represents a technically promising alternative with significant structural benefits for unpaved road structures, particularly under repeated loading conditions.

In summary, the results obtained from the physical tests demonstrated that the use of geocells—both commercial and those manufactured from recycled tires—significantly contributes to the reduction of accumulated settlement under repeated loading. The reinforced configurations exhibited more stable behavior and lower final deformations compared to the unreinforced system. In particular, the RRGI20 configuration stood out due to its performance, suggesting

that increased geocell height can be beneficial in terms of confinement and deformation control. These findings underscore the importance of considering both the geometric characteristics of the reinforcement and its placement within the granular structure, and they provide a solid foundation for the subsequent analyses of settlement rate and segment-wise relative performance.

Figure 4.2 shows the evolution of accumulated settlement in the configurations constructed with *recebo*, evaluated after the maintenance intervention. Overall, a significant improvement in the structural performance of the reinforced sections is evident, reflected in substantially lower final settlements compared to the unreinforced configuration. This behavior can be attributed to the effects of successive compaction of both the subgrade and the granular material, occurring during and after the maintenance process, which increases system stiffness and enhances stress distribution. As a result, the overall structure exhibits reduced deformability under cyclic loading conditions.

The unreinforced system (URR-MANT) continued to exhibit poor performance, with accumulated deformation exceeding 110 mm after 100,000 cycles, confirming its structural vulnerability to repeated loading, even after maintenance. In contrast, all reinforced configurations showed final settlements below 60 mm, with differences of less than 20 mm among them, indicating a consistent and favorable performance.

Among the evaluated alternatives, the RRCI-MANT configuration, reinforced with commercial geocell, exhibited the lowest accumulated deformation, remaining below 40 mm, highlighting its effectiveness as a reinforcement material. On the other hand, the RRGM15-MANT configuration, which uses a 15 cm high recycled-tire geocell placed at mid-depth of the granular layer, demonstrated highly stable behavior throughout the entire test. This alternative reached its maximum deformation early on and maintained an almost zero slope during the remainder of the loading period, indicating rapid consolidation and excellent confinement capacity.

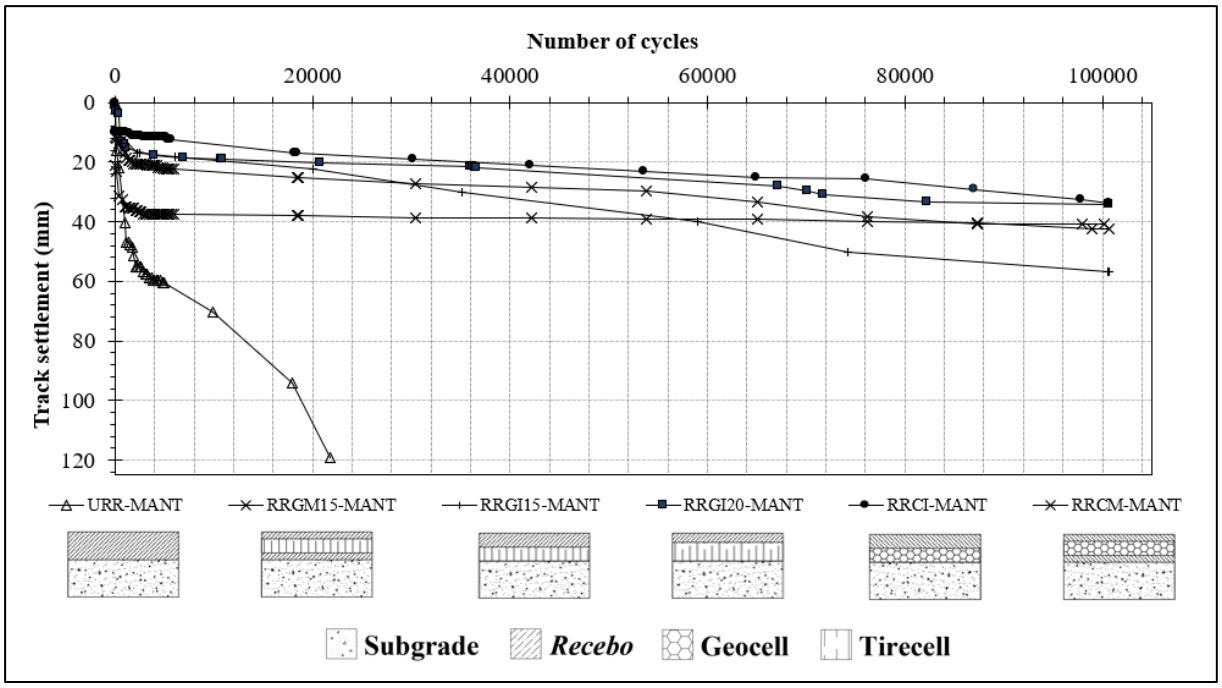

Figure 4.2 - Accumulated Settlements for the *recebo* Material after Maintenance.

Although the RRGI20-MANT configuration, incorporating a taller recycled-tire geocell, exhibited good performance, it did not outperform the commercial geocell in terms of behavior. Nevertheless, it remained within the efficiency range of the other reinforced alternatives, suggesting that all reinforced configurations offer significantly improved structural performance compared to the unreinforced condition.

In conclusion, the post-maintenance results confirm that the configurations reinforced with geocells—both commercial and those made from recycled tires—provide longer service life and lower accumulated deformations. This stable performance demonstrates that the use of geocells is a successful technical strategy for reinforcing unpaved road structures constructed with *recebo*, even after maintenance interventions.

4.1.2. Evaluation of Accumulated Settlements in Base-Type Material

Figure 4.3 illustrates the accumulated deformation behavior in the configurations constructed with base-type granular material. The analysis reveals a clear distinction between the unreinforced configuration and the reinforced alternatives. The unreinforced test (UR) reached a final settlement of approximately 240 mm, confirming a rapid and progressive structural

failure from the early loading cycles, and reflecting a limited capacity to withstand repeated loads without confinement.

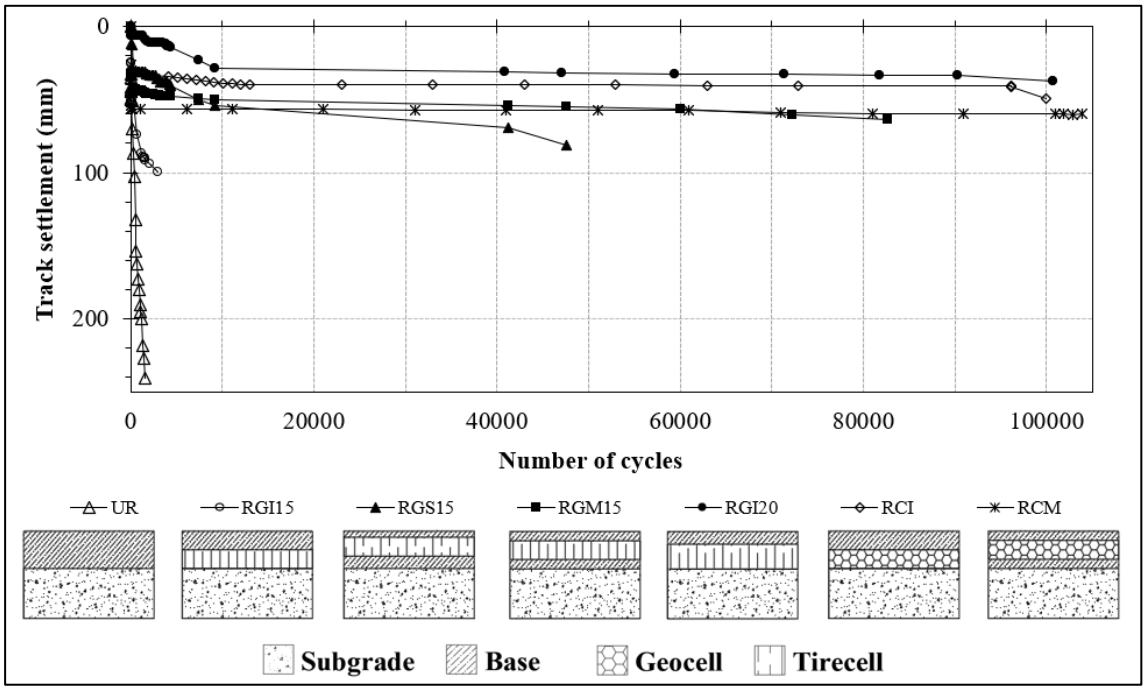

Figure 4.3 - Accumulated Settlements for the Base Material under Initial Conditions.

In contrast, all reinforced configurations exhibited a significant reduction in accumulated deformation, with final settlements below 120 mm, representing a decrease of over 50%. In this case, the RGI20 configuration, which uses 20 cm high tirecell-type geocells placed at the bottom of the granular layer, showed the lowest accumulated settlement, with a value close to 30 mm. This represents an 87.5% reduction compared to the unreinforced test, highlighting it as one of the most efficient alternatives for material confinement and the control of permanent deformations.

On the other hand, the RGI15 configuration, also positioned at the bottom but with a 15 cm high geocell, demonstrated less favorable behavior. Although it succeeded in reducing deformation relative to the unreinforced system, its curve reveals a rapid progression toward structural failure, reaching high deformation levels in fewer than 40,000 cycles. This behavior suggests that a reduced geocell height may be insufficient to provide adequate confinement under repeated loading conditions, particularly when combined with high-stiffness materials such as base-type aggregates.

The RGS15 configuration, the only one with reinforcement placed at the top of the granular layer, also exhibited poor performance. It showed an accelerated increase in deformation after 30,000 cycles, accompanied by a visibly more elastic structural response. During the tests, greater surface deformation was observed in the loading area, along with significant vibration in the equipment frame, posing a risk to the integrity of the testing system. For this reason, no additional replicates were conducted. This behavior confirms that placing the reinforcement at the top does not provide effective confinement of the granular material nor adequate stress redistribution.

The configurations with reinforcement placed at mid-depth (RGM15 and RCM), as well as the RCI configuration (with commercial geocells at the base), exhibited intermediate but stable results, with final deformations ranging between 80 and 100 mm. These alternatives showed a progressive evolution without signs of instability, demonstrating an effective capacity to control accumulated settlements and enhance the durability of the road structure.

In conclusion, the use of base-type granular material in combination with geocells—particularly when the geocells are placed at the bottom of the structural layer and have greater height—proves to be highly effective for deformation control under repeated traffic loads. The RGI20 configuration reaffirms its outstanding performance, establishing itself as a technically robust option. In contrast, configurations with thinner reinforcements (such as RGI15) or those positioned in less effective locations within the structural profile (such as RGS15) demonstrated less favorable behavior.

Figure 4.4 presents the behavior of accumulated settlements in the sections constructed with base-type granular material, evaluated after the maintenance intervention. In general terms, a substantial improvement in the structural performance of all reinforced configurations is observed, with significant reductions in accumulated deformation compared to the unreinforced system.

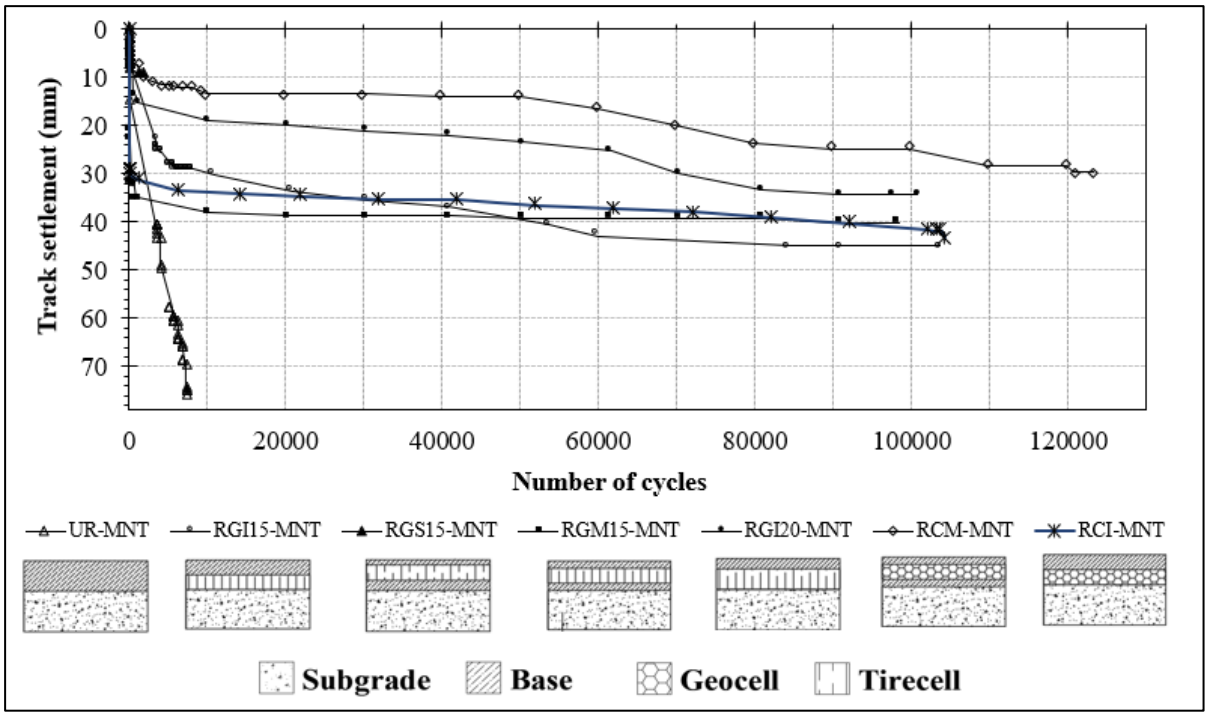

Figure 4.4 - Accumulated Settlements for the Base Material under Post-Maintenance Conditions.

The unreinforced configuration (UR-MNT) exhibited rapid deformation accumulation, reaching 75 mm (7.5 cm) in fewer than 10,000 cycles, indicating early structural failure and limiting the functionality of this type of solution even after compaction or surface restoration.

In contrast, all reinforced configurations maintained accumulated deformations below 50 mm throughout the 100,000 cycles, demonstrating notable structural efficiency and a clear extension of the system's service life. This widespread improvement confirms the effectiveness of geocell reinforcement in confining the material and controlling post-maintenance deformations.

Among the evaluated alternatives, the RCI-MNT configuration (commercial geocell at the base) and the RGM15-MNT configuration (recycled-tire geocell placed at mid-depth) stood out due to their nearly identical performance, remaining the sections with the lowest final settlement. This similarity in behavior demonstrates that proper placement of the reinforcement—even when using recycled materials—can achieve efficiency levels comparable to those of commercial solutions.

The RGI20-MNT configuration, with a 20 cm high geocell placed at the bottom of the layer, also demonstrated outstanding performance, with a maximum settlement of 34 mm. This

confirms that increased reinforcement height significantly contributes to deformation control, even under post-maintenance conditions.

At the opposite end, the RGI15-MNT configuration showed the highest settlement among the reinforced sections, slightly exceeding 45 mm. Nevertheless, it successfully withstood the 100,000 loading cycles without exhibiting structural failure—consistent with the performance of the other reinforced configurations—reflecting an overall structural improvement following the maintenance intervention.

In summary, the post-maintenance analysis confirms that the use of geocells—whether commercial or made from recycled tires—provides an effective solution for reinforcing structures built with base-type granular material, improving structural performance under repeated loading and reinforcing their technical viability. The fact that all reinforced configurations-maintained deformations below 5 cm and successfully withstood 100,000 loading cycles without failure serves as strong evidence of their functionality. In contrast, the poor performance of the unreinforced system highlights the necessity of incorporating confinement elements to ensure the stability and durability of unpaved roads.

4.1.3. Influence of Geocell Type and Infill Material under the Same Placement Position

This section analyzes the influence of the reinforcement type and the infill material in configurations where the reinforcement location remains the same. Figure 4.5 presents the accumulated deformations corresponding to the tests in which the reinforcement was installed near the subgrade.

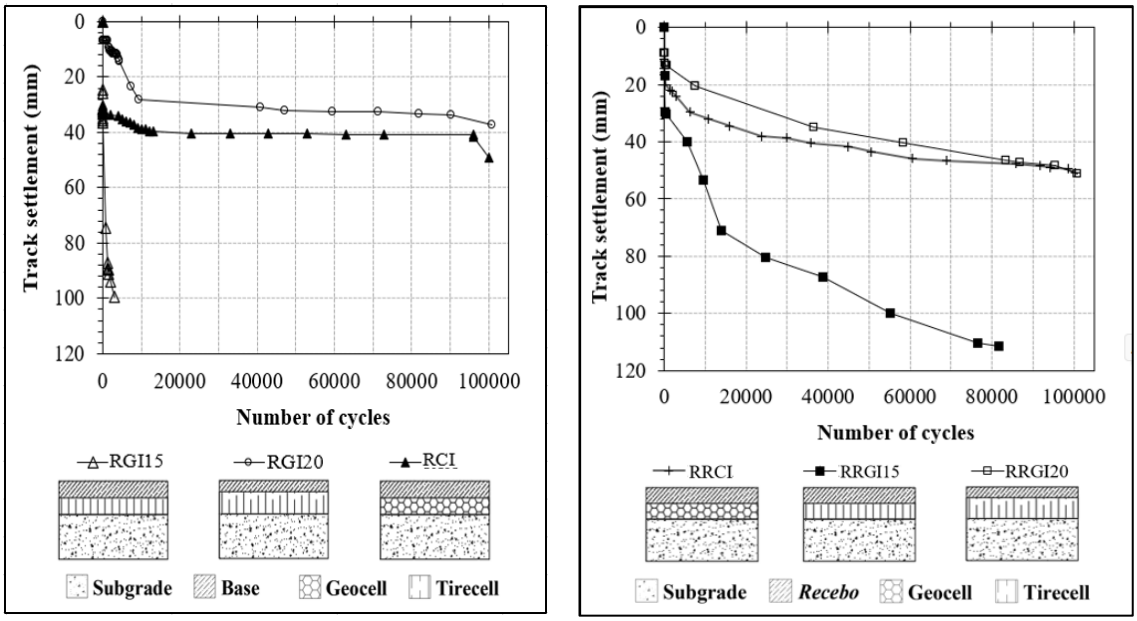

(a) (b)

Figure 4.5 - Accumulated deformation in tests with reinforcement placed directly over the subgrade: (a) using base material and (b) using *recebo* material.

When comparing the different infill materials, it is observed that the base-type material tends to stabilize deformation more rapidly and exhibits lower accumulated deformation compared to *recebo*. This indicates better structural performance of the system when a higher-quality material is used, highlighting the significant influence of the infill type on the overall behavior of the reinforcement.

Regarding the type of reinforcement used in this location, the best performance is achieved with the 20 cm high recycled-tire geocell. This configuration shows the lowest levels of deformation regardless of the granular material used, even outperforming commercial geocells in terms of structural efficiency.

Additionally, configurations using the 15 cm high recycled-tire geocell installed directly on the subgrade—whether with base or *recebo* infill—exhibited less favorable behavior, characterized by higher levels of accumulated deformation.

Figure 4.6 shows the accumulated deformation from the tests conducted with the reinforcement placed at the mid-depth of the granular layer. The influence of the infill material is more pronounced in the configurations using commercial geocells, where the use of *recebo* results in

over 10 mm greater deformation compared to the use of base-type material. In contrast, when employing higher-quality base material, the difference in deformation between both geocell types is significantly smaller—around 5 mm—indicating that this type of reinforcement is less sensitive to variations in infill material quality.

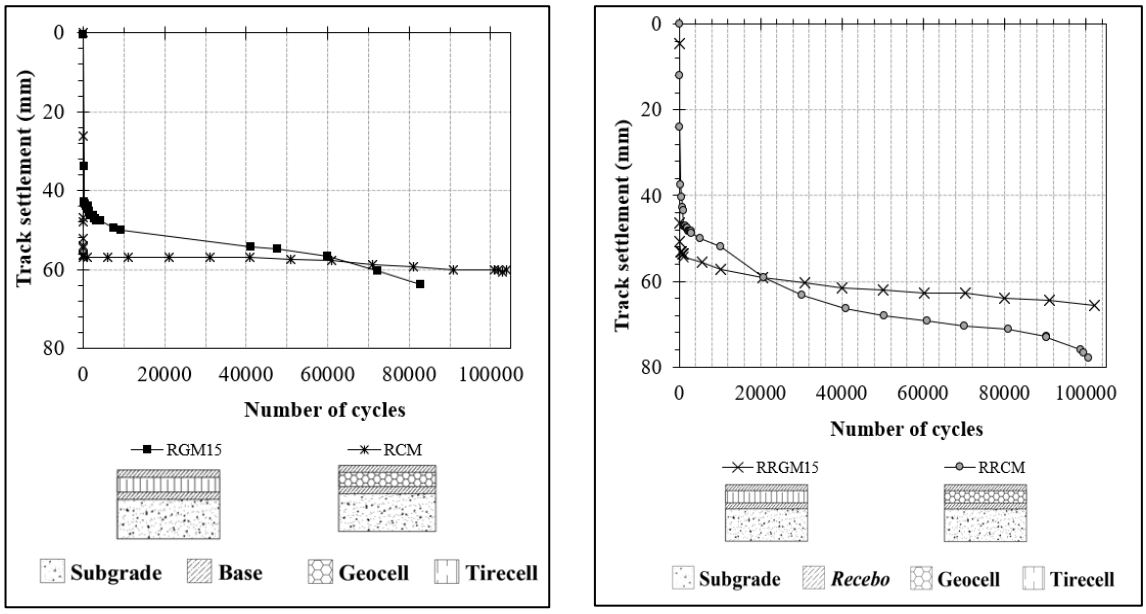

(a) (b)

Figure 4.6 - Accumulated deformation from tests with mid-depth reinforcement: (a) using base material and (b) using *recebo* material.

Regarding the geocell type, it is observed (as shown in Figure 4.5 and Figure 4.6) that the commercial geocell tends to stabilize its deformation more quickly, exhibiting a curve with a decreasing slope from the early stages of the test, which suggests a tendency toward stabilization under repeated loading. However, when comparing both types of reinforcement using base material, their behaviors are similar. In the case of *recebo*, the geocell made from recycled tires demonstrates better performance, as evidenced by lower accumulated deformation.

In summary, these results confirm that the type of infill material significantly influences the performance of the reinforced system. As with other reinforcement placements, the use of higher-quality granular material improves the structural efficiency of the system. Furthermore, the 15 cm recycled-tire geocell exhibits competitive behavior when compared to commercial geocells, reinforcing its potential as a sustainable and technically viable alternative for unpaved road applications.

4.1.4. Deformation Rate for Tests Using *Recebo*-Type Material

The evaluation of settlement rate or deformation rate is essential for understanding the dynamic structural behavior of road sections subjected to cyclic loading. Unlike cumulative analysis, this approach allows for the identification not only of the magnitude of deformation, but also the speed at which it occurs and how it evolves with the number of applied cycles.

The analysis of the deformation rate, calculated from the local slope between consecutive data points obtained during the test, made it possible to identify three distinct stages of structural behavior under cyclic loading.
This classification was developed as part of the present research, based on the experimental results, and the reference thresholds for the deformation rate (mm/cycle) were established a posteriori to interpret the structural performance of the tested sections.

- Active deformation: rate > 0.5 mm/cycle, associated with an unstable or uncontrolled response. This behavior was mainly observed in unreinforced sections and in those with lower geocell heights, which reached the termination criterion after a reduced number of cycles.

- Moderate deformation: between 0.5 and 0.2 mm/cycle, corresponding to a structural transition phase toward stabilization. This range was observed in reinforced configurations with intermediate geocell heights, where the accumulation of deformation gradually decreased with the number of cycles.

- Low deformation: < 0.2 mm/cycle, representing a stabilized phase that indicates good structural performance. This behavior was recorded in reinforced sections with higher or commercial geocells, which exhibited the lowest accumulation of permanent deformation.

This classification provided a clear basis for comparing the structural behavior of reinforced and unreinforced sections, demonstrating the effectiveness of cellular confinement in reducing accumulated deformation under repeated loading.

Figure 4.7 shows the transition of deformation rate over the initial loading cycles of the tests, revealing notable differences between the unreinforced test and those with reinforcement.

It can be observed that the URR configuration (unreinforced) exhibited the most critical acceleration rate behavior among all evaluated alternatives. From the very first cycles, it presented an extremely high initial deformation rate—exceeding 2.5 mm/cycle—indicating a system with poor confinement capacity and low resistance to deformation accumulation. Although the system transitioned from the active phase (> 0.5 mm/cycle) to a moderate phase (0.5–0.2 mm/cycle) within just a few cycles (between cycles 7 and 9), this transition cannot be interpreted as a stabilization process, since the system never reached the low deformation phase (< 0.2 mm/cycle). As a result, the system continued to undergo progressive failure until the test was terminated.

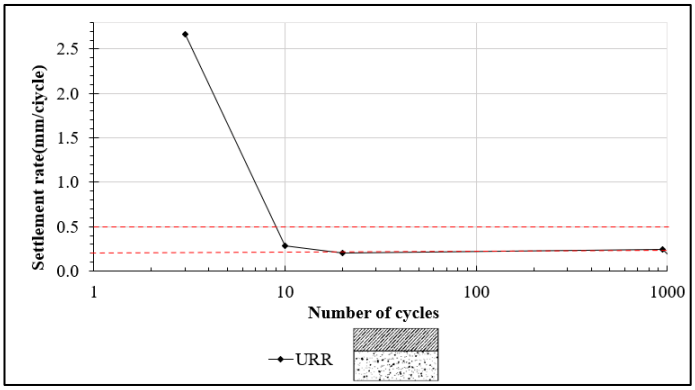

(a)

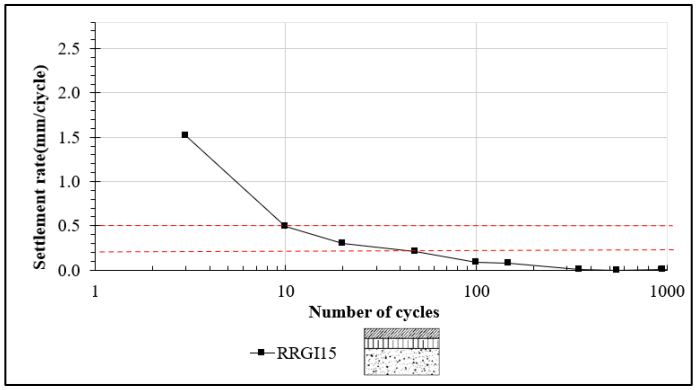

(b)

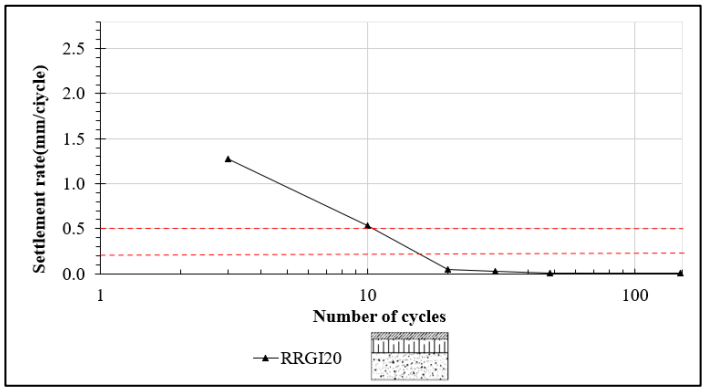

(c)

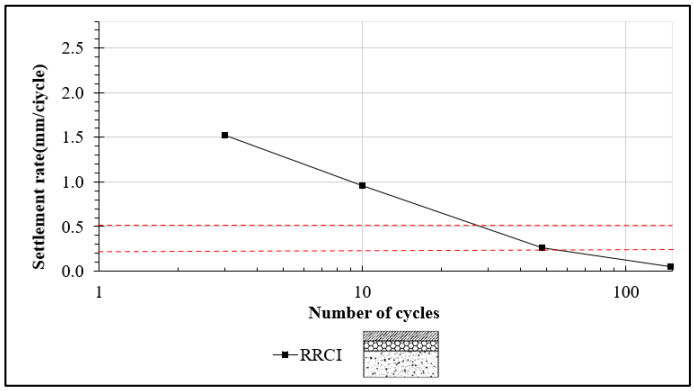

(d)

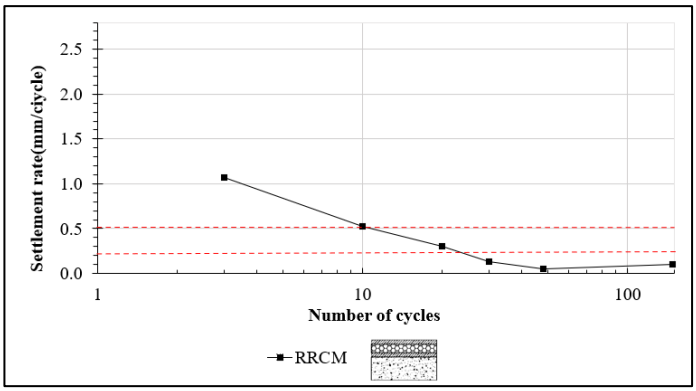

(f)

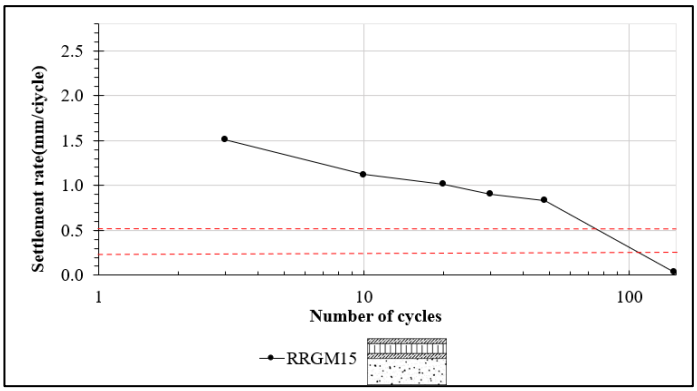

(g)

Figure 4.7 - Settlement rate for Each Test Configuration with local typical material (*Recebo*) (a) URR, (b) RRGI15, (c) RRGI20, (d) RRCI, (e) RRCM, and (f) RRGM15.

Table 4.1 shows the number of cycles during which each configuration remained within the active and moderate deformation phases, until reaching the low phase, which represents the desired condition of structural stabilization—characterized by settlement rates below 0.2 mm/cycle. This progression is key to interpreting the effectiveness of the confinement induced by the different reinforcements used.

The reinforced tests showed favorable performance, as all configurations exited the active deformation phase within the first 20 loading cycles. This behavior, identified directly from the experimental data, indicates a rapid stabilization of the reinforced layers, with deformation rates falling below 0.5 mm/cycle from the early stages. The results confirm that the use of geocells, both commercial and recycled-tire types, effectively enhances structural stability under repeated loading.

Of all the evaluated configurations, the ones that reached the low-deformation phase in the fewest cycles were the one reinforced with the taller recycled-tire geocell (RRGI20), which stabilized around cycle 19, and the one with the commercial geocell at mid-depth (RRCM), which stabilized around cycle 22. This similarity in behavior underscores the positive impact of increased cell height on the lateral confinement of granular material and the substantial influence of the reinforcement's location within the structural profile on system efficiency. This enables greater energy dissipation and improved deformation control.

Table 4.1 - Summary of settlement rate (mm/cycle) behavior for tests using recebo material.

		Configuration					
Phase		**URR**	**RRGI15**	**RRGI20**	**RRCI**	**RRCM**	**RRGM15**
Active	**Phase Start**	1	1	1	1	1	1
	Phase End	9	10	13	20	10	80
	Number of cycles in Phase	8	9	12	19	9	79
Moderate	**Phase Start**	9	10	13	20	10	80
	Phase End	N/A	50	19	50	22	110
	Number of cycles in Phase	N/A	40	6	30	12	30
Low	**Phase Start**	N/A	50	19	50	22	110

The term *N/A* (not applicable) was used in cases where the test section did not reach the stabilized phase, defined by a deformation rate below 0.2 mm/cycle. In these configurations, the deformation rate remained above this threshold throughout the test duration, indicating that the section did not attain the low-deformation stage. Therefore, the value was not computed, as the section exhibited continuous deformation without clear stabilization.

Taken together, these results reinforce the importance of strategic and geometric reinforcement design—particularly in terms of height and placement—to ensure a rapid transition toward structural stability in unpaved roads subjected to repeated traffic loading.

4.1.5. Deformation Rate for Tests Using Base Material

The UR configuration, corresponding to the unreinforced system, exhibited the least efficient behavior among all tests in terms of settlement rate. It began with a rate exceeding 2.8 mm/cycle, indicating rapid deformation from the very first cycles, with no capacity for stress control or redistribution. Although this configuration transitioned from the active to the moderate phase, and eventually to the low phase near cycle 80, this progression did not reflect true structural stabilization. On the contrary, a progressive collapse was observed, where the decrease in rate resulted from system exhaustion rather than improved performance.

In contrast, the configurations reinforced with geocells demonstrated more controlled behavior from the early stages of testing. Among them, the RGI20 configuration—featuring a 20 cm high geocell made from recycled tires—stood out for its efficiency, entering the moderate phase by

cycle 3 and reaching the low phase before cycle 20. This result suggests that a greater geocell height enhances the confinement capacity of the granular material, enabling more effective control of accumulated deformation. Similarly, the RCI configuration, using a commercial geocell placed at the base, also entered the low phase early and maintained low and stable settlement rate values throughout the test.

Other configurations, such as RGI15, RGM15, and RCM, also reached the low phase, although they did so after a greater number of cycles. In particular, RGM15 exhibited a prolonged duration in the active phase, but without reaching critical deformation levels or showing signs of failure. RGS15, despite being the only configuration with the geocell placed at the top of the granular layer, achieved early stabilization; however, physical tests revealed surface vibrations that could compromise the system's operational stability. Overall, all reinforced systems demonstrated more efficient control of settlement rate, validating the positive contribution of geocells to the stabilization of structural behavior under repeated loading.

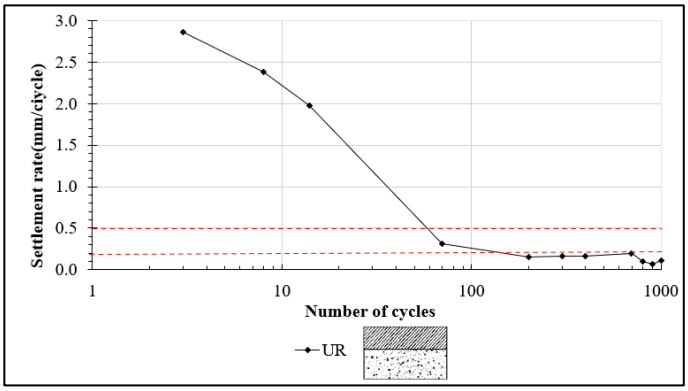

(a)

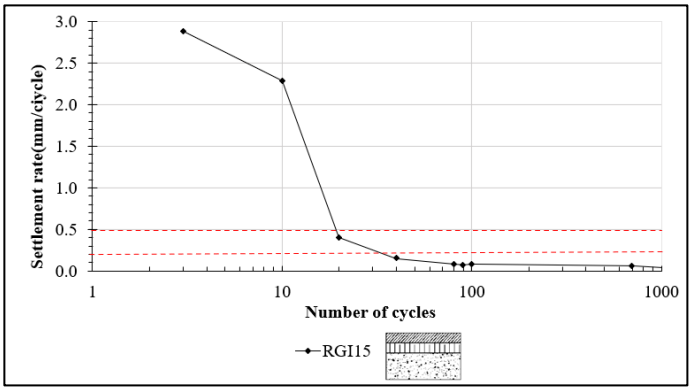

(b)

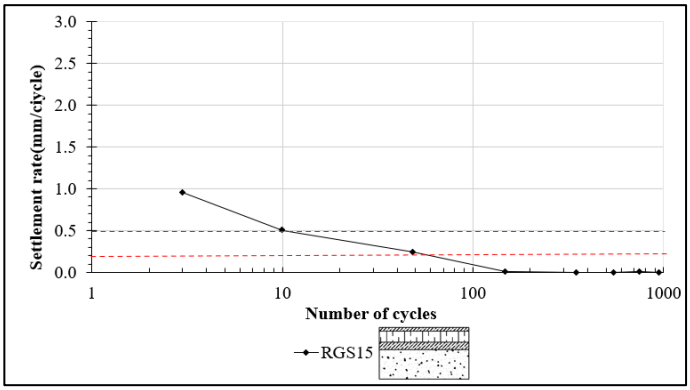

(c)

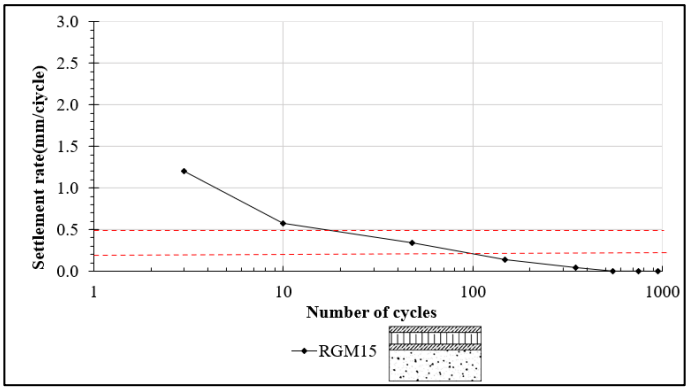

(d)

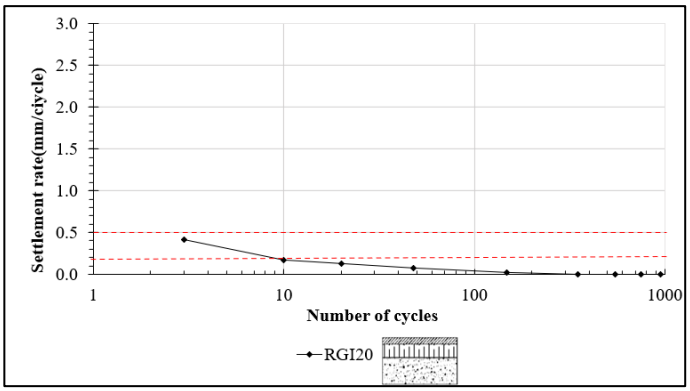

(e)

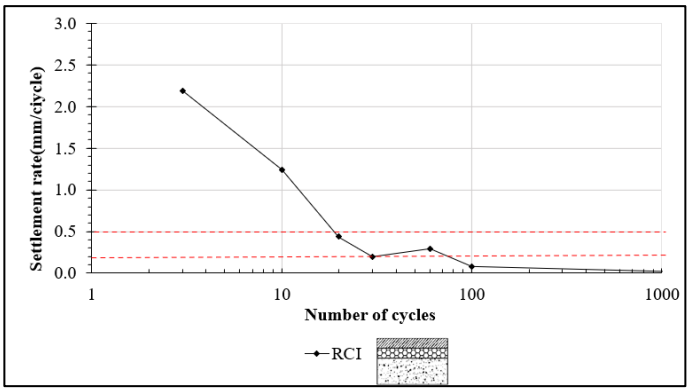

(f)

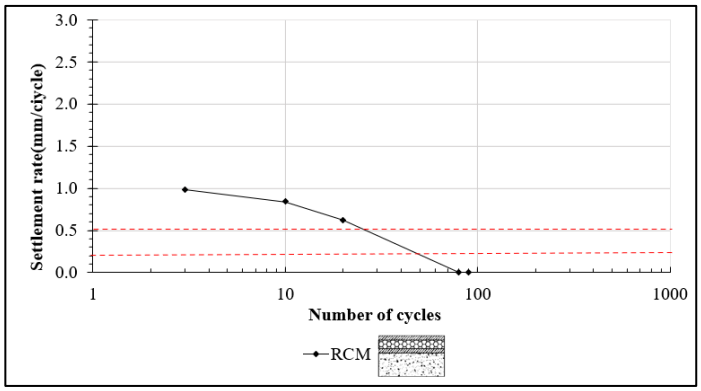

(g)

Figure 4.8 - Deformation rate for each test configuration using base material. (a) UR, (b) RGI15, (c) RGS15, (d) RGM15, (e) RGI20, (f) RCI, and (g) RCM.

Table 4.2 presents the duration of each configuration within the active, moderate, and low deformation phases, based on the settlement rate observed during the first 100 cycles. The unreinforced test (URR) remained in the active phase for 49 cycles and in the moderate phase for 50 cycles, reaching the low phase only at cycle 100. This confirms its poor performance, characterized by a slow transition and a lack of real control over progressive deformation. In contrast, reinforced configurations such as RGI20 and RCI exited the active phase early (at cycles 25 and 24, respectively) and reached the low phase before cycle 100, indicating a more efficient stabilization of the system.

Table 4.2 - Summary of the deformation rate behavior for the tests with base material.

		Configuration						
Phase		**UR**	**RGI15**	**RGS15**	**RGM15**	**RGI20**	**RCI**	**RCM**
Active	**Phase Start**	1	1	1	1	N/A	1	1
	Phase End	50	20	28	50	N/A	25	80

	Number of cycles in Phase	49	19	27	49	N/A	24	79
Moderate	**Phase Start**	50	20	28	50	1	25	80
	Phase End	100	35	100	110	7	100	110
	Numero de ciclos Fase	50	15	72	60	6	75	30
Low	**Phase Start**	100	35	100	110	7	100	50

The results obtained allow to conclude that the settlement rate is a key indicator for evaluating the structural behavior and flexibility of the tested systems. Configurations reinforced with geocells—both commercial and those made from recycled tires—were able to quickly transition from active deformation phases to moderate and low phases, demonstrating early stabilization. The unreinforced system (URR) exhibited a very high initial deformation rate and failed to stabilize, resulting in early structural failure. These findings reinforce the importance of using reinforcements with strategic geometries and placement to extend the service life of unpaved structures under repeated loading conditions.

4.1.6. System Flexibility Analysis

In the context of this research, flexibility refers to the capacity of the reinforced or unreinforced system to accommodate cyclic loading through progressive deformation without losing structural stability. This property is directly related to the deformation rate observed during the initial loading cycles, which reflects how the system redistributes stresses and adapts to repeated loads. A more flexible system tends to exhibit higher deformation rates at the beginning of loading but can subsequently reach stabilization if adequate confinement is provided. Therefore, analyzing flexibility allows evaluating the system's ability to adjust to load application while maintaining overall integrity during the early stages of repeated loading.

This study introduces a flexibility index as a performance indicator to compare reinforcement efficiency during the early stages of loading. The index is computed from the deformation rate (mm/cycle) evaluated at cycle 3, taken as the onset of the system's structural response. In this research, inspection of the deformation-rate curves showed that the early response is clearly expressed within the first few cycles and is consistently captured at cycle 3 across the tested configurations, which justifies adopting this cycle for comparative analysis. This cycle has been shown to be critical according to studies such as Pokharel et al, (2009), (Jitendra K. Thakur,

2016) y Moghaddas Tafreshi & Dawson, (2012). The selection of this cycle is justified by its ability to clearly capture the initial deformation rate, providing relevant insight into the system's structural adaptability from the very first loading applications.

The analysis aims to identify which configurations promote a progressive transition toward stabilization without compromising the integrity of the system. To visualize these results, a heat map is used to classify the performance of each configuration: the most favorable values are represented in shades of blue, while the less favorable results are shown in shades of red. This approach allows for a quick and intuitive interpretation of the relative behavior among the evaluated cases.

Figure 4.9 and Figure 4.10 present the heat maps constructed from the results of the Flexibility Index (FI). This index quantifies the efficiency of the reinforcement during the initial stage of the test by comparing the deformation rate relative to the unreinforced system. An FI value equal to zero indicates that the reinforcement had no effect, as the settlement rate is identical to that of the unreinforced system. In contrast, values closer to one reflect a greater reduction in the deformation rate, indicating improved performance of the reinforced system.

Among the configurations analyzed with *recebo* (Figure 4.9), the best results are observed in the RRGI20 test, which corresponds to a geocell made from recycled tires with a height of 20 cm, and in RRCM, which uses a commercial geocell placed at mid-depth of the granular layer. Both alternatives achieve the highest index values, indicating a greater capacity to control deformations from the early cycles. It is worth noting that all reinforced configurations show positive FI values, confirming that, in all cases, the use of geocells contributed to improving the structural performance compared to the unreinforced system

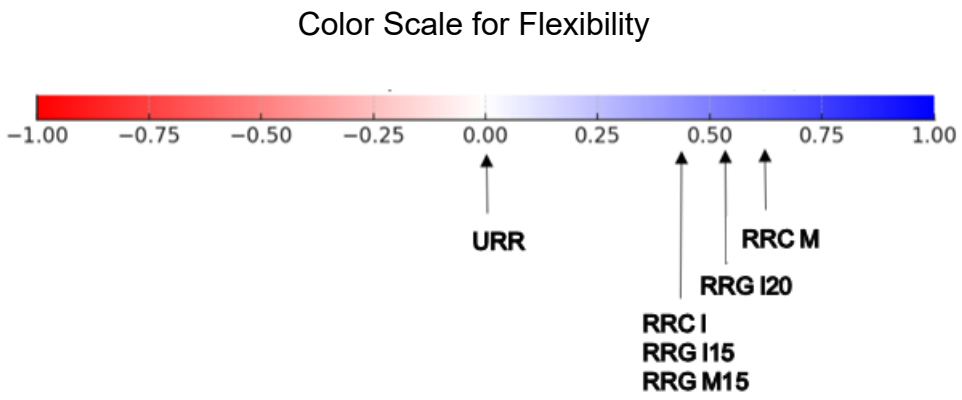

Figure 4.9- Comparative scale of structural performance using the Flexibility Index (FI) from tests with material such as local typical material fill.

Figure 4.10 presents the Flexibility Index (FI) results for the configurations tested with base material. It can be observed that the RGI20 test, corresponding to the geocell made from recycled tires with a height of 20 cm, reached an FI value of approximately 0.78, the closest to one, indicating high reinforcement efficiency in reducing the deformation rate during the initial loading stages.

In contrast, the RGI15 test, with a 15 cm high recycled tire geocell placed at the bottom of the granular layer, shows behavior similar to that of the unreinforced system (UR), with an FI close to zero. This suggests that this configuration did not result in significant improvements in terms of structural flexibility. The remaining reinforced configurations (RCM, RCI, RGM15, and RGS15) show favorable behavior, with FI values greater than 0.5, indicating an effective reduction in the settlement rate compared to the unreinforced system.

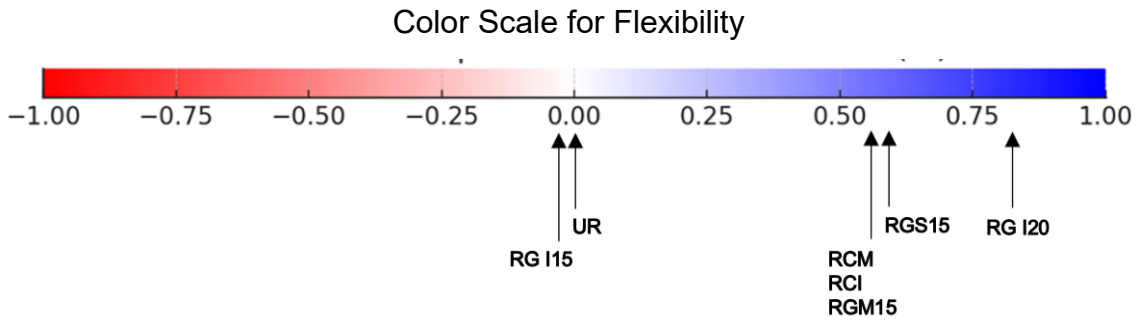

Figure 4.10 - Comparative scale of structural performance using the Flexibility Index (FI) from tests with base material.

The Flexibility Index (FI) emerges as a valuable tool for understanding how a reinforced system responds from its early loading cycles. By focusing on the speed of initial deformation, it allows for the comparison of reinforcement configurations that could make a significant difference in real mechanical performance.

4.1.7. Assessment of Maintenance Efficiency Using the Post-Maintenance Relative Deformation Index (PM-RDI)

After maintenance, the deformations observed in the tests were visibly reduced compared to those recorded prior to the intervention. To quantify this effect, the Post-Maintenance Relative

Deformation Index (PM-RDI) was calculated, defined as the percentage of accumulated settlement after maintenance relative to the pre-maintenance settlement. This indicator allows for the assessment of maintenance efficiency in controlling residual deformations.

Figure 4.11 shows the PM-RDI values for the tests conducted using base granular material as fill. The results indicate that the RGI20-MNT configuration (recycled tire geocell, 20 cm in height) and RCI-MNT (commercial geocell placed directly above the subgrade) exhibited the lowest index values, with only 8% and 11.8% of deformation relative to their pre-maintenance condition, respectively. These values reflect a high level of structural efficiency following the maintenance intervention. In contrast, the unreinforced test (UR-MNT) reached a PM-RDI of 68.8%, revealing a limited capacity for stabilization after intervention.

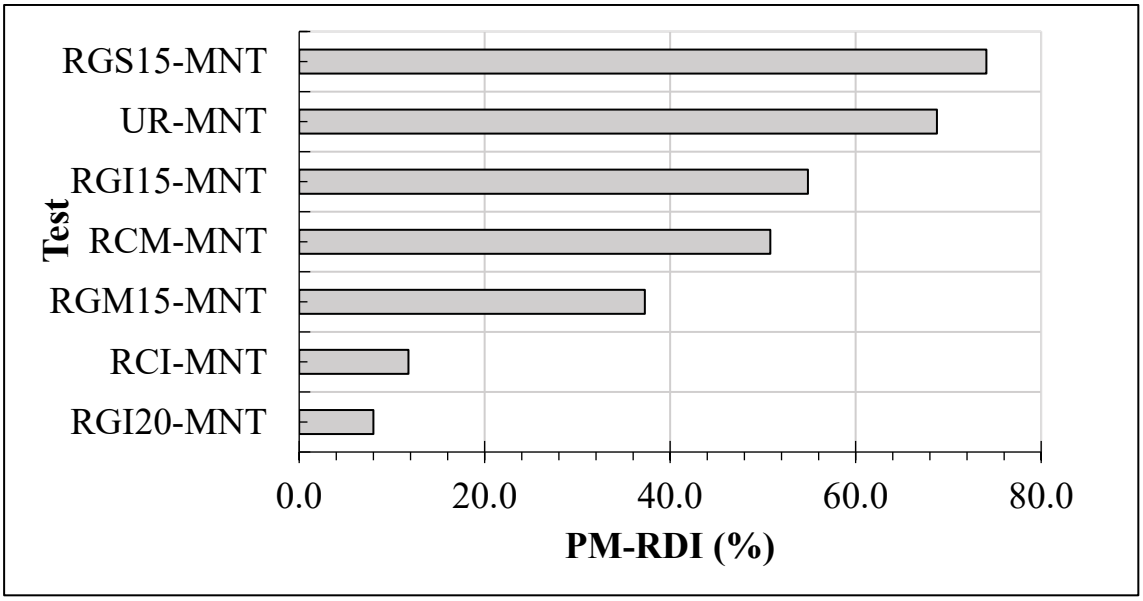

Figure 4.11 - Comparison of maintenance efficiency using the Relative Deformation Index (PM-RDI) for tests with base material.

These findings indicate that most of the reinforced configurations maintain effective control over settlement after maintenance, promoting system stabilization. Among the evaluated configurations, the best performance was achieved by the recycled tire geocell with greater height (RGI20-MNT), even outperforming configurations that used commercial geocells in various locations. This suggests that the height of the reinforcement plays a decisive role in post-maintenance efficiency.

Figure 4.12 presents the results of the Post-Maintenance Relative Deformation Index (PM-RDI) for the configurations tested with *recebo* material. It is evident that the RGI20-MNT configuration, which incorporates a geocell made from recycled tires with a height of 20 cm, exhibited the best structural performance. This alternative reduced post-maintenance deformation to approximately 33% of the accumulated deformation prior to the intervention, reflecting a notable efficiency of the reinforced system in controlling residual settlements.

In second place, the RCI-MNT configuration, corresponding to the commercial geocell installed above the subgrade, also achieved a significant reduction in post-maintenance deformation. Both cases reaffirm that the geometric design of the reinforcement (such as cell height) and its proper placement within the structure play a key role in post-maintenance performance.

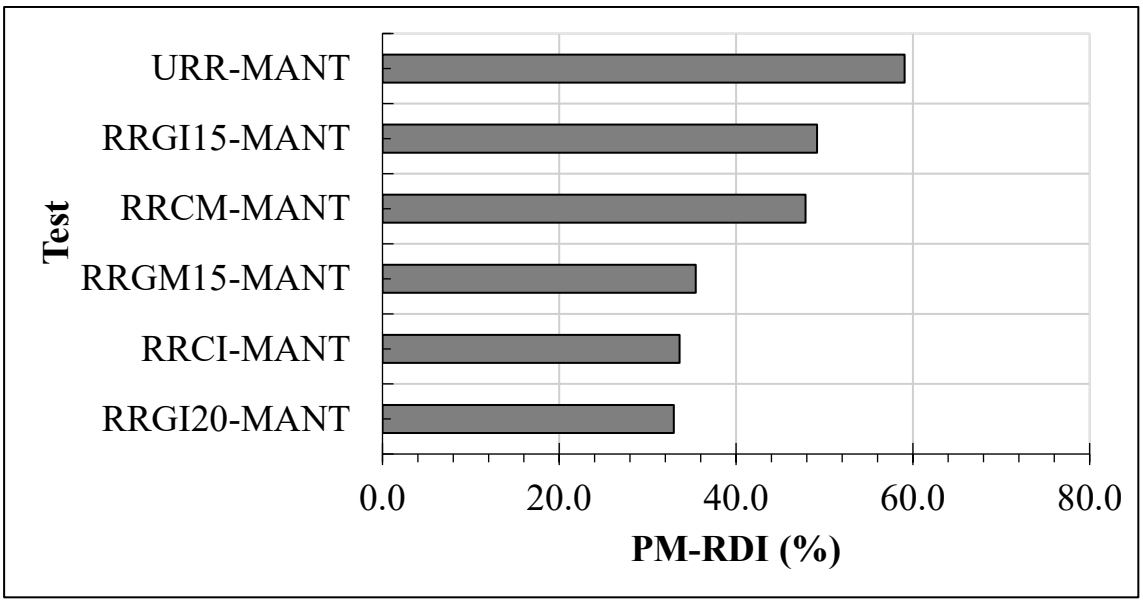

Figure 4.12 - Comparison of maintenance efficiency using the Relative Deformation Index (PM-RDI) for tests with recebo fill material.

4.2.EVALUATION OF THE TRAFFIC BENEFIT RATIO (TBR)

The Traffic Benefit Ratio (TBR) is used to evaluate the structural efficiency of geocell reinforcement by comparing the load-bearing capacity of a reinforced section against an unreinforced section, under the same deformation limit criterion. Table 4.3 and Table 4.4

present the TBR values obtained from the tests conducted with recebo and granular base materials, respectively, for an accumulated deformation of 40 mm.

Table 4.3 - Calculation of the TBR for tests with *recebo* fill material.

Test	Nr	Nu	TBR
URR	385	385	1
RRGI15	5514	385	14.32
RRGI20	58263	385	151.33
RRCI	35813	385	93.02
RRCM	548	385	1.42
RRGM15	48	385	0.12

Table 4.4 - Calculation of the TBR for tests with base material.

|	Nr	Nu	TBR
UR	30	30	1
RGI15	100	30	3.33
RGS15	4392	30	146.4
RGM15	348	30	11.6
RGI20	100728	30	3357.6
RCI	96085	30	3202.83
RCM	30	30	1

In the case of tests using *recebo* material, the results demonstrate a substantial improvement in structural performance when geocells are incorporated as reinforcement. The RRGI20 configuration stands out in particular, achieving a TBR of 151.33, indicating that the section reinforced with 20 cm-high geocells made from recycled tires can withstand 151 times more load cycles before reaching the same level of deformation as the unreinforced section (URR). Configurations such as RRCI (with commercial geocell) also show notable performance, with a TBR of 93.02, validating the effectiveness of cellular confinement in materials with lower structural quality.

Meanwhile, the tests with granular base material reveal that reinforcement also have a significant impact, although the relative effect is even more pronounced due to the inherent properties of the material. The RGI20 configuration, corresponding to a 20 cm recycled tire geocell, achieved a TBR of 3357.7, representing an exceptional structural improvement. This result confirms that the combination of high-quality material and well-designed and properly placed reinforcement can exponentially extend the service life of unpaved road systems.

Previous studies, such as that by Asha et al. (2017), have also reported positive TBR values for systems with geocells, although in different contexts and configurations. In that study, the TBR values obtained under a 40 mm deformation were significantly lower compared to those achieved in the present research, which underscores the importance of fill material type, reinforcement height, and its placement within the system.

In conclusion, the TBR values obtained in this research validate the use of geocells as an effective alternative for the reinforcement of unpaved roads, both with low-quality materials such as *recebo* and with granular bases. The improvement observed is not only technical but also functional, as it extends the service life of the pavement, reduces maintenance needs, and promotes the sustainable use of recycled materials, such as end-of-life tires.

4.3. EVALUATION OF TOTAL STRESSES

This item presents and analyzes the total stress results measured at the subgrade of the physical models. As explained in the methodology section, three load cells were installed to record total stresses at different points within the subgrade. Cell B is located directly beneath the applied load, at the center of the model; Cell A is also positioned under the load but at an additional depth of 15 cm; and Cell C is placed toward the lateral edge of the system, away from the point of direct loading.

4.3.1. Evaluation of Total Stresses in the Tests Conducted with Granular Base Material

The results obtained from the tests conducted with granular base material confirm that Cell B records the highest values of total stress, as expected given its central location. This is followed by Cell A, with intermediate values, while Cell C shows the lowest pressures due to its peripheral position. In general, the pressure values tend to remain relatively constant throughout the test, showing minimal variation between the beginning and the end of the experiment. In most cases, a slight increase in pressure is observed with the number of loading cycles, which can be attributed to the progressive rearrangement of the material and the cumulative effect of the repeated loads.

Figure 4.13, Figure 4.14 and Figure 4.15, illustrate the distribution of total stresses measured at positions A, B, and C, respectively, corresponding to the tests conducted using granular base material. These figures provide a detailed representation of the stress behavior at different locations within the subgrade throughout the loading cycles, offering critical insights into the system's load redistribution capacity and its effectiveness in mitigating localized stress concentrations.

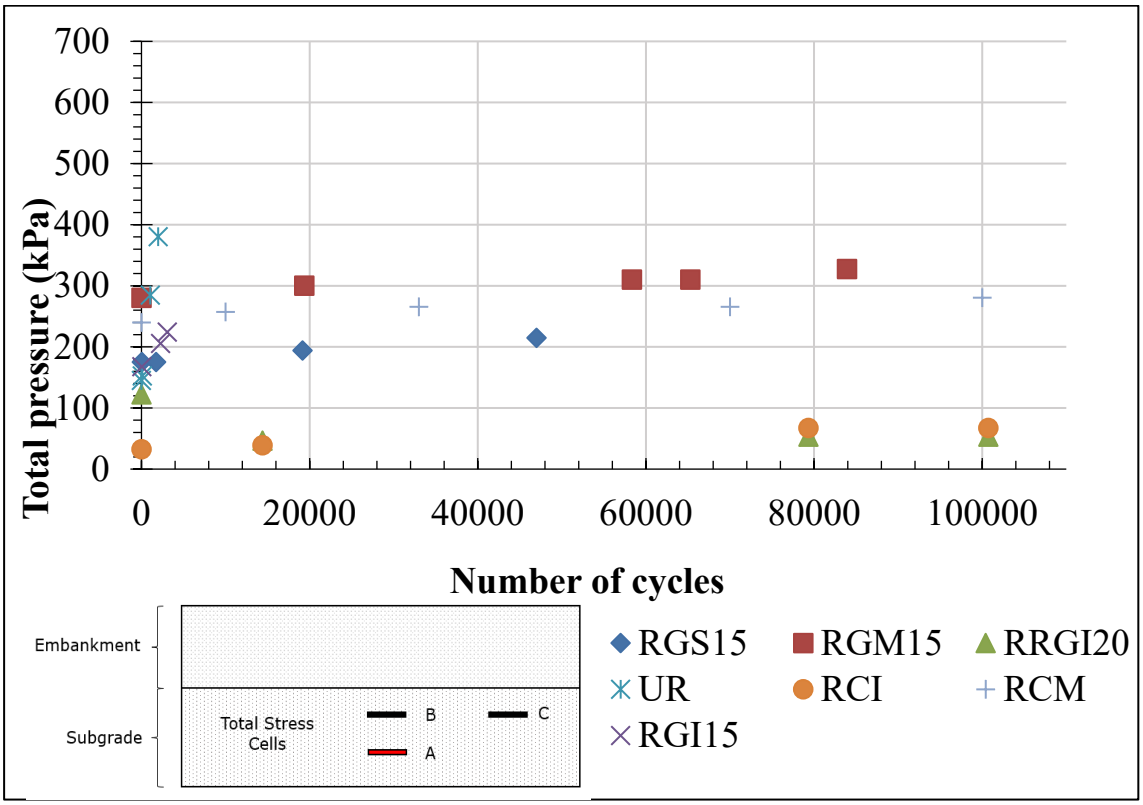

Figure 4.13 - Total stresses in initial condition tests in stress cell A for tests with base material.

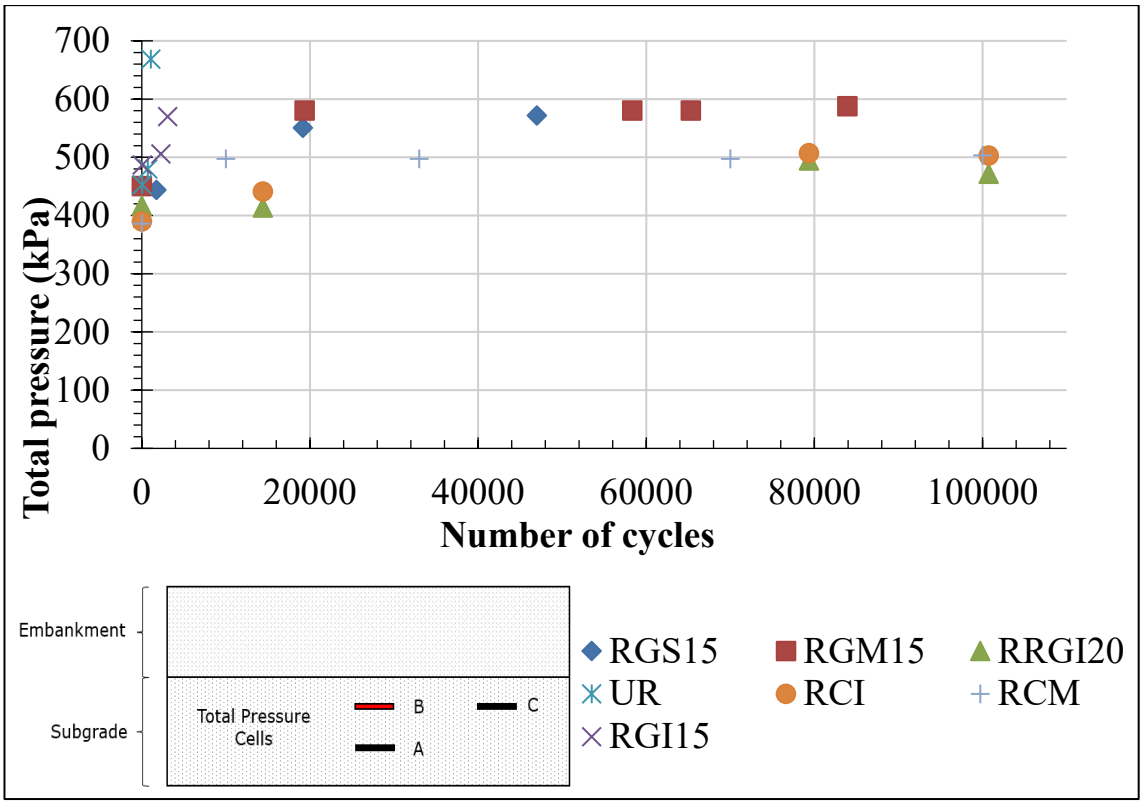

Figure 4.14 - Total stresses in initial condition tests in stress cell B for tests with base material.

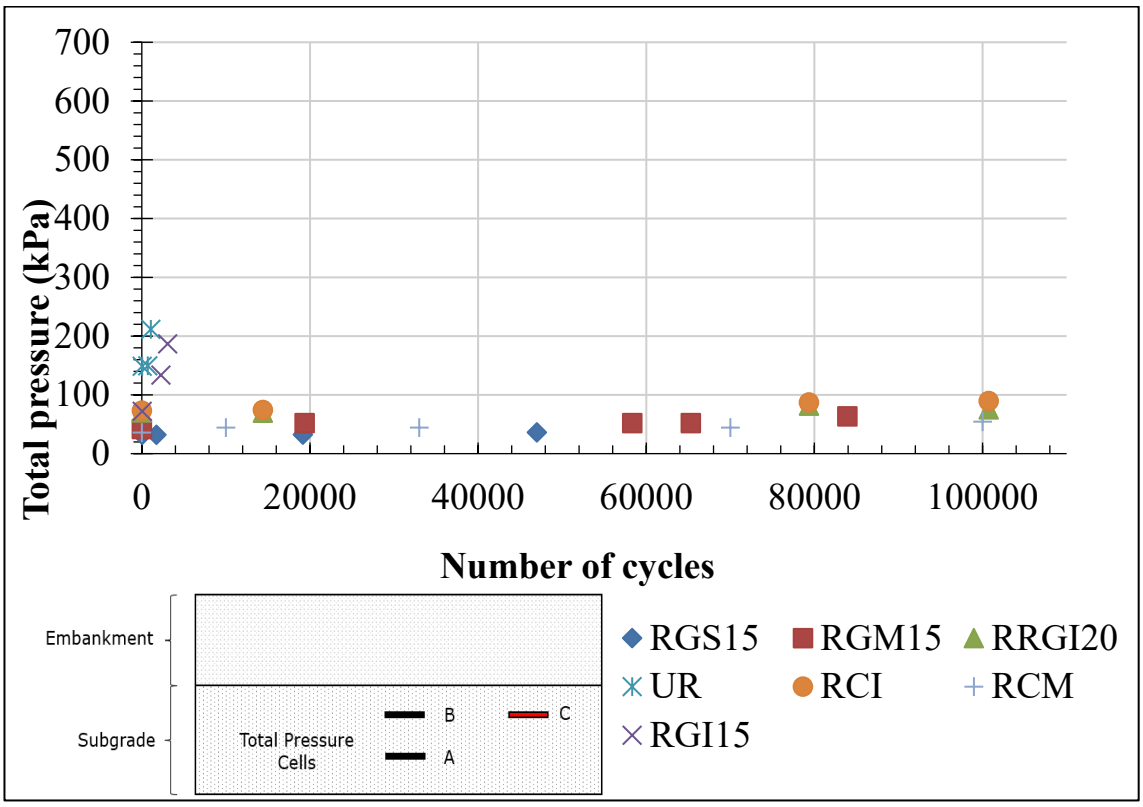

Figure 4.15 - Total stresses in initial condition tests in stress cell C for tests with base material.

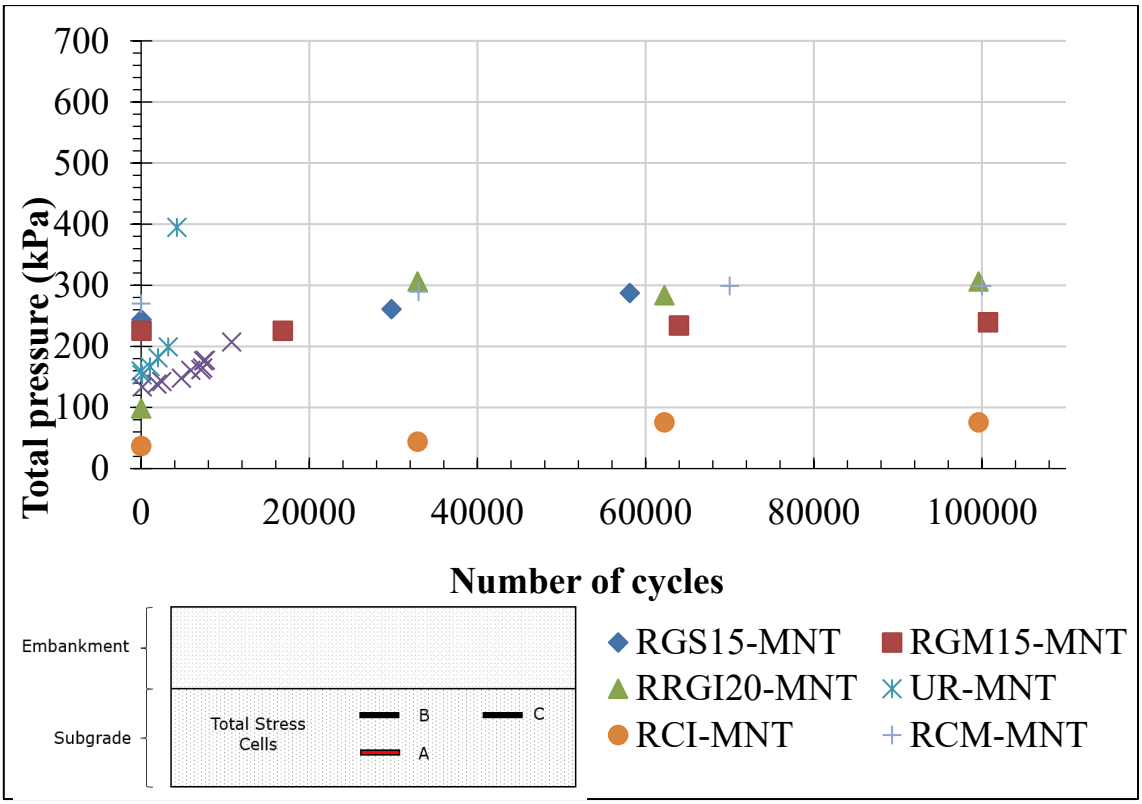

Figure 4.16 - Total stresses in post-maintenance condition tests in stress cell A for tests with base material.

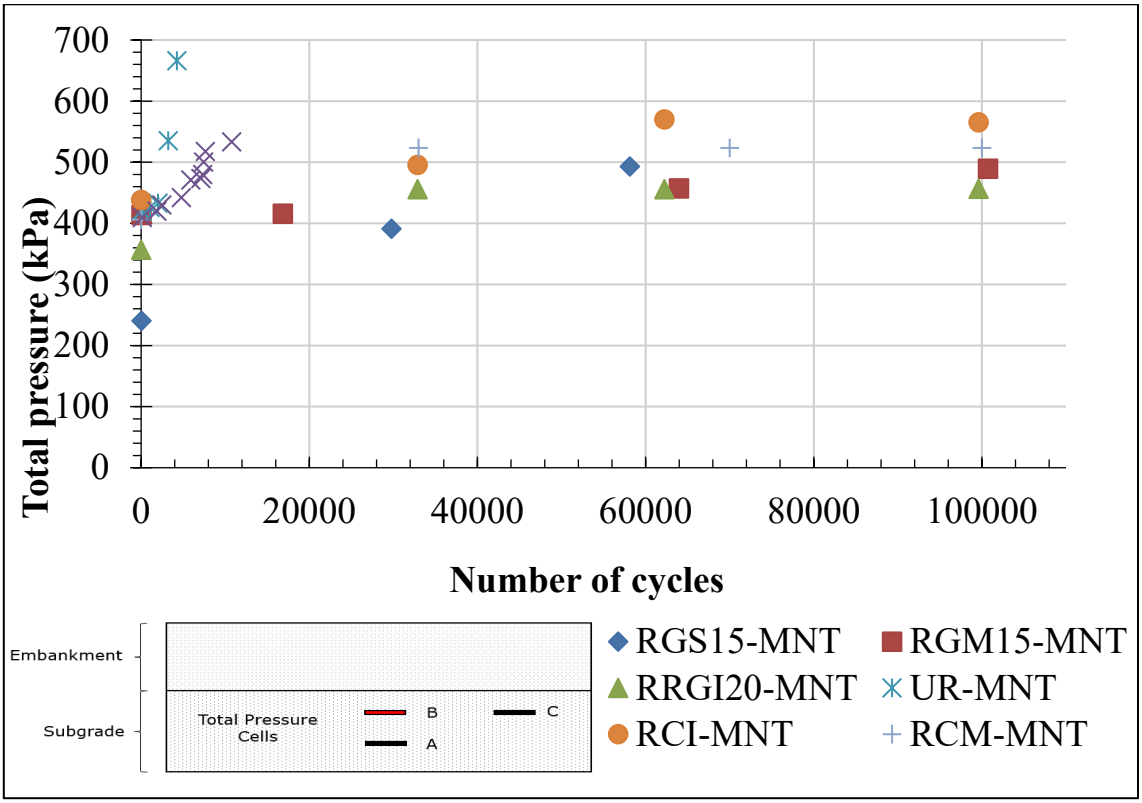

Figure 4.17 - Total stresses in post-maintenance condition tests in stress cell B for tests with base material.

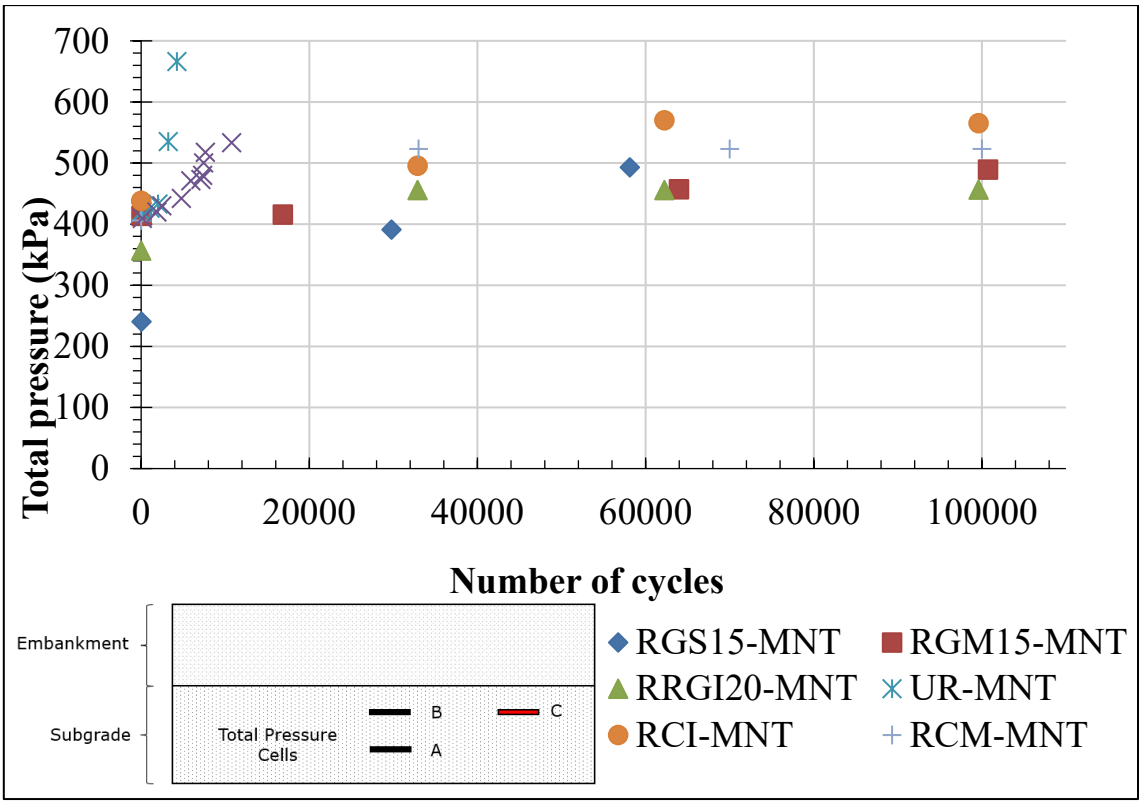

Figure 4.18 - Total stresses in post-maintenance condition tests in stress cell C for tests with base material.

In all analyzed cases, the unreinforced sections exhibited significantly higher vertical stress values compared to those reinforced with geocells. This indicates that the use of geocells effectively contributes to the reduction of vertical stresses transmitted to the subgrade. These findings are consistent with previous studies such as those by Banerjee et al. (2025), Evirgen et al. (2024) and Li et al. (2025), which demonstrated that the inclusion of geocells in pavement systems enhances load distribution, reduces stress concentrations on the subgrade, and improves overall structural performance.

From Figure 4.19 to Figure 4.31, the total stresses recorded during the tests with base-type granular material are presented. These figures show pressure ranges reaching up to a maximum of 700 kPa. It is evident that the unreinforced tests exhibit higher total stress values, highlighting the beneficial effect of geocells in improving stress distribution within the subgrade.

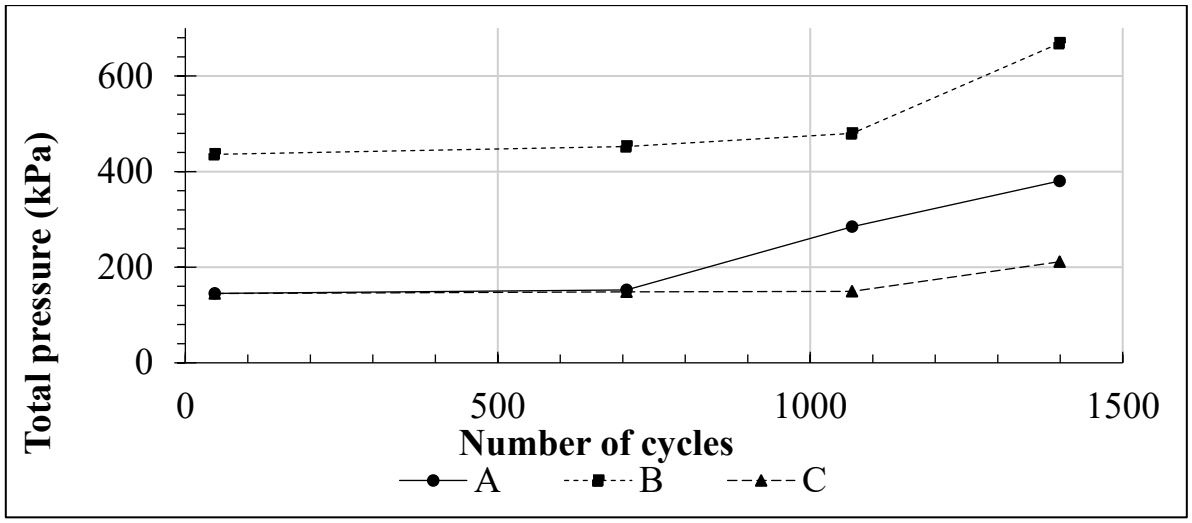

Figure 4.19 - Total stresses during the UR test (without reinforcement with base material pre-maintenance).

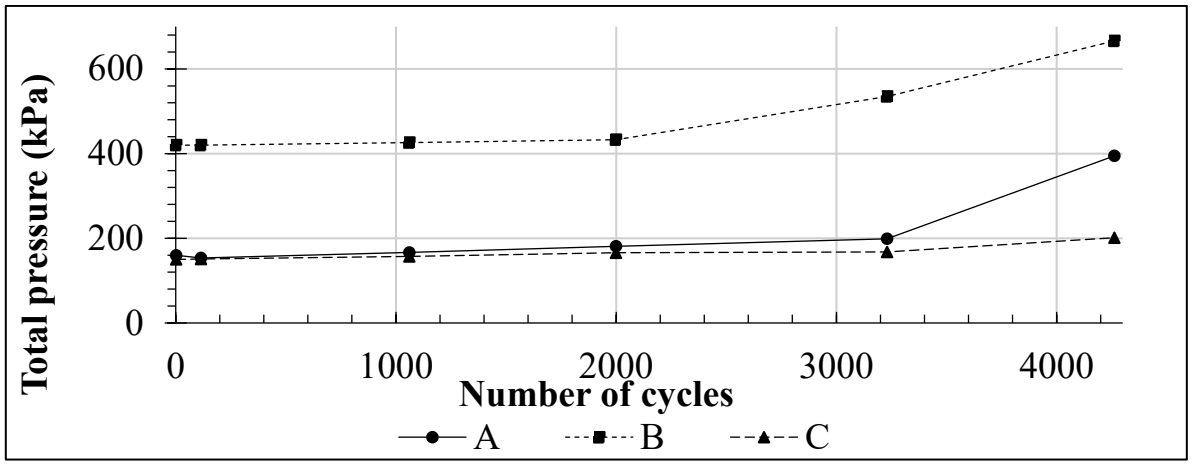

Figure 4.20 - Total stresses during the UR-MNT test (without reinforcement with base material, post-maintenance)

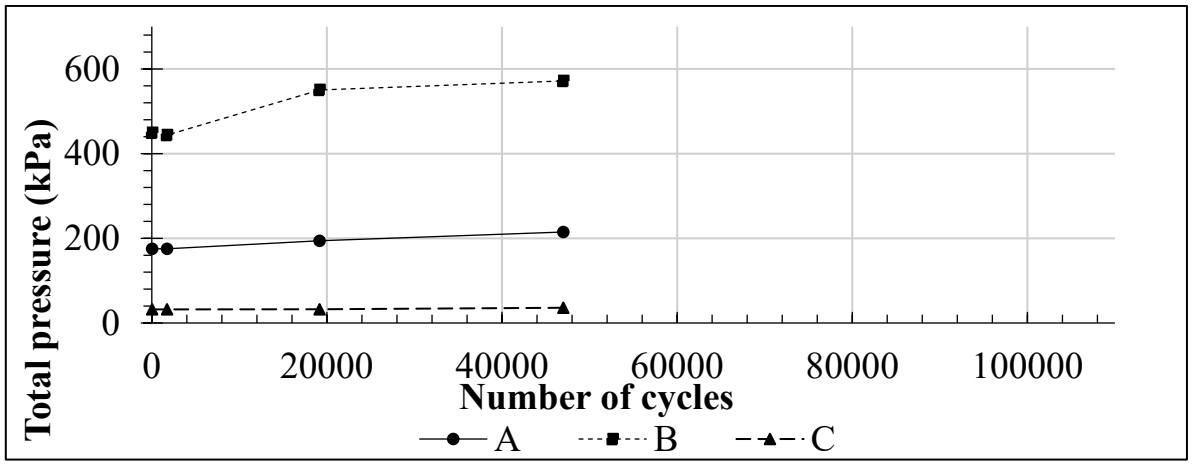

Figure 4.21 - Total stresses recorded in the RGS15 test (test with 15 cm geocell, surface location, base material, pre-maintenance).

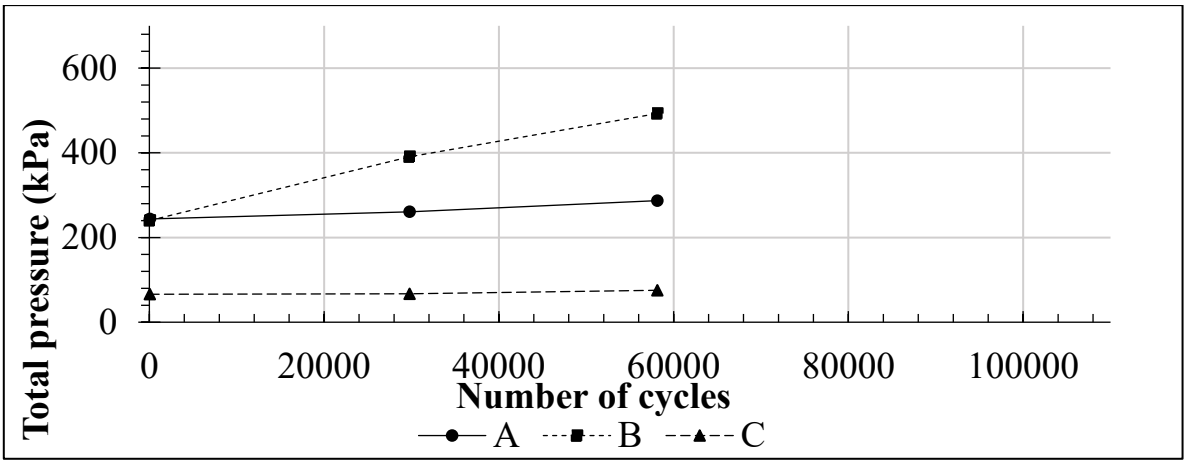

Figure 4.22 - Total stresses during the RGS15-MNT test (test with 15 cm geocell, surface location, base material, post-maintenance).

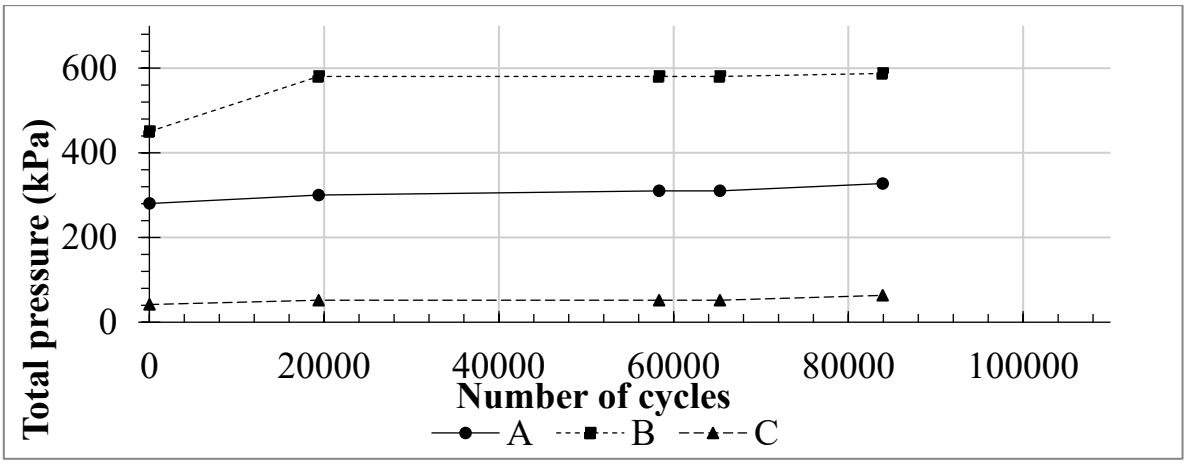

Figure 4.23. Total stresses recorded in the RGM15 test (test with 15 cm tire geocell, medium location, base material, pre-maintenance).

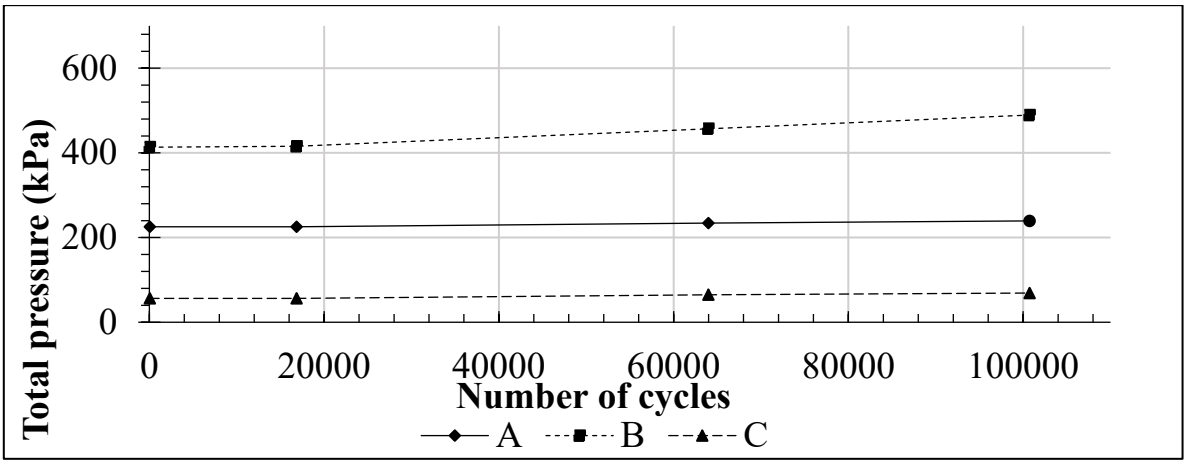

Figure 4.24 - Total stresses recorded in the RGM15 test (test with 15 cm tire geocell, medium location, base material, post-maintenance).

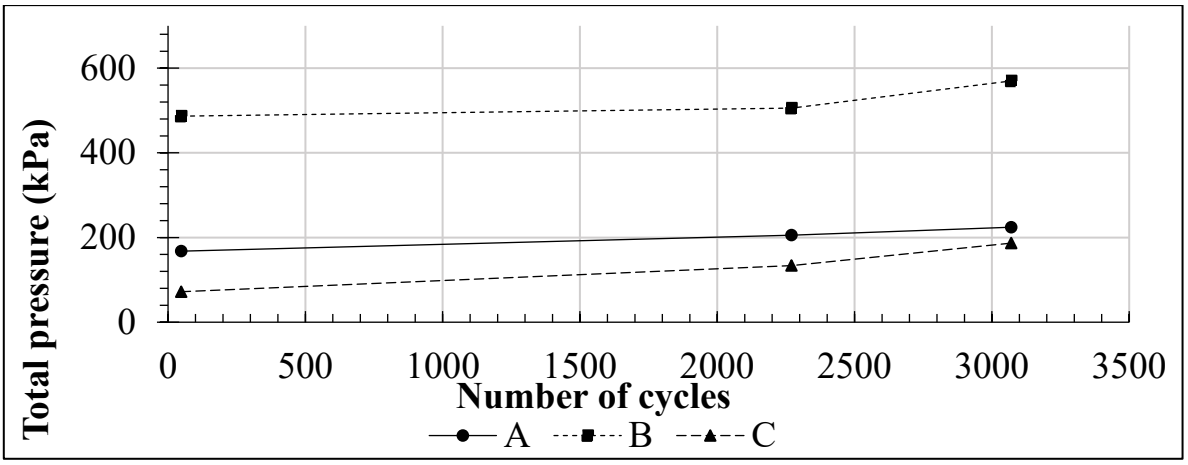

Figure 4.25. Total stresses recorded in the RGI15 test (test with 15 cm tire geocell, subgrade location, base material, pre-maintenance).

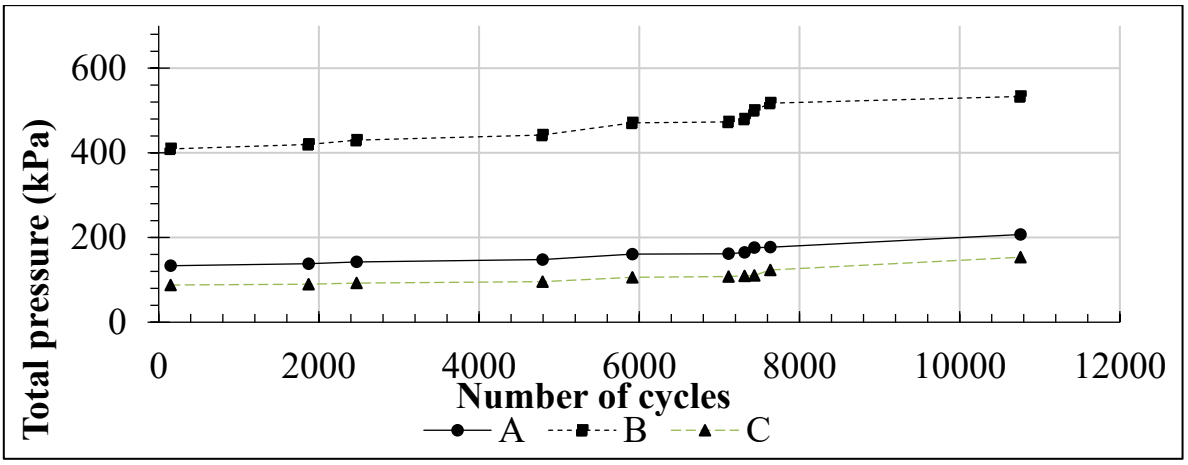

Figure 4.26. Total stresses recorded in the RGI15 test (test with 15 cm tire geocell, subgrade location, base material, post-maintenance).

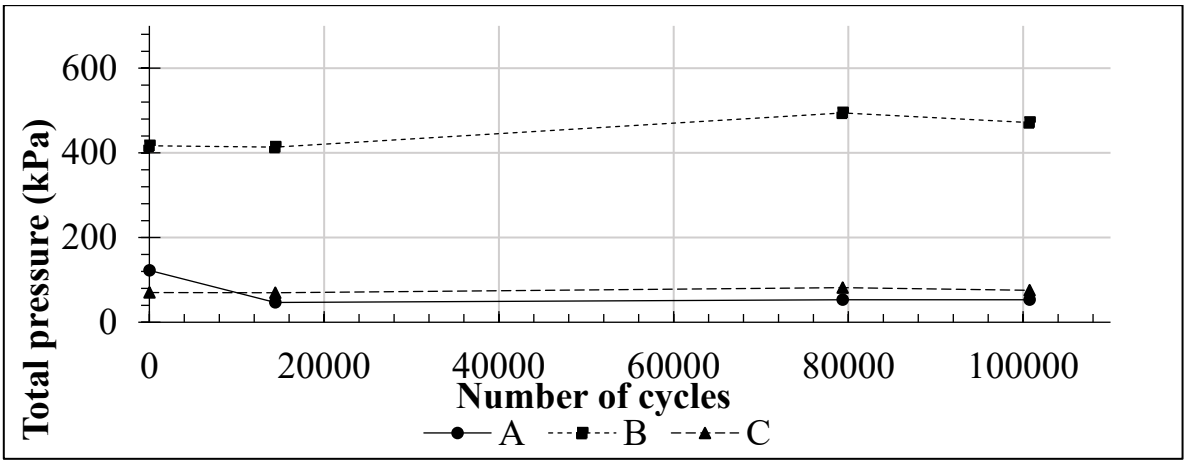

Figure 4.27. Total stresses recorded in the RGI20 test (test with 20 cm tire geocell, subgrade location, base material, pre-maintenance).

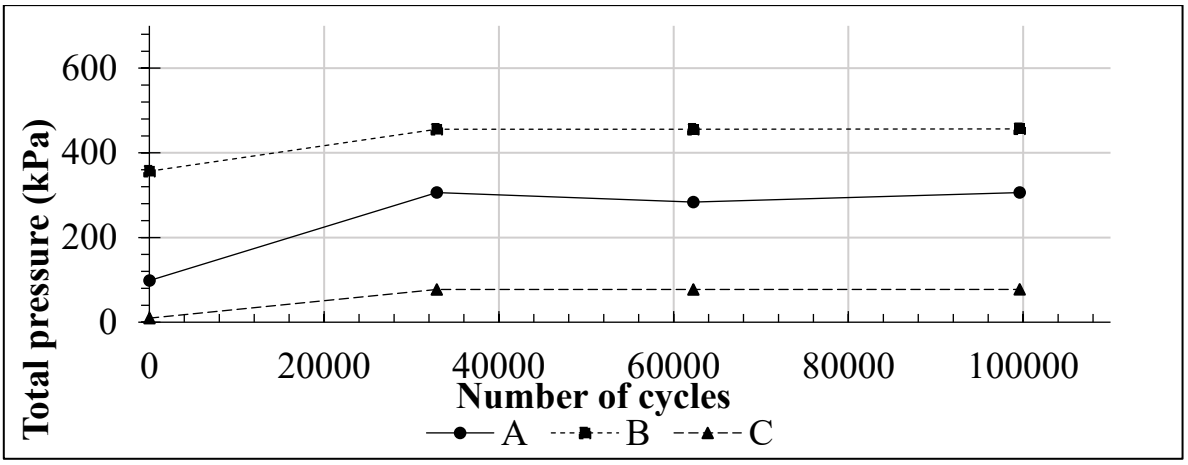

Figure 4.28 - Total stresses recorded in the RGI20 test (test with 20 cm tire geocell, subgrade location, base material, post-maintenance).

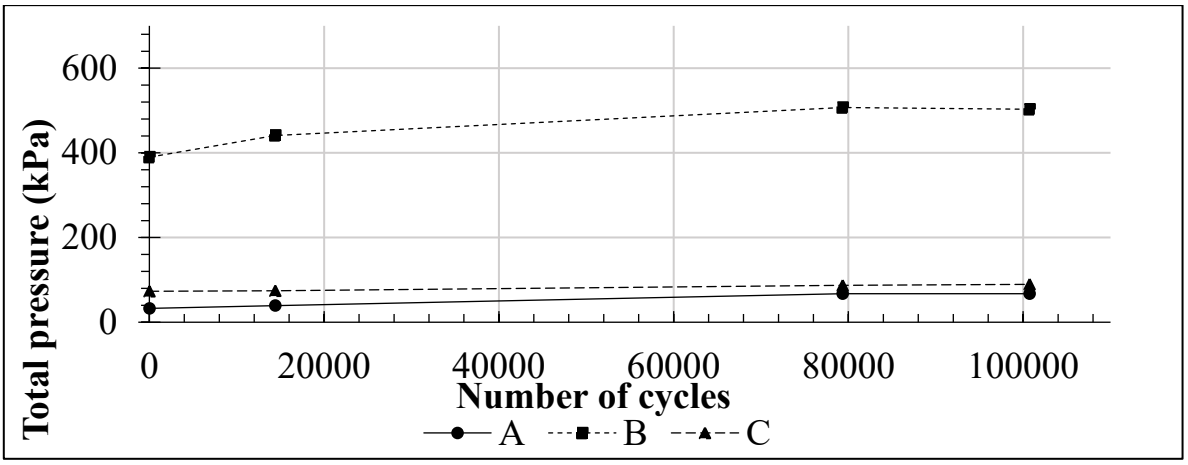

Figure 4.29 - Total stresses recorded in the RCI test (test with commercial geocell, subgrade location, base material, pre-maintenance).

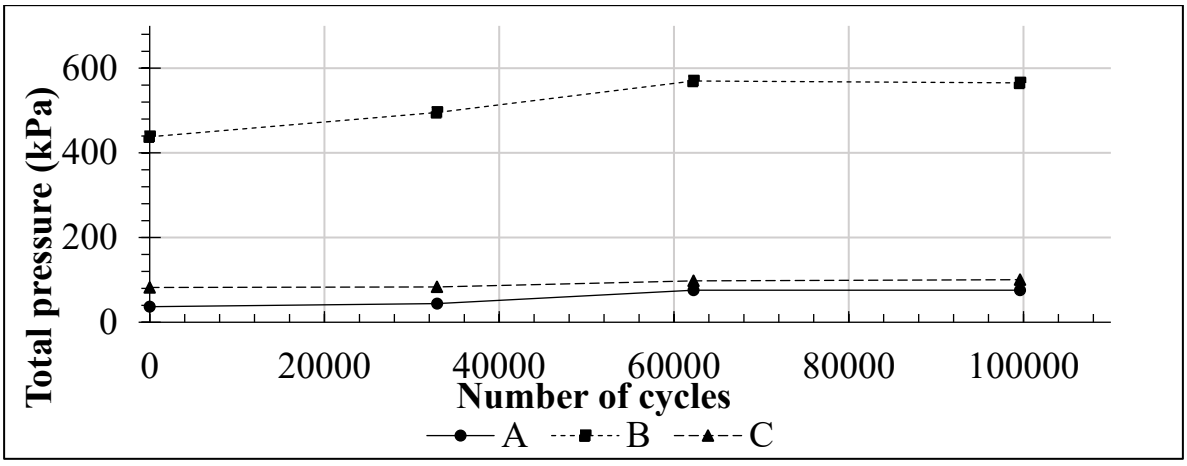

Figure 4.30 - Total stresses recorded in the RCI test (test with commercial geocell, subgrade location, base material, post-maintenance).

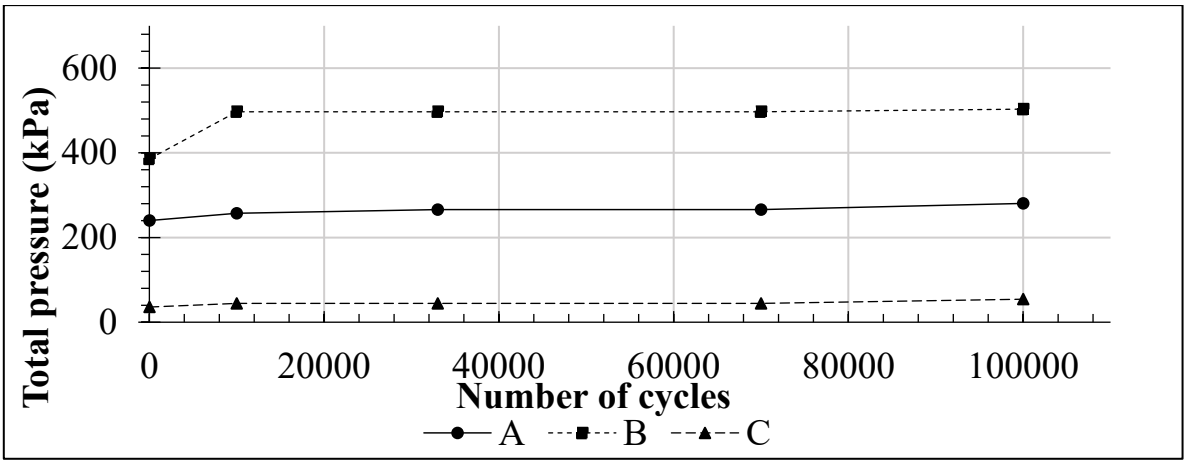

Figure 4.31 - Total stresses recorded in the RCM test (test with commercial geocell, center location of the base layer, base material, pre-maintenance).

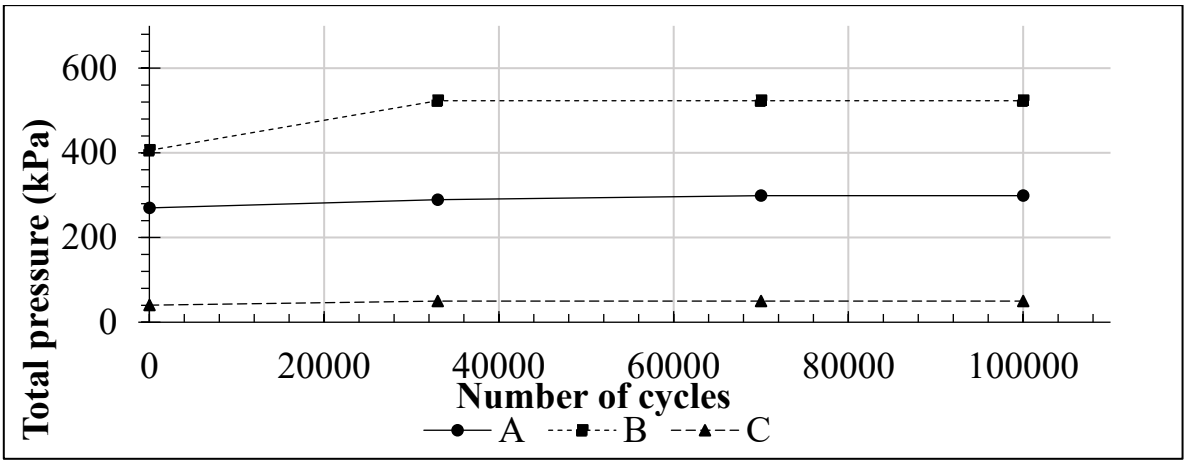

Figure 4.32 - Total stresses recorded in the RCM test (test with commercial geocell, center location of the base layer, base material, post-maintenance).

Figure 4.33 presents the total stresses measured by the pressure cells in the various tests conducted using base-type material. The results show a significant reduction in total stress for all reinforced systems compared to the unreinforced system (UR), highlighting the positive effect of the confinement provided by the geocells.

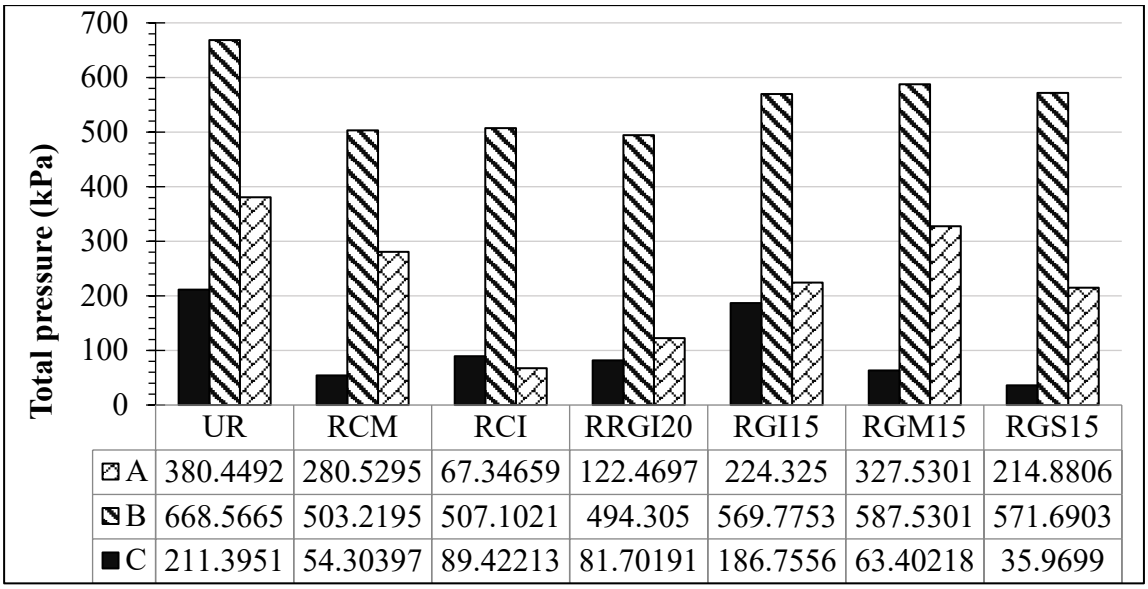

	UR	RCM	RCI	RRGI20	RGI15	RGM15	RGS15
A	380.4492	280.5295	67.34659	122.4697	224.325	327.5301	214.8806
B	668.5665	503.2195	507.1021	494.305	569.7753	587.5301	571.6903
C	211.3951	54.30397	89.42213	81.70191	186.7556	63.40218	35.9699

Figure 4.33 - Maximum total stresses in each of the tests conducted with base material.

As shown in Figure 4.34, the analysis of total stress behavior in the maintenance stage tests reveals that the maximum recorded values in the unreinforced configuration (UR-MNT) are significantly higher than those observed in the reinforced sections. This indicates that the absence of geocells results in higher stress transmission to the subgrade, thereby increasing the risk of permanent deformation in the road structure.

Moreover, the variation in stress recorded at cell C is smaller than that measured at position A, suggesting that stress concentration is more pronounced directly beneath the load application area.

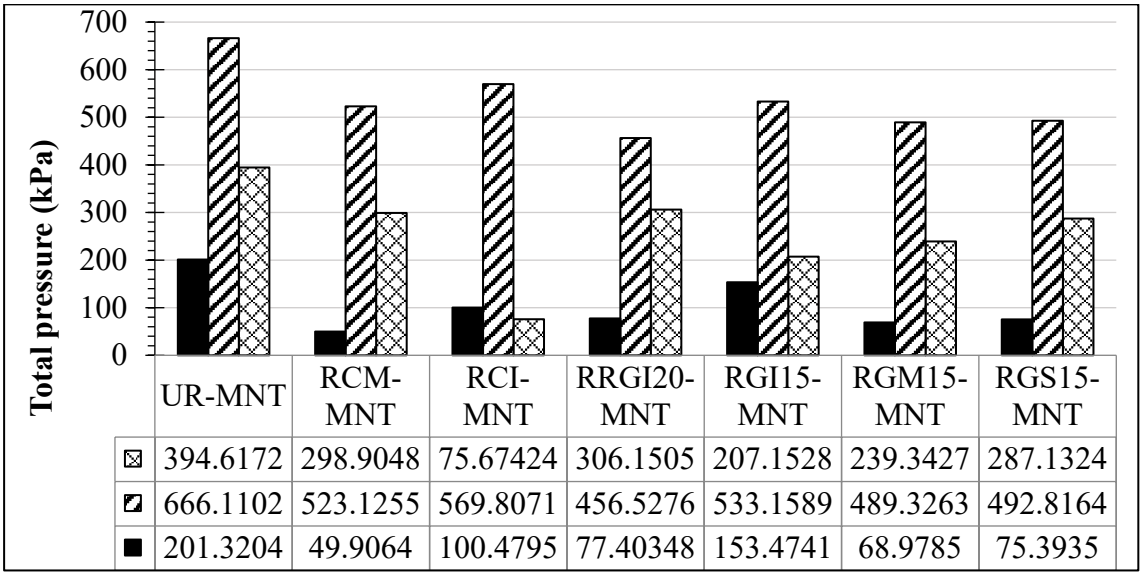

	UR-MNT	RCM-MNT	RCI-MNT	RRGI20-MNT	RGI15-MNT	RGM15-MNT	RGS15-MNT
	394.6172	298.9048	75.67424	306.1505	207.1528	239.3427	287.1324
	666.1102	523.1255	569.8071	456.5276	533.1589	489.3263	492.8164
	201.3204	49.9064	100.4795	77.40348	153.4741	68.9785	75.3935

Figure 4.34 - Maximum total pressure for reinforced and unreinforced tests with base material after maintenance.

Specifically, pressure cell B, located directly beneath the load application point, records the highest magnitude of pressure in all cases. The test reinforced with a geocell made from recycled tires and 20 cm in height (RRGI20) achieved a reduction of approximately 26 % compared to the unreinforced configuration, representing the highest efficiency among the alternatives analyzed. This behavior is consistent with the results obtained in the tests using commercial geocells (RCI and RCM), which show similar reductions, confirming that both the geometry and stiffness of the reinforcement directly influence the redistribution of stresses. In contrast, the tests with 15 cm high geocells also show improvements, although of smaller magnitude, suggesting that a greater cell height creates a stiffer and more confined zone capable of better absorbing and dispersing the loads transmitted to the subgrade.

In conclusion, these results support the assertion that the use of geocells enhances the structural efficiency of the system by reducing concentrated stresses on the subgrade, thereby promoting improved performance under repeated loading and increased durability of the unpaved road structure.

4.3.1. Evaluation of Total Stresses in Tests Conducted with Selected Fill Material (*Recebo*)

Recebo, commonly used in base or subbase layers of unpaved roads in Colombia, exhibits variable characteristics depending on its origin and gradation, which directly influence the distribution of stresses transmitted to the subgrade. This section presents the results obtained from the tests conducted, focusing on the analysis of the magnitude and behavior of total vertical stresses, with the aim of identifying their evolution as a function of the reinforcement type, confinement configuration, and measurement location within the testing system.

Figure 4.35 through Figure 4.40 present the total stress values measured at different locations within the subgrade. In most cases, a reduction in stress is observed for the reinforced sections, both under initial conditions and after maintenance, when using recebo as the fill material. This reduction is attributed to the load distribution effect provided by the geocells Studies such as Sujit Kumar, (2019) y Banerjee et al., (2024) affirm that the use of geocells improves stress distribution in the subgrade by expanding the load application area, thereby reducing the vertical pressure transmitted to the subgrade.

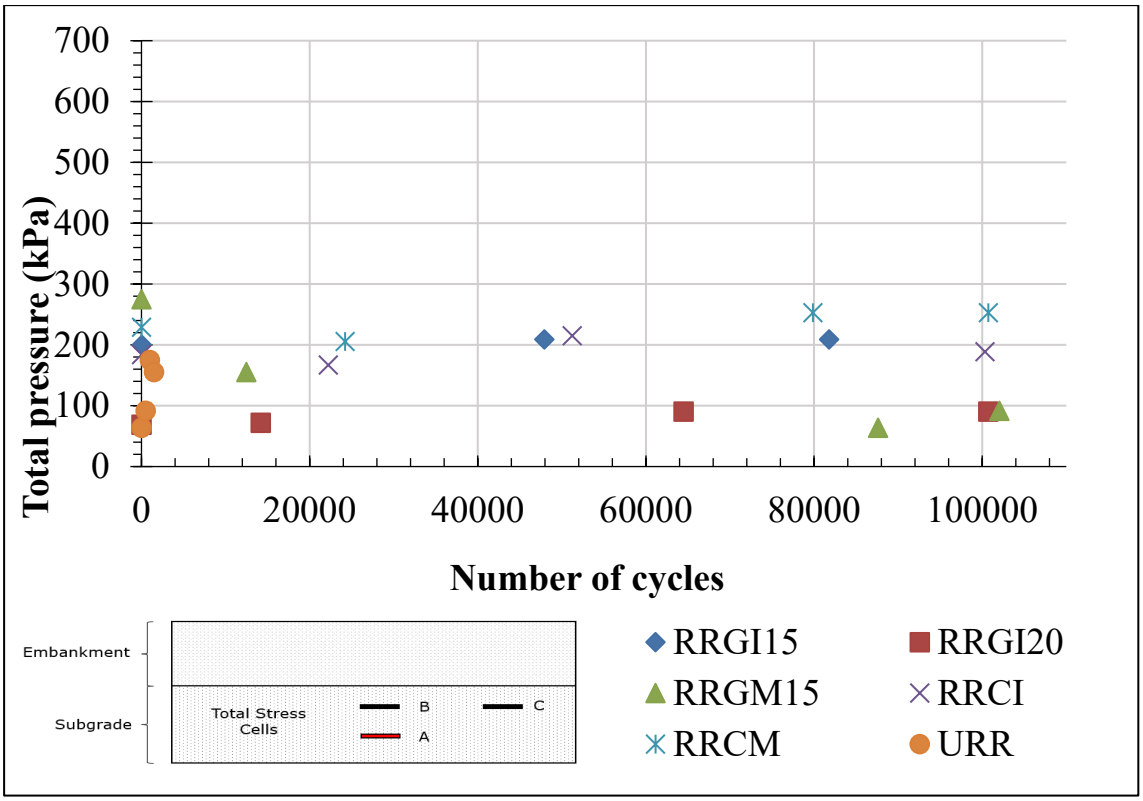

Figure 4.35 - Initial condition tests in stress cell A for tests with *recebo* fill material.

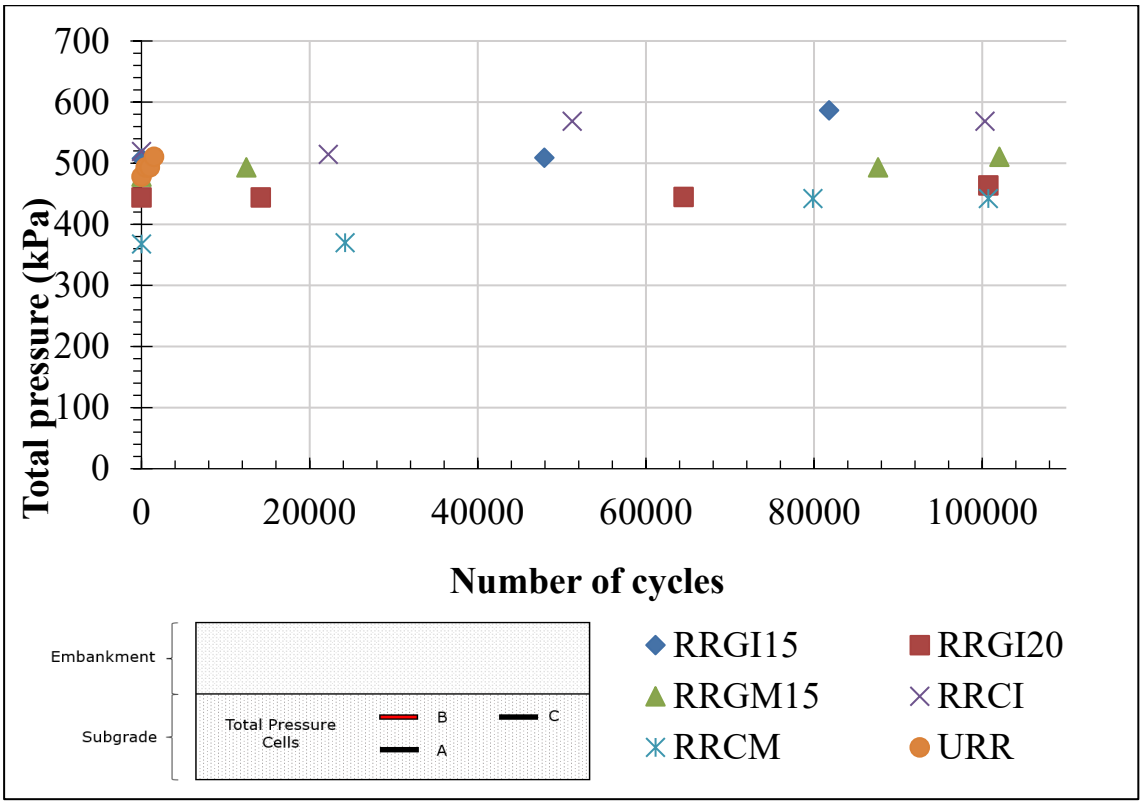

Figure 4.36 - Initial condition tests in stress cell B for tests with *recebo* fill material.

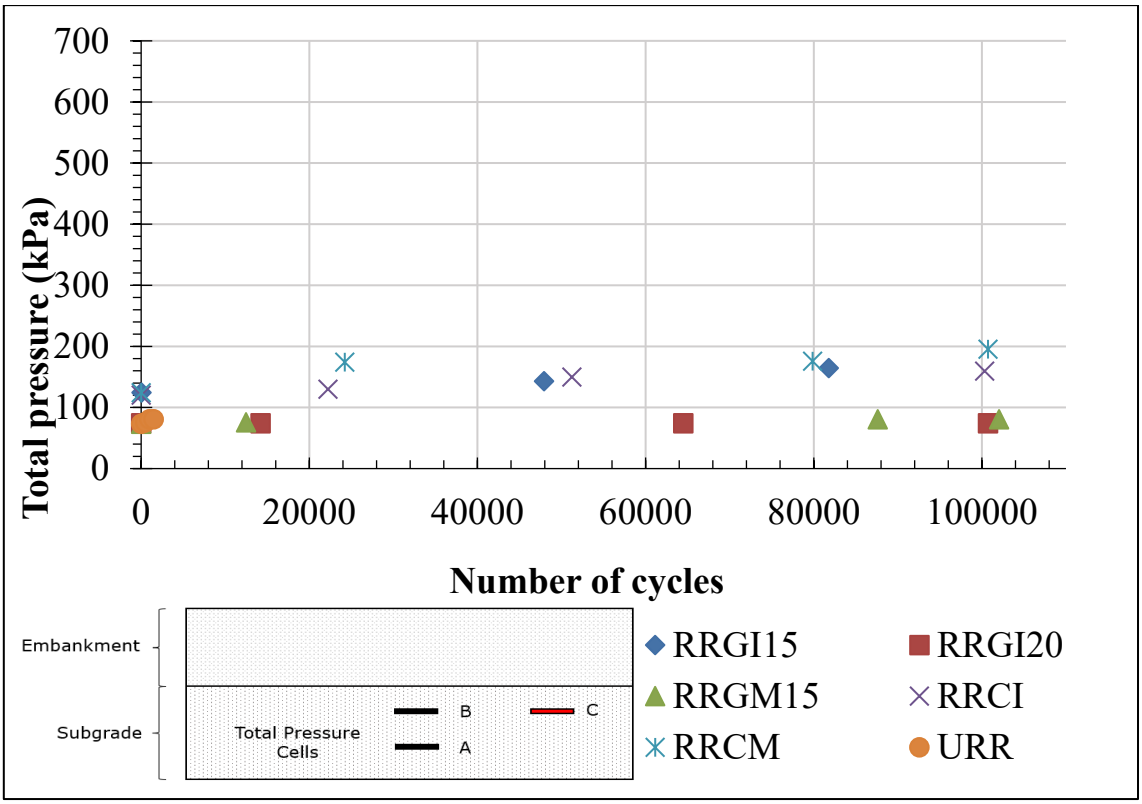

Figure 4.37 - Initial condition tests in stress cell C for tests with *recebo* fill material.

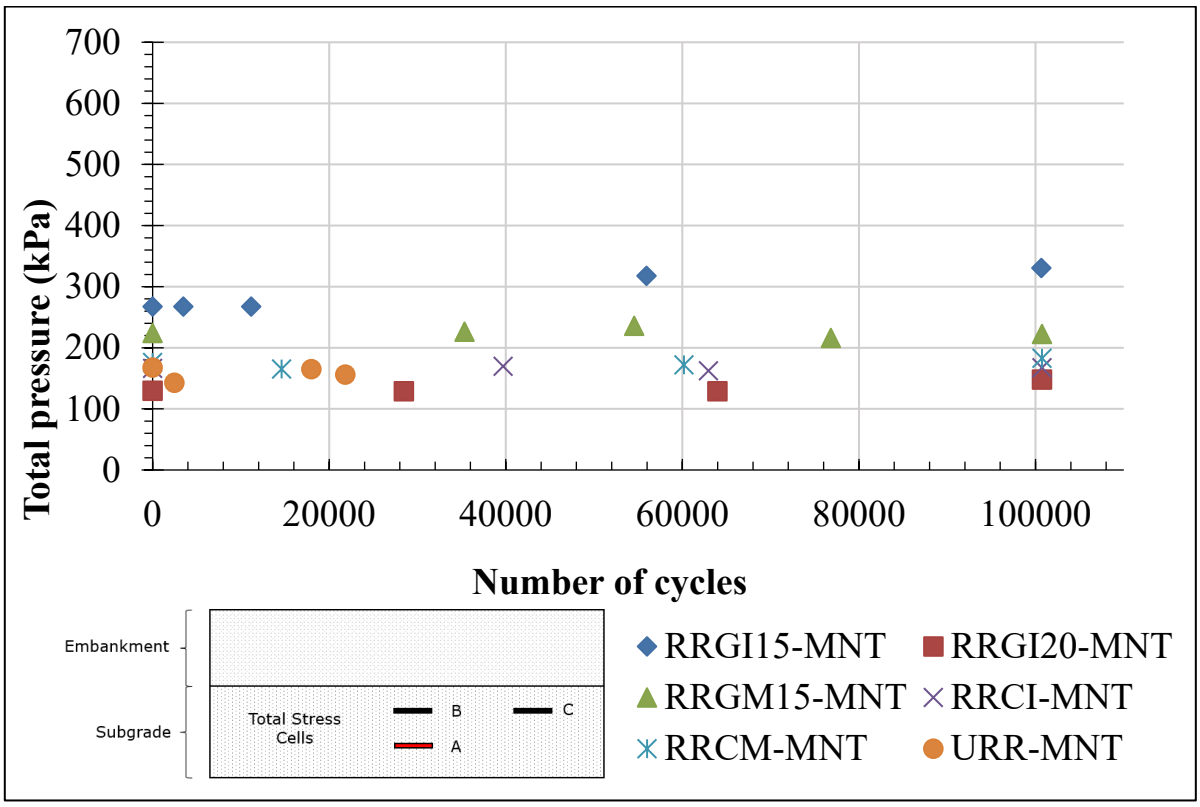

Figure 4.38 - Post-maintenance condition tests in stress cell A for tests with *recebo* fill material.

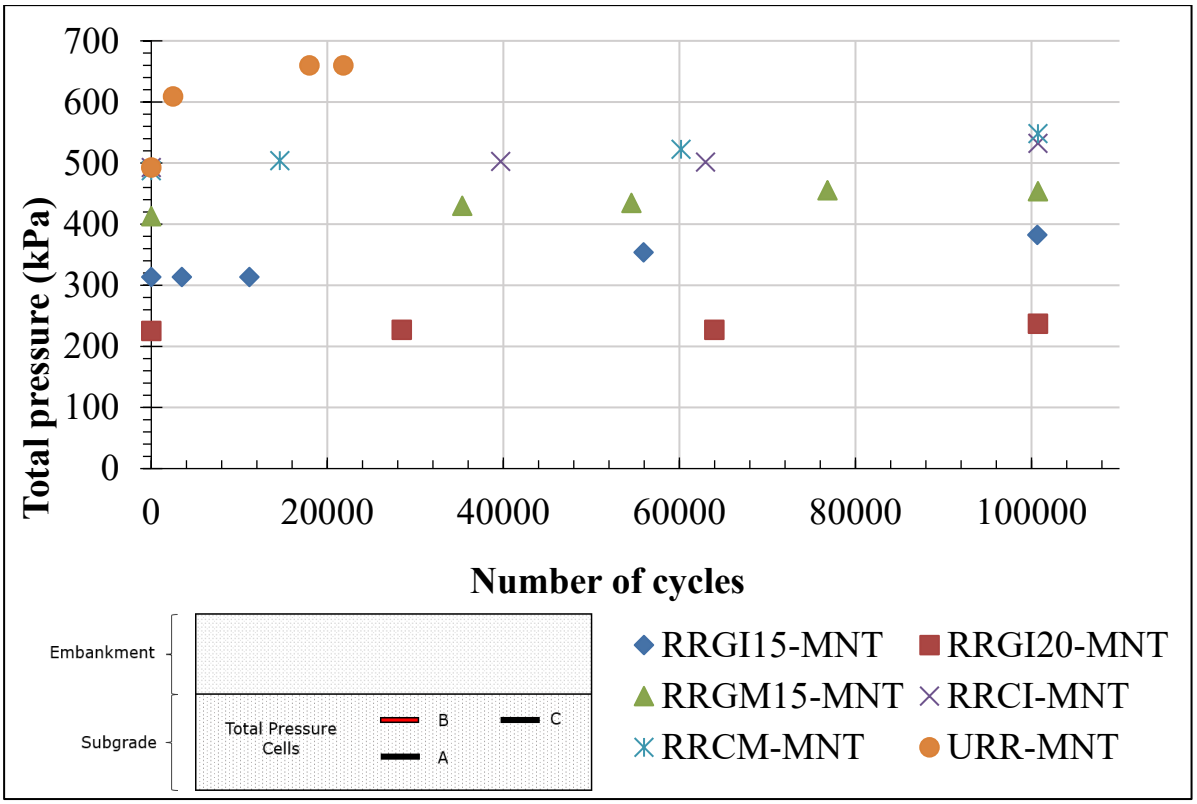

Figure 4.39 - Post-maintenance condition tests in stress cell B for tests with *recebo* fill material.

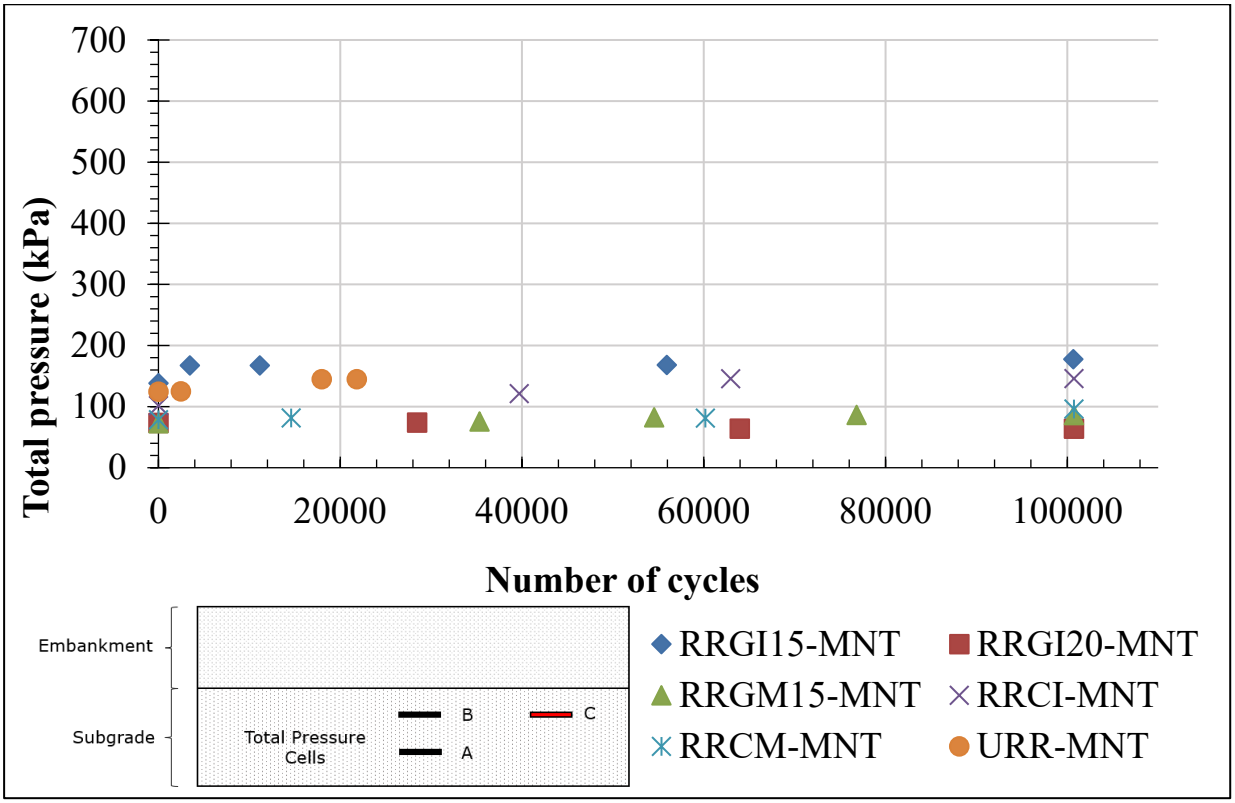

Figure 4.40 - Post-maintenance condition tests in stress cell C for tests with recebo fill material.

Figure 4.41 through Figure 4.52 show the total stress curves recorded during the tests conducted using *recebo* as the structural layer. Similar to the tests performed with granular base material, a trend of relatively constant total stress values is observed throughout the applied loading cycles, indicating system stabilization. Cell B, located directly beneath the load application point, consistently registers the highest-pressure values, as expected due to its strategic position. It is important to highlight that the unreinforced test displays the highest ranges of total stress, while the reinforced tests show a significant reduction in these values. This demonstrates a more effective redistribution of loads transmitted to the subgrade, attributed to the confinement effect provided by the geocells.

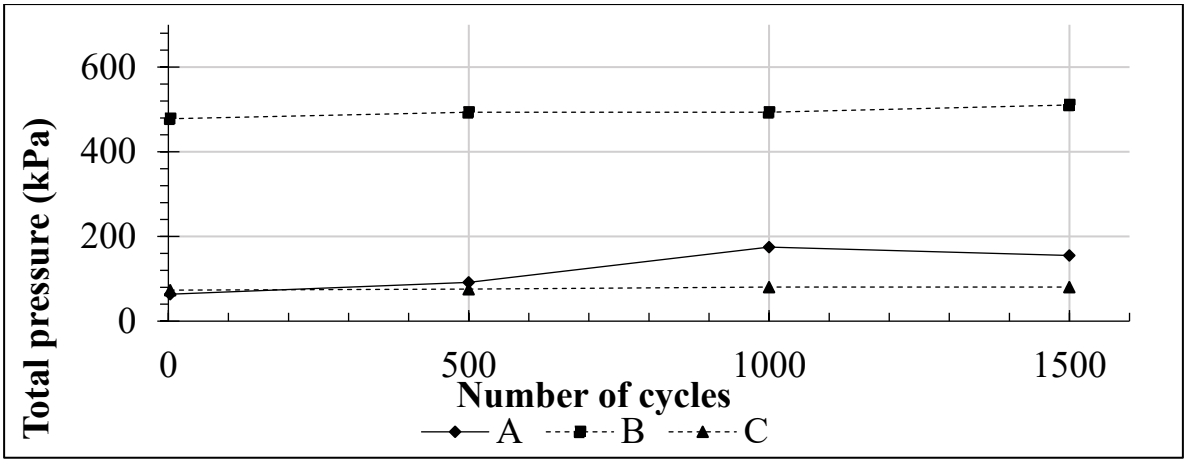

Figure 4.41 - Total stresses during the URR test (test without reinforcement with *recebo* fill material, pre-maintenance).

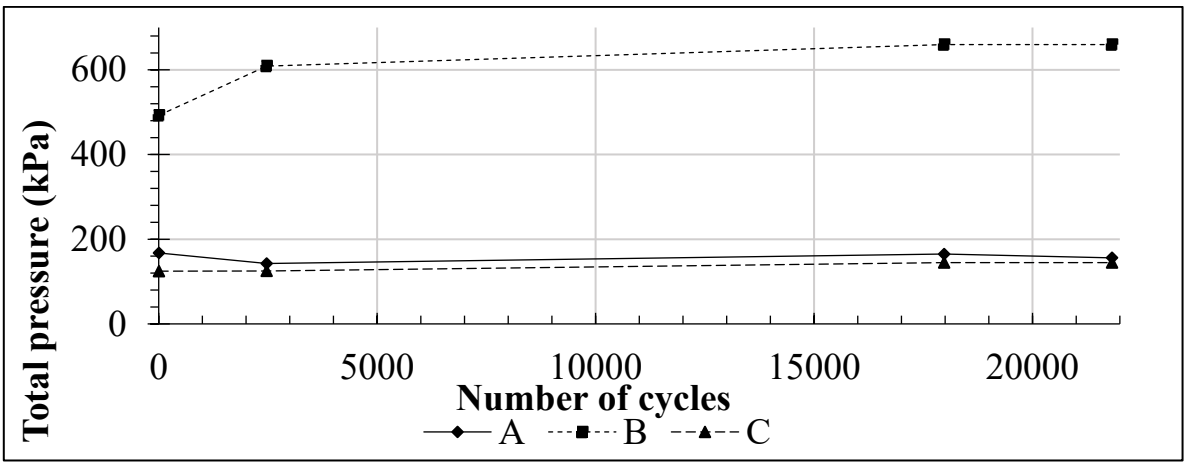

Figure 4.42 - Total stresses during the SRR-MNT test (test without reinforcement with *recebo* fill material, post-maintenance).

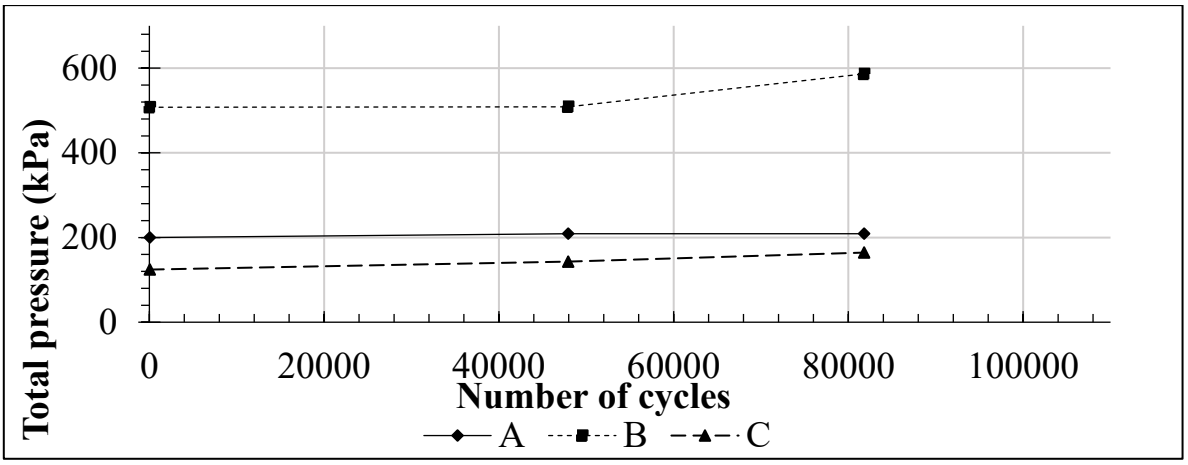

Figure 4.43 - Distribution of total stresses in the RRGI15 test (test with 15 cm recycled tire geocell, located on the subgrade, with *recebo* fill material, pre-maintenance).

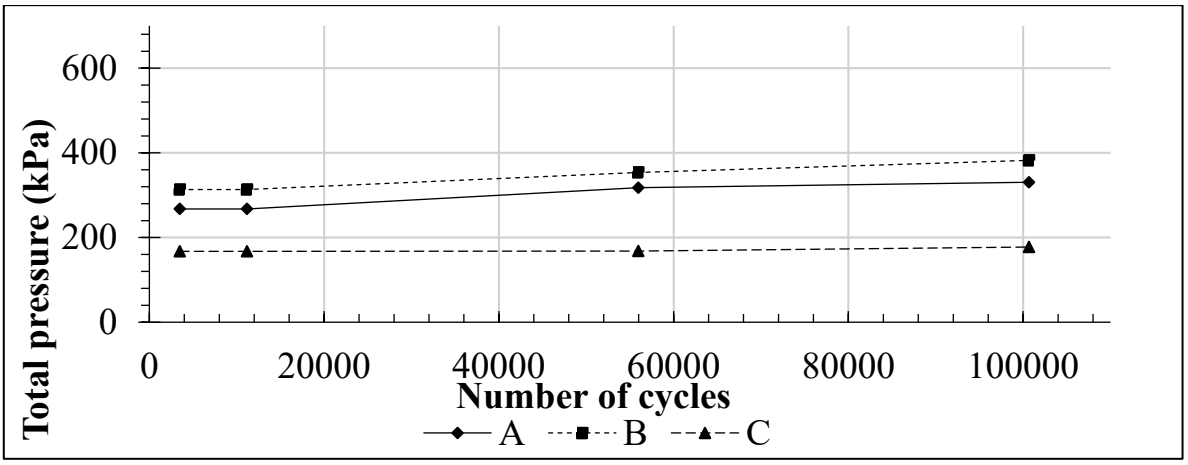

Figure 4.44. Distribution of total stresses in the RRGI15 test (test with 15 cm recycled tire geocell, located on the subgrade, with *recebo* fill material, post-maintenance).

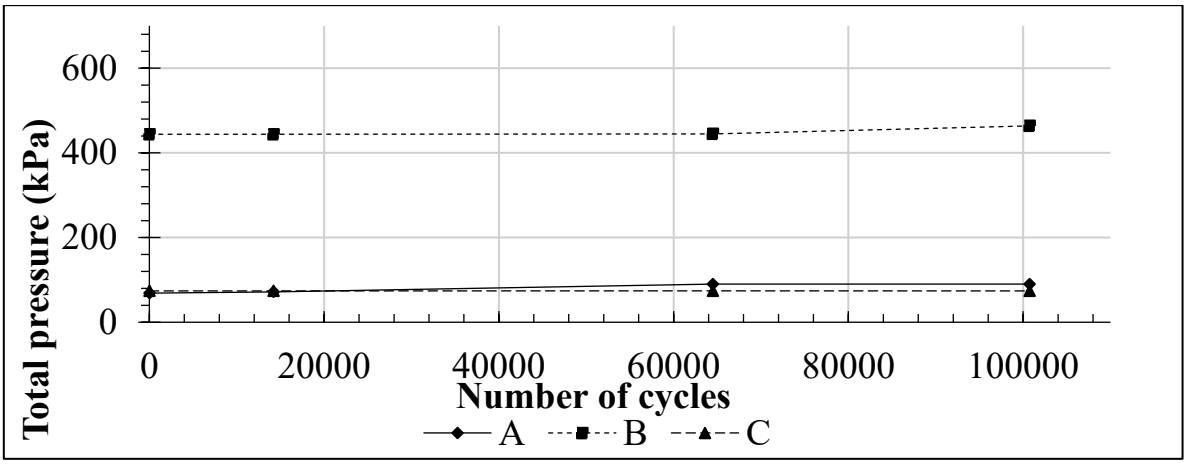

Figure 4.45. Distribution of total stresses in the RRGI20 test (test with 20 cm recycled tire geocell, located on the subgrade, with *recebo* fill material, pre-maintenance).

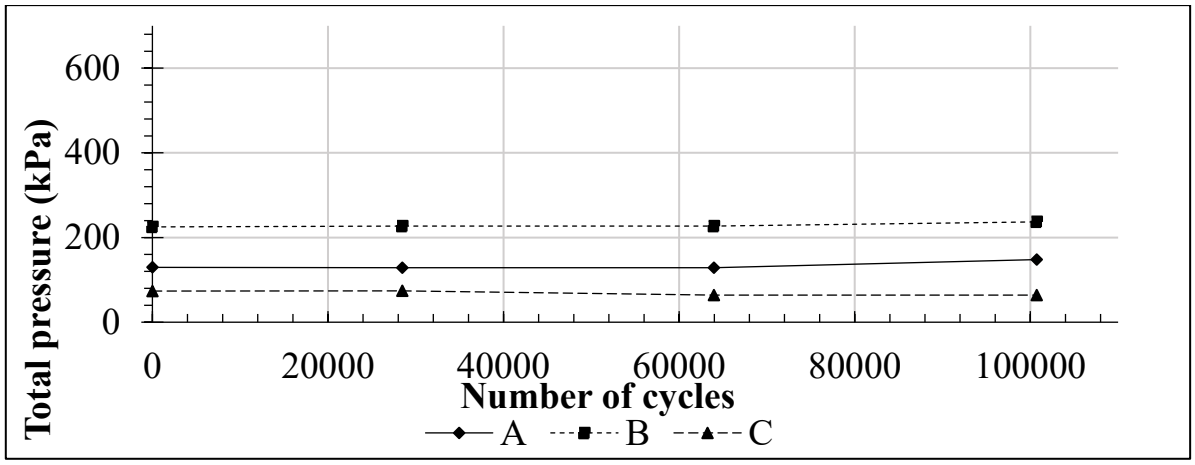

Figure 4.46. Distribution of total stresses in the RRGI20 test (test with 20 cm recycled tire geocell, located on the subgrade, with *recebo* fill material, post-maintenance).

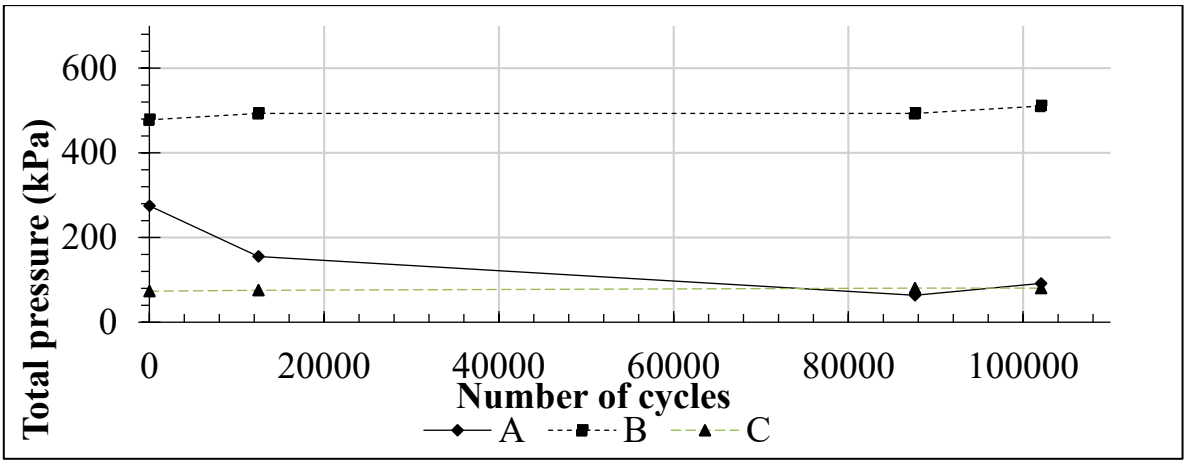

Figure 4.47 - Distribution of total stresses in the RRGM15 test (test with a 15 cm recycled-tire geocell, placed at mid-depth of the structural layer, with local granular material (*recebo)*, pre-maintenance condition).

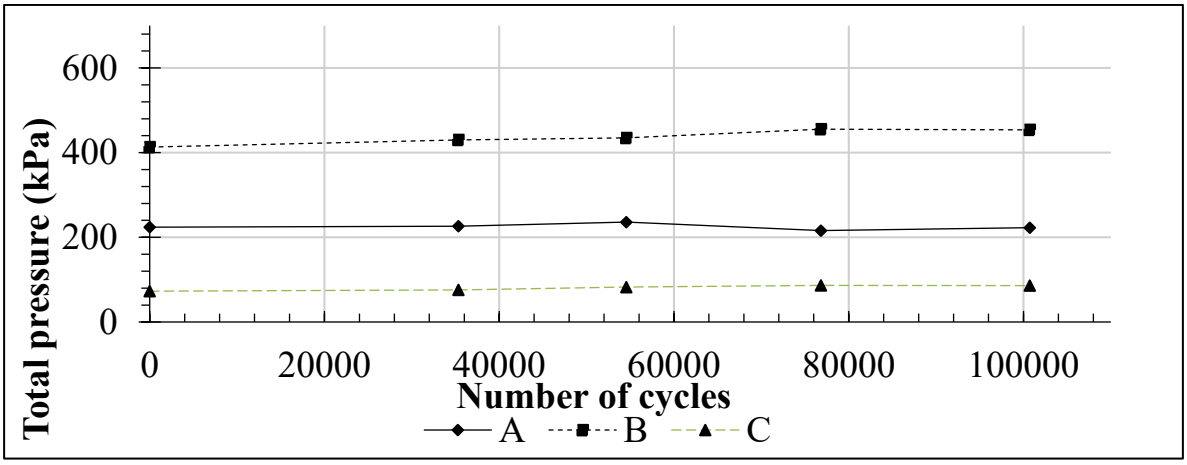

Figure 4.48. Distribution of total stresses in the RRGM15 test (test with a 15 cm recycled-tire geocell, placed at mid-depth of the structural layer, with local granular material (*recebo*), post-maintenance condition).

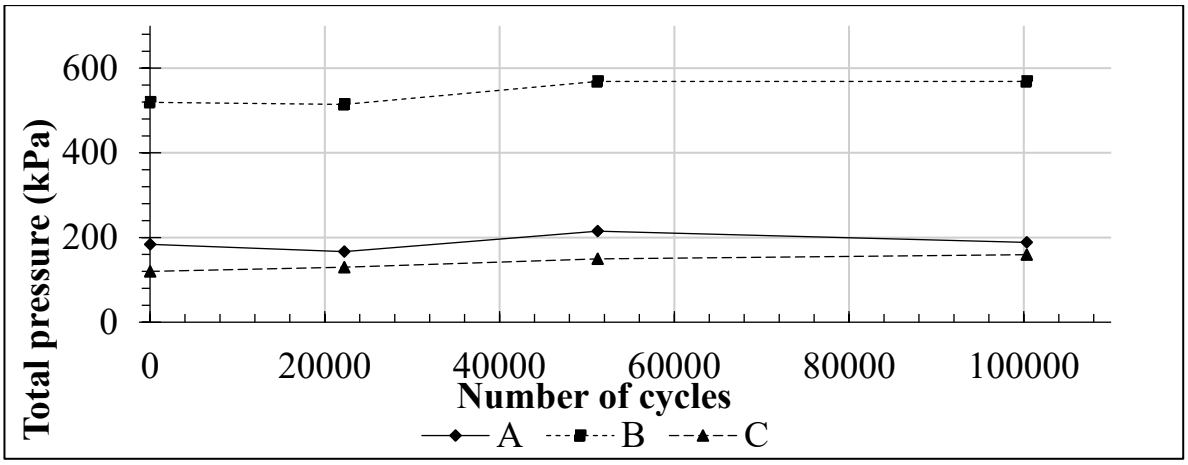

Figure 4.49. Distribution of total stresses in the RRCI test (test with a commercial geocell, placed on top of the subgrade, using typical local fill material *(recebo)*, pre-maintenance condition).

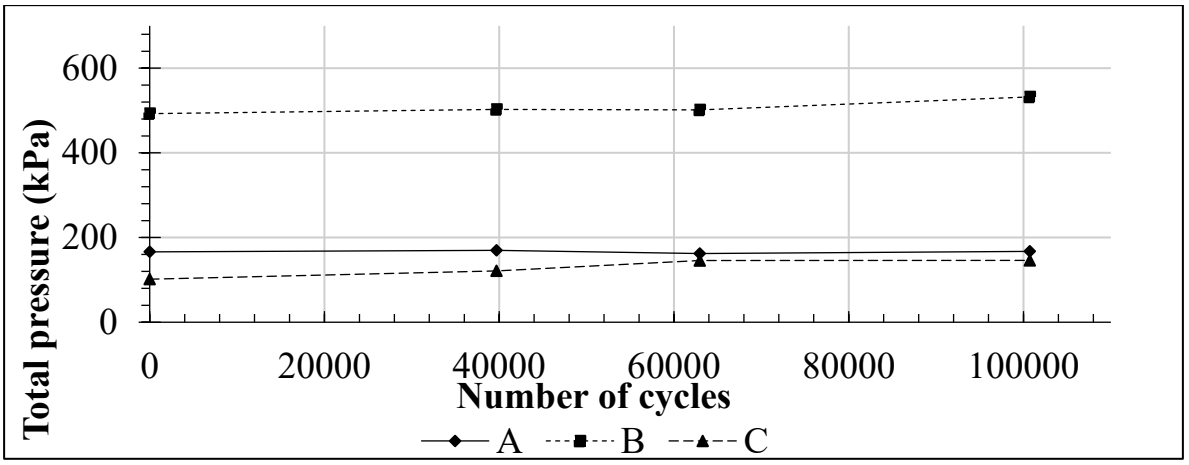

Figure 4.50. Distribution of total stresses in the RRCI test (test with a commercial geocell, placed on top of the subgrade, using typical local fill materia*l (recebo*), post-maintenance condition).

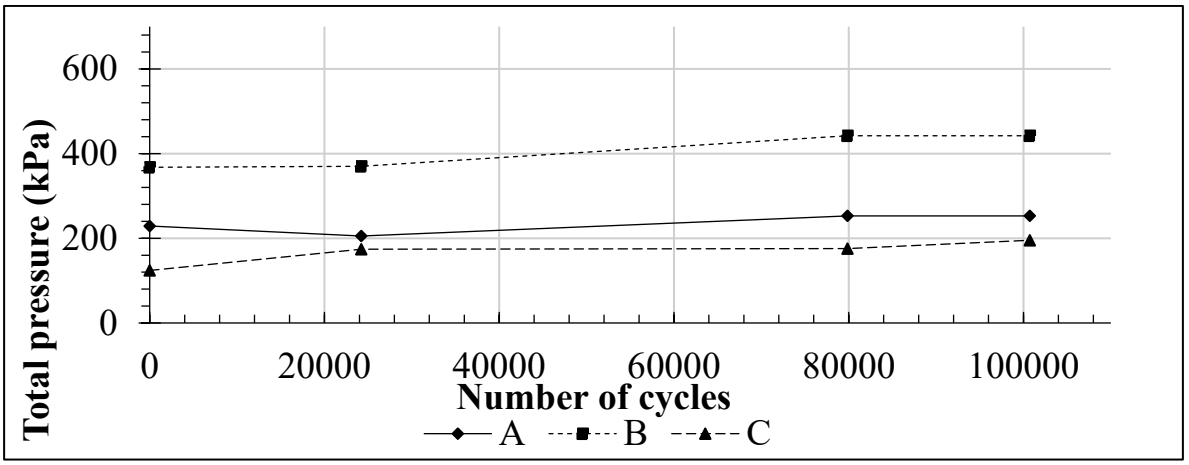

Figure 4.51 - Distribution of total stresses in the RRCM test (test with a commercial geocell, placed at mid-depth of the structural layer, using typical local fill material *(recebo*), pre-maintenance condition).

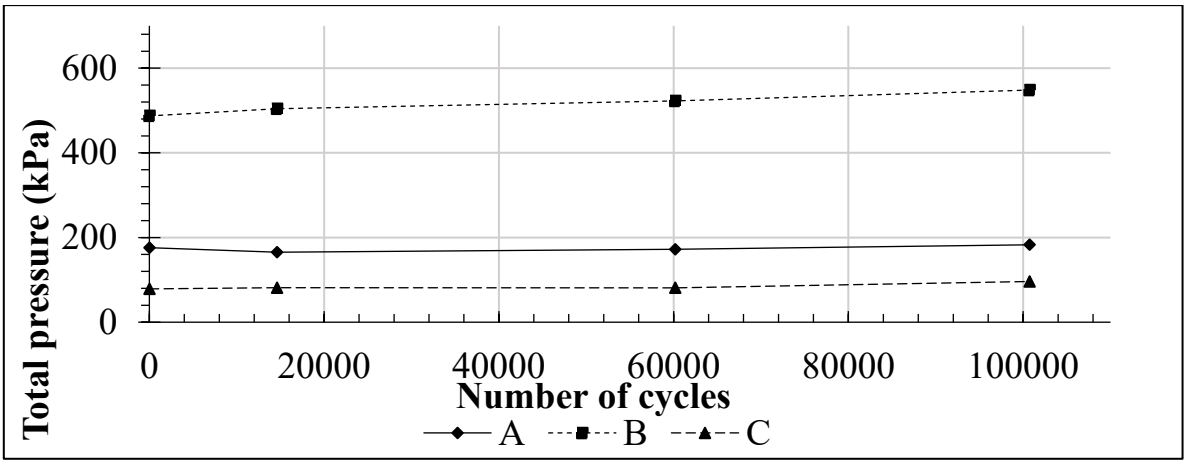

Figure 4.52 - Distribution of total stresses in the RRCM test (test with a commercial geocell, placed at mid-depth of the structural layer, using typical local fill material (*recebo*), post-maintenance condition).

Figure 4.53 shows the maximum stresses recorded during each test conducted with typical local fill material (*recebo*).

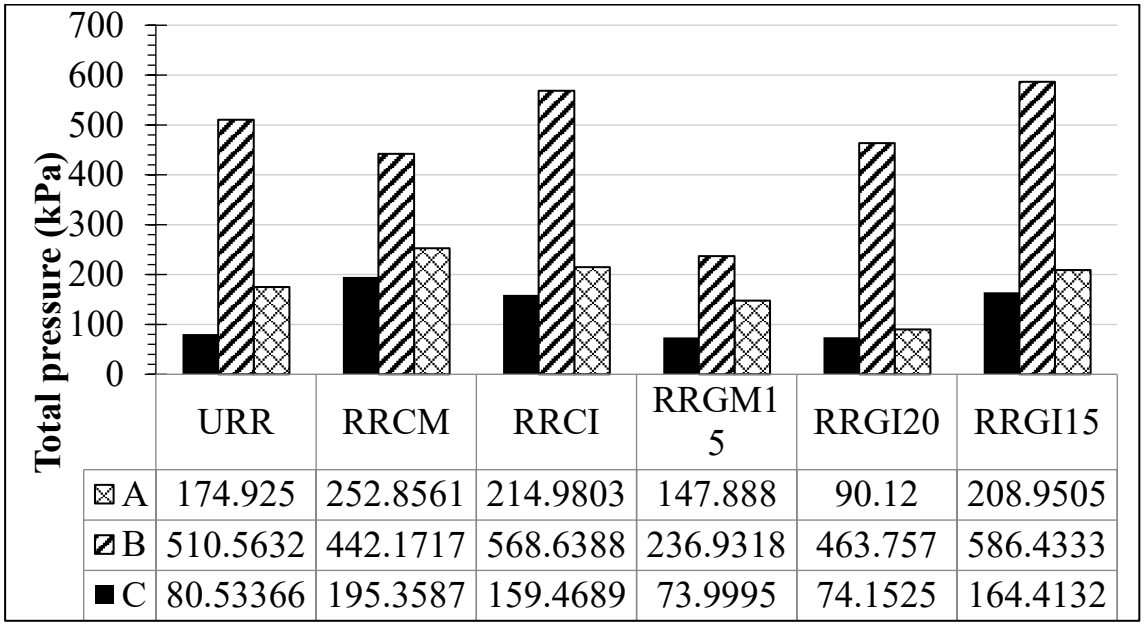

	URR	RRCM	RRCI	RRGM15	RRGI20	RRGI15
A	174.925	252.8561	214.9803	147.888	90.12	208.9505
B	510.5632	442.1717	568.6388	236.9318	463.757	586.4333
C	80.53366	195.3587	159.4689	73.9995	74.1525	164.4132

Figure 4.53 - Maximum total stresses in each of the tests conducted with typical local fill material (r*ecebo*).

Analysis of total stresses after maintenance in tests conducted with *recebo*-type material (see Figure 4.54) shows that the reinforced configurations follow the same trend as observed in the initial phase, effectively reducing stress peaks compared to the unreinforced section (URR-MNT). Furthermore, it is evident that the cells located directly beneath the centre of load application register the highest stress values, while also demonstrating a more significant

reduction compared to the initial condition. This confirms the effectiveness of the reinforcement in redistributing stresses following the intervention.

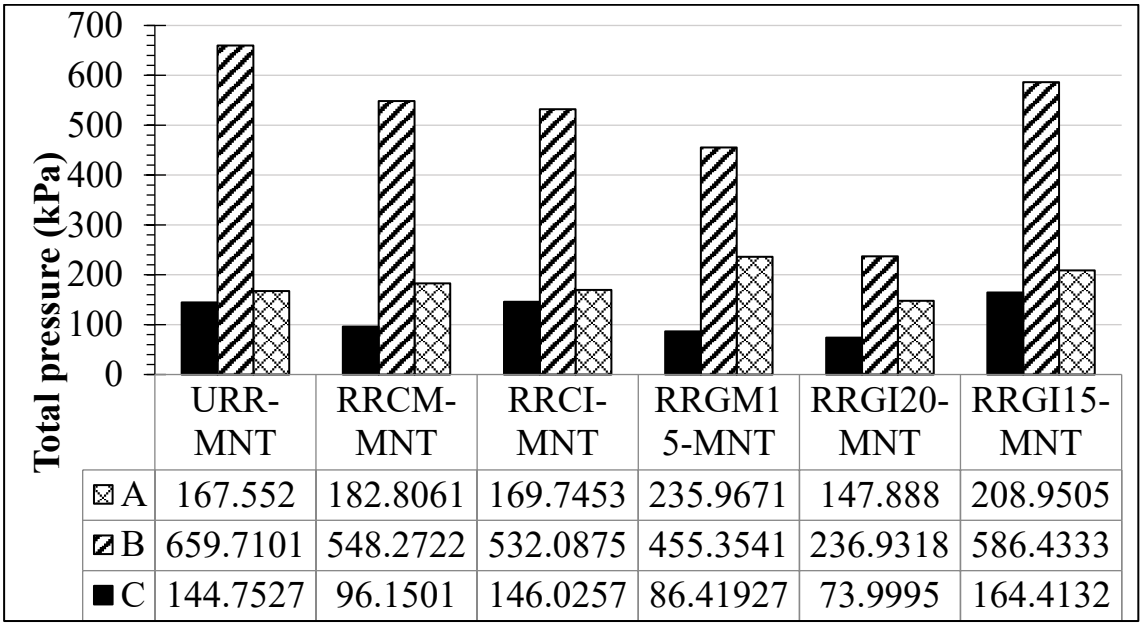

	URR-MNT	RRCM-MNT	RRCI-MNT	RRGM15-MNT	RRGI20-MNT	RRGI15-MNT
A	167.552	182.8061	169.7453	235.9671	147.888	208.9505
B	659.7101	548.2722	532.0875	455.3541	236.9318	586.4333
C	144.7527	96.1501	146.0257	86.41927	73.9995	164.4132

Figure 4.54 - Maximum total stresses in each of the tests conducted with typical local fill material (*Recebo*).

The results obtained regarding the reduction of stresses within the foundation material through the use of geocells as reinforcement are consistent with numerous previous studies (Feng et al., 2024; J. O. Avesani Neto, 2015; Krishna, 2023; Martins, 2024), which have extensively documented the membrane effect and stress dispersion mechanisms and their contribution to enhancing the structural performance of reinforced soils.

4.4. BREAKAGE INDEX (BG%)

Figure 4.55 shows the behavior of the grain breakage index (Bg%) for the different configurations evaluated, compared to the reference value of the unreinforced system (URR, represented by the red dashed line). At first glance, it can be seen that the unreinforced test exhibits a lower Bg% than all the reinforced systems, which might be interpreted as a more "flexible" behavior in terms of unrestricted aggregate deformation. However, this interpretation must be approached with caution.

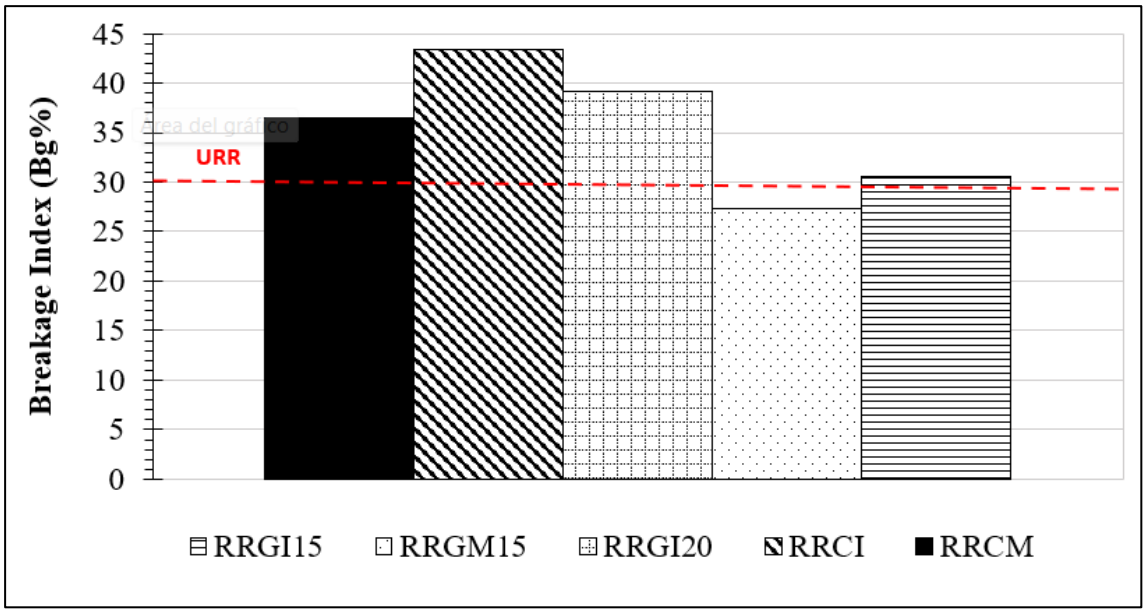

Figure 4.55 - Break index of the tests conducted with typical local fill material (*recebo*).

The lower Bg% value observed in the URR configuration may be influenced by the fact that it was the system with the shortest duration, reaching failure in less than 25,000 cycles. As a result, the aggregate was subjected to fewer loading cycles, limiting the accumulation of fractures. Furthermore, in the absence of confinement, the material was able to redistribute and rearrange freely, reducing the likelihood of particle breakage due to confined friction for such lower number of load cycles.

In contrast, the RRGI20 test, which employed 20 cm-high geocells made from recycled tires, exhibited the highest grain breakage index. This response can be attributed to the strong lateral confinement provided by the geocell, which creates a semi-rigid slab-like structure that restricts horizontal movement of the material. This confinement leads to stress concentration at contact points, increasing the probability of particle breakage.

Additionally, it was observed that the RRGM15 and RRGI15 configurations, which employed geocells fabricated from recycled tires, exhibited lower grain breakage indices compared to the RCI and RRCM tests that used commercial geocells. This difference may be attributed to the nature of the reinforcement material: rubber derived from recycled tires exhibits a more elastic and flexible behavior, allowing for a certain degree of energy absorption under cyclic loading, thereby reducing the stiffness of the confinement. In contrast, commercial geocells tend to be

more rigid, which increases the stress concentration at the contact points between particles, promoting their fracture.

This result suggests that the elasticity of the reinforcement directly influences the integrity of the confined aggregate, and that tire-derived geocells may offer a more favorable balance between confinement efficiency and preservation of the granular material.

Figure 4.56 presents the results of the grain breakage index (Bg%) for the configurations using base material. Consistent with the tests conducted with *recebo*, the highest breakage value was observed in the RGI20 test, which incorporated 20 cm-high geocells made from recycled tires, followed by the RGS15 test, corresponding to the geocell located at the top of the granular layer. In contrast, the unreinforced configuration (UR) recorded the lowest grain breakage index. This difference can be explained by two main factors: the lack of lateral confinement, which allowed the particles to rearrange freely, and the short test duration, as this system failed prematurely, thereby limiting exposure to cyclic loading and reducing the potential for progressive aggregate fracture.

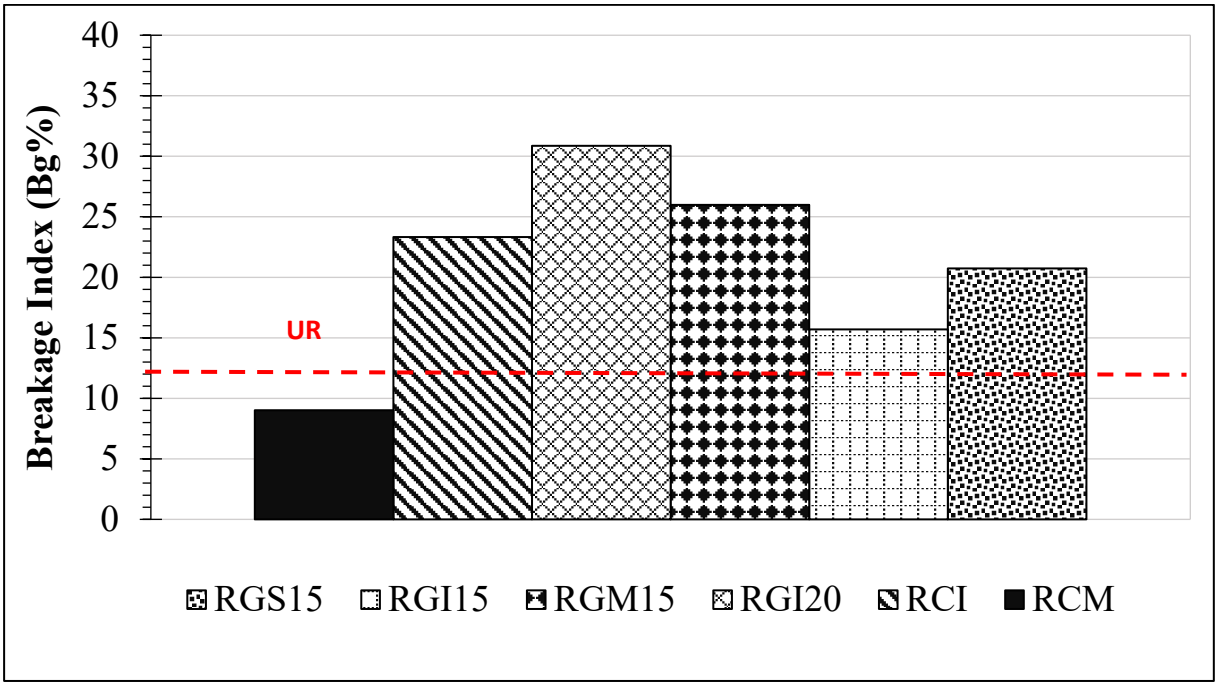

Figure 4.56 - Break index of the tests conducted with base material.

The results of the grain breakage index (Bg%) highlight the combined influence of three key variables: the height of the geocell, the material used for the reinforcement, and its position

within the granular layer. In general, it is observed that greater geocell height results in a higher restriction of particle movement, thereby increasing the likelihood of fracture. Likewise, geocells positioned closer to the surface tend to induce greater levels of surface confinement, concentrating stresses and elevating the breakage index. Finally, it is noteworthy that more rigid materials, such as commercial geocells, produce higher grain breakage values compared to geocells made from recycled tires, whose more elastic behavior allows for a more gradual stress dissipation, resulting in lower aggregate degradation.

The results obtained for the grain breakage index (Bg) raise significant debate due to the variability reported in the literature. Studies such as those bySweta & Hussaini, (2020), Indraratna, et al., (2017) and Thakur et al., (2012) suggest that the use of geosynthetics contributes to a reduction in grain breakage. However, a study conducted by Alkhorshid et al., (2019), which involved confinement in gravel columns, indicates that the use of stiffer geotextiles may increase the Bg in areas where the system exhibits greater rigidity, as a result of the higher confinement induced by the geosynthetics.

This discrepancy in the results may be influenced by factors such as the quality of the material used and the location of the collected samples. These variables could partially explain the observed differences, highlighting the importance of considering the specific conditions of each test when interpreting the data.

4.5. Summary of Results and Performance Evaluation

The comprehensive analysis of the tests revealed the positive influence of geocell reinforcement on the structural behavior of the evaluated sections. The reinforced configurations exhibited notable reductions in accumulated deformation and average deformation rate compared to the unreinforced section, particularly those with a height of 20 cm. Among them, the RGI20 configuration, made from recycled tires, achieved performance values equivalent to the commercial system, demonstrating that cellular confinement enhances the stability of the granular layer and the efficiency of load transfer to the subgrade.

The integration of deformation, transmitted stress, and stiffness results allowed for a more complete characterization of the system's behavior. The reinforced sections showed a progressive decrease in stresses transmitted to the subgrade and a tendency toward increased

stiffness modulus with the number of cycles, reflecting a more stable and efficient structural response. This behavior confirms the effectiveness of the confinement provided by the geocells in redistributing stresses and controlling permanent deformation under repeated loading.

The comparative analysis made it possible to identify both advantages and limitations of the system. The main advantages include the reduction of deformations, the decrease in transmitted stresses, the increase in stiffness with the number of cycles, and the environmental contribution derived from the reuse of recycled materials. The identified limitations are related to the geometric variability of the recycled material, the difficulty of ensuring manufacturing standardization, and the sensitivity of performance to the quality of the infill and initial compaction. Overall, the results validate the technical and environmental feasibility of geocells made from recycled tires as a sustainable and efficient alternative for the reinforcement of unpaved roads.

CHAPTER 5

5. CONCLUSIONS

This research demonstrates that geocells made from recycled tires are an effective, sustainable way to reinforce unpaved roads built on low-load-bearing soils. Using them significantly reduces deformations, thereby improving the mechanical performance of the road structure. The cellular confinement provided by the geocells promoted better load distribution and more stable behavior of the granular layer. Furthermore, the results confirmed that variables such as geocell height, placement within the layer, and type of infill material influence reinforcement efficiency. Recycled-tire geocells exhibited performance comparable to that of commercial products, which supports their technical and environmental feasibility as sustainable alternatives.

The physical and mechanical characterization of geocells manufactured from recycled tires demonstrated that parameters such as height, thickness, strength, flexibility, and durability significantly influence the structural behavior of unpaved roads. The results showed that geocells with greater height and thickness provide improved lateral confinement, which leads to a significant reduction in vertical deformations and stresses transmitted to the subgrade. Moreover, the geocells exhibited adequate mechanical strength and flexibility to withstand repeated loading, and their durability, assessed under laboratory conditions, supports their long-term use.

Comparative tests with and without geocells made from recycled tires revealed substantial improvements in the structural behavior of the pavement system, quantifying the influence of the reinforcement. Geocell reinforcement increased the pavement's load-bearing capacity, promoted more uniform stress redistribution toward the subgrade, and significantly reduced permanent deformation under repeated loading.

Placing geocells within the granular layer significantly impacts the road system's structural behavior. Tests demonstrated that installing geocells at an intermediate depth within the layer optimally balances the confinement of fill material and the redistribution of stresses toward the subgrade. Compared to configurations located near the surface or close to the subgrade, this

position resulted in a greater reduction of vertical deformations and improved structural efficiency under repeated loading.

These findings reinforce the viability of using recycled tires in geocells as a sustainable solution for road infrastructure, particularly in rural or low-traffic areas. Future work could include full-scale validation and long-term field monitoring to solidify their use in engineering practices.

To continue consolidating the knowledge gained, it is important that future research goes beyond the laboratory and includes full-scale tests on unpaved roads, considering different soil, traffic, and climate conditions. This will allow the true potential of geocells made from recycled tires to be verified in practice. Likewise, it is valuable to study how this material behaves over time when exposed to natural cycles of moisture, drought, and temperature changes, since these factors directly affect its durability. With this information, it would be possible to define its service life with greater certainty and to design clearer, more efficient, and sustainable maintenance plans.

Based on the results obtained in this study, several research directions are proposed to further advance the understanding and application of geocells made from recycled tires. It is recommended to expand the application of theoretical formulations to establish correlations between experimental results and analytical models of bearing capacity and cellular confinement. Additionally, conducting numerical analyses using finite element methods would allow the simulation of system behavior under different loading and geometric conditions, enhancing predictive design capabilities. Another relevant area involves performing economic feasibility studies comparing production, installation, and maintenance costs with those of commercial and conventional systems. Finally, it is suggested to investigate the relationship between the tensile strength of the tire material and the overall strength of the geocell system, with the aim of optimizing the selection of recycled materials and improving the structural efficiency of the reinforcement.

REFERENCES

AHMED, S. T., KABIR, M. U., ZAHID, C. Z. B., TAREQUE, T., MIRMOTALEBI, S. (2024). Improvement of subgrade California Bearing Ratio (CBR) using recycled concrete aggregate and fly ash. *Hybrid Advances*, 5: 100153.

ALKHORSHID, N. R., ARAUJO, G. L. S., PALMEIRA, E. M., ZORNBERG, J. G. (2019). Large-scale load capacity tests on a geosynthetic encased column. *Geotextiles and Geomembranes*, 47(5): 632-641.

AVESANI, J. O. (2013). Desenvolvimento de uma metodologia de cálculo e simulações numéricas aplicadas na melhoria da capacidade de carga de solos reforçados com geocélula. Tese de Doutorado, Escola de Engenharia de São Carlos, Universidade de São Paulo, São Carlos, Brasil.

AVESANI NETO, J. O., BUENO, B. S., FUTAI, M. M. (2015). Evaluation of a calculation method for embankments reinforced with geocells over soft soils using finite-element analysis. *Geosynthetics International*, 22(6): 439-451.

AVESANI NETO, J. O., BUENO, B. S., FUTAI, M. M. (2013). *A bearing capacity calculation method for soil reinforced with a geocell. Geosynthetics International,* 20(3): 142–157.

BADIGER, M., MAMATHA, K. H., DINESH, S. V. (2025). Evaluation of commercial and scrap tyre cellular reinforcement infilled with demolition waste for granular sub-base of flexible pavements: A sustainable approach. *International Journal of Transportation Science and Technology*, 18: 29-46.

BANERJEE, S., MANNA, B., SHAHU, J. T. (2024). Experimental investigation of the geometry of geocell on the performance of flexible pavement under repeated loading. *Geotextiles and Geomembranes*, 54: 1-14.

BANERJEE, S., MANNA, B., SHAHU, J. T. (2025). Performance evaluation of geocell-reinforced pavements overlying black cotton soil. *Geotextiles and Geomembranes*, 53(5): 1076-1093.

CHAUVET, P., B., A. (2018). Transporte de carretera en América Latina: evolución de la infraestructura y de sus impactos entre 2007 y 2015. Comisión Económica para América Latina y el Caribe – CEPAL, Santiago, Chile.

CHEN, L., LU, Y., NANAYAKKARA, A. (2023). Rural road connectivity and local economic activity: Evidence from Sri Lanka's iRoad program. *Transport Policy*, 144: 49-64.

CZARNA-JUSZKIEWICZ, D., KUNECKI, P., CADER, J., WDOWIN, M. (2023). Review in waste tire management—potential applications in mitigating environmental pollution. *Materials*, 16(17): 5771

CODASP – Companhia de Desenvolvimento Agrícola de São Paulo. (1988). *Estradas vicinais de terra: Manual técnico para manutenção e conservação*. São Paulo, Brasil, 125 p.

DABIRYAN, H., KARGAR, M., AGHABEIGI, E., MIR MOHAMMAD HOSSEINI, S. M., HOSSEINI VARKIYANI, S. M. (2017). Evaluating the performance of geocells made from needle-punched nonwoven layers in the bearing capacity of reinforced soil. *The Journal of The Textile Institute*, 108(9): 1531-1538.

DANDIN, S., SATHE, S., WAGALE, M., JOMDE, A. (2024). Utilizing PET bottles for sustainable cellular reinforcement: A study on enhancing fly ash backfill bearing strength with innovative geocell alternative. *Construction and Building Materials*, 433: 136641.

DASH, S. K., SIREESH, S., SITHARAM, T. G. (2003). Model studies on circular footing supported on geocell reinforced sand underlain by soft clay. *Geotextiles and Geomembranes*, 21(4): 197-219.

DASH, S.K. & SAIKIA, R. (2019). Contact pressure distribution on subgrade soil underlying geocell reinforced foundation beds. Transportation and Transit Systems, 5(1): 45-52.

DEMIRDOGEN, S., GURBUZ, A., YUNKUL, K. (2024). Parameters affecting performance of fully instrumented model testing of strip footings on geocell-reinforced soils. *Geotextiles and Geomembranes*, 52(6): 1191-1206.

DUDDU, S. R., KOMMANAMANCHI, V., CHENNARAPU, H., BALUNAINI, U. (2024). Field evaluation of deformation modulus of geogrid and geocell-stabilized subgrade soil. *KSCE Journal of Civil Engineering*, 28(11): 4944-4960.

EMERSLEBEN, A., MEYER, N. (2008). The use of geocells in road constructions over soft soil: Vertical stress and falling weight deflectometer measurements. *EuroGeo4 – 4th European Geosynthetics Conference*, IGS, Edinburgh, Scotland, Paper 132, 8 p.

CORREA VALDERRAMA, E. (2017). El rol de las vías terciarias en la construcción de un nuevo país. *Revista de Ingeniería*, 45: 64-71.

EDIL, T. B., BENSON, C. H., TANYU, B. F., SENOL, A., GUTHRIE, W. S., ABU-FARSAKH, M. (2013). Laboratory evaluation of geocell-reinforced gravel subbase over poor subgrades. *Geosynthetics International*, 20(2): 61-72.

FAZELI DEHKORDI, P., MIRABOLGHASEMI DEHKORDI, A., SHIRANI FARADONBE, A. M. (2023). Bearing capacity of two asymmetric differently loaded concrete footings seated on geocell-reinforced sand slopes. *Case Studies in Construction Materials*, 19: e02299.

FENG, L. X., AVESANI NETO, J. O., ZORNBERG, J. G. (2024). Evaluation of the elastic modulus improvement in geocell-reinforced unbound aggregates: Full-scale experimental sections on a highway. *Transportation Geotechnics*, 49: 101444.

GEBRESILASSE, M. (2023). Rural roads, agricultural extension, and productivity. *Journal of Development Economics*, 162: 103048.

GUTIÉRREZ GÓNGORA, I. A. M. (2015). Estradas não pavimentadas reforçadas com geossintéticos: influência de propriedades físicas e mecânicas do reforço. Tese de Doutorado em Geotecnia, Universidade de Brasília, Brasília, Brasil.

HARRAL, C. G., FAIZ, A. (1988). *El deterioro de los caminos en los países en desarrollo: causas y soluciones*. Banco Mundial, Washington, D.C., 31 p.

HASHAMFIROOZ, M., DEHGHANI, M. H., KHANIZADEH, M., AGHAEI, M., BASHARDOOST, P., HASSANVAND, M. S., HASSANABADI, M., MOMENIHA, F. (2025). A systematic review of the environmental and health effects of waste tires recycling. *Heliyon*, 11(2): e41909.

HEGDE, A. M., SITHARAM, T. G. (2015). Experimental and numerical studies on protection of buried pipelines and underground utilities using geocells. *Geotextiles and Geomembranes*, 43(5): 372-381.

HEGDE, A., SITHARAM, T. G. (2015). 3-Dimensional numerical modelling of geocell reinforced sand beds. *Geotextiles and Geomembranes*, 43(2): 171-181.

HIDALGO, C. A., BUSTAMANTE-HERNÁNDEZ, J. J. (2020). A new sustainable geotechnical reinforcement system from old tires: Experimental evaluation by pullout tests. *Sustainability*, 12(11): 4582.

HIDALGO, C., BUSTAMANTE, J. (2018). Sistema de refuerzo geotécnico con llantas recicladas. Patente NC2017/0003522, Colômbia.

HUANG, M., LIN, C., POKHAREL, S. K., TURA, A., MUKHOPADHYAYA, P. (2021). Model tests of freeze-thaw behavior of geocell-reinforced soils. *Geotextiles and Geomembranes*, 49(3): 669-687.

IBAGÓN, L., CAICEDO, B., VILLACRESES, J. P., ACHURY-FLORIAN, Á. (2025). Theoretical modelling of the washboard phenomenon on unpaved roads. *Transportation Geotechnics*, 50: 101484.

INDRARATNA, B., SUN, Q., GRANT, J. (2017). Behaviour of subballast reinforced with used tyre and potential application in rail tracks. *Transportation Geotechnics*, 12: 26-36.

INVIAS. (2013). *INV E 125-13: Determinación del límite líquido de los suelos*. Bogotá, Colombia, 20 p.

INVIAS. (2013). *INV E 126-13: Límite plástico e índice de plasticidad de los suelos*. Bogotá, Colombia, 10 p.

INVIAS. (2013). *INV E 142-13: Relaciones de humedad – peso unitario seco en suelos*. Bogotá, Colombia, 26 p.

INVIAS. (2013). *INV E 148-13: CBR de suelos compactados en el laboratorio y sobre muestra inalterada*. Bogotá, Colombia, 20 p.

INVIAS. (2013). *INV E 102-13: Descripción e identificación de suelos*. En: *Normas de Ensayo de Materiales para Carreteras*. Bogotá, Colombia, p.28-56.

INVIAS. (2013). *INV E 128-13: Determinación de la gravedad específica de las partículas sólidas de los suelos y del llenante mineral, empleando un picnómetro con agua*. Bogotá, Colombia.

KAMALI, M., HEWAGE, K., SADIQ, R. (2019). Conventional versus modular construction methods: A comparative cradle-to-gate LCA for residential buildings. *Energy and Buildings*, 204: 109479.

KEBEDE, H. A. (2024). Gains from market integration: welfare effects of new rural roads in Ethiopia. *Journal of Development Economics*, 168: 103252

KOERNER, R. M. (1994). *Designing with geosynthetics*. 3. ed. Englewood Cliffs: Prentice Hall.

KOLATHAYAR, S., SUJA, P., NAIR, V., KRISHNA, S. & TAMILARASI, G. (2019). Performance evaluation of seashell and sand as infill materials in HDPE and coir geocells. Innovative Infrastructure Solutions, 4(17): 1-9.

KRISHNA, A., LATHA, G. M. (2023). Evolution of geocells as sustainable support to transportation infrastructure. *Sustainability*, 15(15): 11773.

LEI, H.; MA, T.; FENG, S.; WANG, L. (2024). Confinement effect of geocell on the mechanical characteristics of reinforced sand subgrade. Transportation Geotechnics, 48: 101336.

LI, L.; SUN, K.; XU, M.; XIAO, H.; JIANG, S. (2025). Study on the dynamic performance of heavy-load railway reinforced subgrade under flood condition. Geotextiles and Geomembranes, 53(4): 985-998.

MARKIEWICZ, A.; KODA, E.; KIRAGA, M.; WRZESIŃSKI, G.; KOZANKA, K.; NALIWAJKO, M.; VAVERKOVÁ, M. D. (2024). Polymeric products in erosion control applications: a review. Polymers, 16(17): 2490.

MARSAL, R. J. (1967). Large scale testing of rock fill materials. Journal of the Soil Mechanics and Foundations Division, 93(SM2): 27-43.

MARTINS, C., MACEDO, J., PINHO-LOPES, M. (2024). Geocells for unpaved roads: analysis of design methods from the literature. *International Journal of Geosynthetics and Ground Engineering*, 10: 57.

MBABAZI, E. (2019). Impact of unpaved road condition on rural transport services. *Proceedings of the Institution of Civil Engineers – Municipal Engineer*, 172(4): 239-245.

MOHADDAS TAFRESHI, S. N., DAWSON, A. R. (2012). A comparison of static and cyclic loading responses of foundations on geocell-reinforced sand. *Geotextiles and Geomembranes*, 32: 55-68.

ÖNAL, Y., ÇALIŞICI, M., KAYADELEN, C., ALTAY, G. (2023). A comparative experimental study of geocell and geogrid-reinforced highway base layers under repeated loads. *Road Materials and Pavement Design*, 24(12): 2877-2892.

PALMEIRA, E. M. (2018). *Geossintéticos em geotecnia e meio ambiente*. Rio de Janeiro: Editora Oficina de Textos.

PARSA, M.; BAGHERIPOUR, M. H.; NASROLLAHI, S. M.; LO PRESTI, D. (2024). Reinforcement mechanism and the stress-strain behaviors of geocells made by non-woven geotextile. Transportation Geotechnics, 47: 101275.

PHYS.ORG. (2024). From old tires, a new material for making roads. 16 out. 2024. Disponível em: https://phys.org/news/2024-10-material-roads.html. Acesso em: jan. 2025.

POKHAREL, S.K., HAN, J., LESHCHINSKY, D., PARSONS, R.L., HALAHMI, I. (2010). Investigation of factors influencing behavior of single geocell-reinforced bases under static loading. Geotextiles and Geomembranes, 28(6): 570-578.

POKHAREL, S.K., HAN, J., MANANDHAR, C., YANG, X., LESHCHINSKY, D., HALAHMI, I., PARSONS, R.L. (2011). Accelerated pavement testing of geocell-reinforced unpaved roads over weak subgrade. Journal of the Transportation Research Board, 2204(1): 67-75.

POKHAREL, S.K., HAN, J., LESHCHINSKY, D., PARSONS, R.L. (2018). Experimental evaluation of geocell-reinforced bases under repeated loading. Pavement Research and Technology, 11(2): 114-127.

POKHAREL, S.K., HAN, J., LESHCHINSKY, D., PARSONS, R.L. & HALAHMI, I. (2010). Investigation of factors influencing behavior of single geocell-reinforced bases under static loading. Geotextiles and Geomembranes, 28(6): 570-578.

POORAHONG, H., JAMSAWANG, P., THANASISATHIT, N., JONGPRADIST, P., HORPIBULSUK, S. (2024). Enhancing the bearing capacity of unpaved roads on soft clay subgrade using geogrid reinforcement with a triaxial configuration. Construction and Building Materials, 456: 139321.

RAMU, B., BALUNAINI, U., SARIDE, S. (2022). Performance of reinforced base courses of flexible pavements overlying soft subgrades: insights from large-scale model experiments. International Journal of Geomate, 22(89): 80-86.

SARIDE, S., RAMANA, G.V., VASAN, V. (2015). Evaluation of rutting behaviour of geocell reinforced sand subgrades under repeated loading. Indian Geotechnical Journal, 45: 378-388.

SEGUI, L., et al. (2018). Gestión de residuos y economía circular. EAE Business School, Madrid, set. 2018.

SHERIN, K.S., CHANDRASEKARAN, S., NAIR, S.N. (2017). Effect of geocell geometry and multi-layer system on the performance of geocell reinforced sand under a square footing. International Journal of Geosynthetics and Ground Engineering, 3(20): 1-12.

SHIMIZU, M., ISHIMOTO, T. (1990). Increase in the bearing capacity of ground with geotextile wall frame. 4th International Conference on Geotextiles, Geomembranes and Related Products, IFAI, The Hague, Netherlands, 1: 50-254.

SHIN, E.C., KANG, H.H., PARK, J.J. (2017). Reinforcement efficiency of bearing capacity with geocell shape and filling materials. KSCE Journal of Civil Engineering, 21(5): 1648-1656.

SINGH, M., TRIVEDI, A., SHUKLA, S.K. (2022). Evaluation of geosynthetic reinforcement in unpaved road using moving wheel load test. Geotextiles and Geomembranes, 50(4): 581-589.

SIREESH, S., SITHARAM, T.G., DASH, S.K. (2009). Bearing capacity of circular footing on geocell–sand mattress overlying clay bed with void. Geotextiles and Geomembranes, 27(2): 89-98.

STYER, J., TUNSTALL, L., LANDIS, A. & GRENFELL, J. (2024). Innovations in pavement design and engineering: A 2023 sustainability review. Heliyon, 10(13): e33602.

SWETA, K. & HUSSAINI, S.K.K. (2020). Effect of geogrid on deformation response and resilient modulus of railroad ballast under cyclic loading. Construction and Building Materials, 264: 120690.

TAFRESHI, S.N.M. & DAWSON, A.R. (2010). Comparison of bearing capacity of a strip footing on sand with geocell and with planar forms of geotextile reinforcement. Geotextiles and Geomembranes, 28(1): 72-84.

TERZAGHI, K. (1943). Theoretical soil mechanics. John Wiley & Sons, New York, 510 p.

THAKUR, J.K., HAN, J., POKHAREL, S.K. & PARSONS, R.L. (2012). Performance of geocell-reinforced recycled asphalt pavement (RAP) bases over weak subgrade under cyclic plate loading. Geotextiles and Geomembranes, 35: 14-24.

THAKUR, J. K., HAN, J., PARSONS, R. L. (2016). Factors influencing deformations of geocell-reinforced recycled asphalt pavement bases under cyclic loading. *Journal of Materials in Civil Engineering*, 29(3): 04016248.

TUTUMLUER, E., KANG, M. & QAMHIA, I.I.A. (2025). Geosynthetic stabilization of road pavements, railroads, and airfields. Transportation Geotechnics, 50: 101321.

VESIC, A. (1972). Analysis of ultimate loads of shallow foundations. Proceedings of the Conference on Soil Mechanics and Foundations Engineering, Performance of Earth and Earth-Supported Structures, ASCE, Purdue University, 2: 75-145.

XLENDER, B., LENART, S., JELUSIC, P. & MEDVED, S. (2016). Modeling of a geocell-reinforced pavement: An experimental validation. Acta Geotechnica Slovenica, 13: 14-23.

YANG, X., HAN, J. & PARSONS, R. (2010). Three-dimensional numerical modeling of single geocell-reinforced sand. Frontiers of Architecture and Civil Engineering in China, 4: 233-240.

YOON, Y.W., HEO, S.B. & KIM, K.S. (2008a). Geotechnical performance of waste tires for soil reinforcement from chamber tests. Geotextiles and Geomembranes, 26(1): 100-107.

ZHAO, Y., LU, Z., JIANG, L. & YAO, H. (2023). Influence of different infill materials on the performance of geocell-reinforced cohesive soil beds. Scientific Reports, 13: 12330.

ZHAO, Y., LU, Z., GEDELA, R., TANG, C., FENG, Y., LIU, J. & YAO, H. (2025). Performance and geocell-soil interaction of sand subgrade reinforced with high-density

polyethylene, polyester, and polymer-blend geocells: 3D numerical studies. Computers and Geotechnics, 178: 106949.

ZHAO, Y., LU, Z., LIU, J. & YAO, H. (2024). Numerical study on shear behavior of geocell-reinforced layer based on large-scale direct shear tests. KSCE Journal of Civil Engineering, 28(7): 2613-2624.